

Improved ring potential of QED at finite temperature and in the presence of weak and strong magnetic field

N. Sadooghi* and K. Sohrabi Anaraki

Department of Physics, Sharif University of Technology, P.O. Box 11155-9161, Tehran-Iran

Using the general structure of the vacuum polarization tensor $\Pi_{\mu\nu}(k_0, \mathbf{k})$ in the infrared (IR) limit, $k_0 \rightarrow 0$, the ring contribution to QED effective potential at finite temperature and non-zero magnetic field is determined beyond the static limit, $(k_0 \rightarrow 0, \mathbf{k} \rightarrow \mathbf{0})$. The resulting ring potential is then studied in weak and strong magnetic field limit. In the limit of weak magnetic field, at high temperature and for $\alpha \rightarrow 0$, the improved ring potential consists of a term proportional to $T^4 \alpha^{5/2}$, in addition to the expected $T^4 \alpha^{3/2}$ term arising from the static limit. Here, α is the fine structure constant. In the limit of strong magnetic field, where QED dynamics is dominated by the lowest Landau level (LLL), the ring potential includes a novel term consisting of dilogarithmic function $(eB)\text{Li}_2\left(-\frac{2\alpha}{\pi} \frac{eB}{m^2}\right)$. Using the ring improved (one-loop) effective potential including the one-loop effective potential and ring potential in the IR limit, the dynamical chiral symmetry breaking of QED is studied at finite temperature and in the presence of strong magnetic field. The gap equation, the dynamical mass and the critical temperature of QED in the regime of LLL dominance are determined in the improved IR as well as in the static limit. For a given value of magnetic field, the improved ring potential is shown to be more efficient in decreasing the critical temperature arising from one-loop effective potential.

PACS numbers: 11.10.Wx, 11.15.Ex, 12.38.Mh

I. INTRODUCTION

A. Motivation

The existence of phase transitions in the early universe has been a question that has preoccupied a generation of cosmologists. Early on, Kirzhnits [1] found that the symmetry between the weak and electromagnetic interactions would be restored at high temperatures. This result was soon complemented by similar works by Weinberg [2], Dolan and Jackiw [3], Kirzhnits and Linde [4]. In particular, there has been much interest in the nature of the electroweak phase transition (EWPT), which is closely related to the still unsolved problem of baryogenesis. It has been known since Sakharov's work that there are three necessary (but not sufficient) conditions for the baryon asymmetry of the Universe to develop [5]. *First*, we need interactions that do not conserve baryon number B , otherwise no asymmetry could be produced in the first place. *Second*, C and CP symmetry must be violated, in order to differentiate between matter and antimatter, otherwise the same rate of baryons and antibaryons would be produced leading to zero

*Electronic address: sadooghi@physics.sharif.edu

net baryon number. *Third*, the universe in his history, must have experienced a departure from thermal equilibrium. In other words, the above C and CP violating processes should have been occurred in a state out of equilibrium, otherwise the net baryon number cannot change in time. The Standard Model (SM) of electroweak interaction meets all the above requirements to generate a baryon asymmetry during the EWPT, provided that this last be of first order.

The type of symmetry restoring phase transition is determined by the behavior of the effective or thermodynamic potential. The fact that the symmetry is restored at high temperatures is a result of the $T^2 m^2(v)$ term as the leading order contribution from the thermal fluctuations of the field. This term appears in the perturbatively calculable one-loop effective potential. Here, T is the temperature and m^2 is the mass squared proportional to the expectation value of some classical scalar (Higgs) field v . As the temperature is increased, the contribution from thermal fluctuation dominates the negative-mass-squared term in the tree level potential and symmetry will be restored. According to this one-loop approximation, it can be shown that the phase transition is of second order [1]-[4] and that the effective potential includes terms proportional to $m^3(v)T$ and therefore is imaginary when the mass squared is negative. As it was shown in [6], however, the appearance of imaginary terms in the one-loop effective potential indicates the breakdown of the semiclassical loop expansion through IR singularities. As it is then argued in [7], these IR singularities are included in the ring (plasmon or daisy) diagrams of the theory. In [7], the nonperturbative ring contribution to the effective potential is calculated. It is shown to have the general structure

$$V_{ring}(v) = \frac{T}{12\pi} \text{Tr} \left(\left[m^2(v) + \Pi_{00}(0) \right]^{3/2} - m^3(v) \right), \quad (\text{I.1})$$

where $\Pi_{00}(0) \equiv \Pi_{00}(n = 0, \mathbf{k} \rightarrow \mathbf{0})$ is the vacuum polarization in the *static (zero momentum) limit*.¹ Adding this contribution to the one-loop effective potential, it is then shown that the SM has indeed a first order phase transition and the critical temperature is much lower than the temperature arising from one-loop effective potential [7]. As for the question of baryon asymmetry, however, it is known that neither the amount of CP violation within the minimal SM nor the strength of the EWPT are enough to generate sizable baryon number [8].²

In the recent years, due to the observation that magnetic fields are able to generate a stronger first order EWPT [9]-[13], the electroweak baryogenesis is revisited within the minimal SM and in the presence of external hypermagnetic fields (for a review see [11]). In [10], the ring improved effective potential of SM, including one-loop effective potential and ring contributions, is calculated explicitly. Here, as in [7], the ring potential is determined in the *static (zero momentum) limit*, where, in the presence of external magnetic field B , $\Pi_{00}(0)$ in (I.1) is defined by $\Pi_{00}(0) \equiv \Pi_{00}(n = 0, \mathbf{k} \rightarrow \mathbf{0}; eB)$. It is found that for the field strengths $10^{23} - 10^{24}$ Gauß, the phase transition is of first order but the baryogenesis condition $\frac{\langle v \rangle}{T_c} > 1 - 1.5$ is still not satisfied.³ To improve this condition one is looking for possibilities to decrease the critical temperature T_c of EWPT.

¹ In [10, 11], this limit is called the “Debye mass” limit.

² Other possibilities to explain the generation of baryon number during the EWPT include minimal and non-minimal supersymmetric model.

³ In the electroweak SM at finite T , the existence of baryon number violation is realized by means of its vacuum structure through sphaleron mediated processes. The sphaleron transition between different topological distinct vacua is associated to baryon number $n_B - n_{\bar{B}}$ violation and can either induce or wash out a baryon asymmetry. In order to satisfy the

Motivated by the previous facts and as the first step to improve the results in [10]-[13] to solve the problem of baryogenesis within the minimal SM, we will go in this paper *beyond the static (zero momentum) limit* and will calculate the ring improved effective potential of QED at finite temperature and in the presence of constant magnetic field in a certain *IR limit*. As we have seen above, the ring part of the ring improved effective potential is given by QED vacuum polarization tensor, $\Pi_{\mu\nu}(n, \mathbf{k})$, at finite temperature. In this paper, in contrast to previous works, *e.g.* [7, 10, 14], we will determine the ring potential using the vacuum polarization tensor in the *IR limit*, which is particularly characterized by $(n = 0, \mathbf{k} \neq \mathbf{0})$.⁴

This paper consists of two parts: In the first part of the paper, using the diagonalized form of the vacuum polarization tensor in the IR limit $\Pi_{\mu\nu}(n = 0, \mathbf{k} \neq \mathbf{0})$, the general structure of the ring potential will be determined. Then, the ring potential in the improved IR limit will be calculated explicitly in the presence of weak and strong magnetic field and the resulting expressions will be compared with the conventionally used static ring potential in these limits. In the second part of the paper, the dynamical chiral symmetry breaking of QED at finite temperature and in the presence of strong magnetic field will be studied. Our main goal to study this example is to answer the question how efficient the improved IR approximation is in decreasing the critical temperature of the above dynamical chiral symmetry breaking. Comparing the effect of the ring potential in the IR limit numerically with the effect of the ring potential in various static limits, we arrive at the conclusion that the improved IR limit is more efficient in decreasing the critical temperature arising from one-loop effective potential $T_c^{(1)}$. Here, $T_c^{(1)}$ is the critical temperature that arises from one-loop effective potential in the lowest order of α correction (ladder approximation). Defining a ring improved critical temperature \mathcal{T}_c containing the contribution of one-loop effective potential in ladder approximation and the ring contributions, it turns out that the difference of the efficiency factors defined as $\eta \equiv 1 - \frac{T_c^{(1)}}{\mathcal{T}_c}$ is more than 60% for the magnetic field $B \approx 10^{16}$ Gauß. The above conclusion is promising in view of the problem of EWPT in the electroweak SM in the presence of weak/strong hypermagnetic field [10]-[13]. Here, one is looking for a possibility to decrease the critical temperature of EWPT in order to improve the baryogenesis condition $\frac{\langle v \rangle}{T_c} > 1 - 1.5$. Using the improved ring potential in the IR limit in determining the critical temperature of EWPT in SM may improve the results from [10]-[13].

The organization of this paper is as follows: In Sect. I.B, we will review some technical details on ring diagrams in thermal field theory without magnetic field. In particular, we will review the well-known results of QED ring contribution to the effective potential in the static limit [14]. In Sect. II, we will determine the vacuum polarization tensor of QED in the IR limit, $\Pi_{\mu\nu}(n = 0, \mathbf{k} \neq \mathbf{0}; eB)$. Here, we will use some results from [15] and [16]. In particular, we will the method in [15] to diagonalize the vacuum polarization tensor in certain basis. In Sect. III, using the diagonalized $\Pi_{\mu\nu}(n = 0, \mathbf{k} \neq \mathbf{0}; eB)$, we will be able to determine the general structure of the ring contribution to QED effective potential in the presence of external magnetic field at finite temperature. In Sect. III.A and III.B, the resulting ring improved effective potential in the IR limit will be considered first in the weak and then in the strong magnetic

baryon asymmetry condition during the baryogenesis process the rate of baryon violating transitions between different topological vacua must be suppressed in the broken phase, when the universe returns to thermal equilibrium. In other words, the sphaleron transitions must be slower than the expansion of the universe and this in turn translates into the condition $\frac{\langle v \rangle}{T_c} > 1 - 1.5$, where $\langle v \rangle$ is the Higgs mass [8, 12].

⁴ See Sect. I.B for technical details.

field limit.

In the weak magnetic field limit, at high temperature and for $\alpha \rightarrow 0$, the ring potential in the IR limit consists of a term proportional to $T^4 \alpha^{5/2}$, in addition to the expected $T^4 \alpha^{3/2}$ term arising from the static limit. Here, $\alpha \equiv \frac{e^2}{4\pi}$ is the fine structure constant. This term can be viewed as a nonperturbative correction to QED effective potential in addition to the perturbative loop corrections to this potential in the corresponding $\alpha^{5/2}$ order. Note that, using Hard Thermal Loop (HTL) expansion [17], similar contributions of order $\alpha_s^{3/2}$ and $\alpha_s^{5/2}$ are previously found in QCD effective potential at finite temperature and zero magnetic field (see [18] and the references therein).

In the strong magnetic field limit, the ring potential of QED at finite temperature includes a novel term consisting of a dilogarithmic function $(eB)\text{Li}_2\left(-\frac{2\alpha}{\pi} \frac{eB}{m^2}\right)$. As in the weak magnetic field limit, similar contribution to QCD effective potential at finite temperature and zero magnetic field is calculated in [19]. Here, going beyond the static limit, it is shown that QCD effective potential consists of an unexpected $g_s^4 \ln g_s$ term. The appearance of a similar term in the QED ring potential at finite temperature and in the presence of strong magnetic field is however expected due to the well-known phenomenon of magnetic catalysis [20, 22]⁵; In the limit of strong magnetic field, QED dynamics is believed to be dominated by the Lowest Landau Level (LLL), where the chiral symmetry of the theory is broken by a dynamically generated fermion mass. As a consequence of a dimensional reduction from D to $D-2$, four dimensional QED exhibits confining properties like ordinary confining Abelian or non-Abelian gauge theories without magnetic field [20, 22].⁶

To compare the ring potential in the IR limit from III.B with the static ring potential in the LLL, we will calculate in Sect. III.C and III.D, the static ring potential in the strong magnetic field limit in two different methods. In the first approach, we will calculate the ring potential after taking the limit $eB \rightarrow \infty$. In the second approach, we will take the limit $eB \rightarrow \infty$ after calculating the ring potential mathematically. We will arrive at two different results. This difference can be interpreted as a direct consequence of the dynamics of QED in the LLL and the above-mentioned dimensional reduction in the regime of LLL dominance.

In the second part of the paper, we will use the results from III.B-III.D to study the dynamical chiral symmetry breaking of QED at finite temperature and in the presence of strong magnetic field in [see Sect. IV.]⁷ As we have mentioned before, we are indeed interested in the effect of our improved ring potential in decreasing the critical temperature of chiral symmetry breaking of QED at finite temperature and in the presence of strong magnetic field. Using the ring improved effective potentials in the IR and the static limit, the gap equation, the dynamical mass and the critical temperature T_c of QED in the LLL are determined. To have a first estimate on the efficiency of the improved IR limit in decreasing the critical temperature arising from one-loop effective potential in the ladder approximation, $T_c^{(1)}$, we will compare the ratio $u \equiv T_c^{(1)}/T_c$ for magnetic field eB in the interval $[10^{-8}, 1]$ GeV². Here, T_c is the improved critical temperature in the ladder approximation. This range corresponding to $B \in [1.7 \times 10^{12}, 1.7 \times 10^{20}]$ Gauß, is phenomenologically relevant in the astrophysics of neutron stars, where the strength of the

⁵ The magnetic catalysis has wide applications in condensed matter physics [23] and cosmology [24].

⁶ A two dimensional Schwinger model is an example of a confining Abelian gauge theory. It is known that four dimensional QED in the presence of strong magnetic field is reduced to a two dimensional theory, very similar to the ordinary Schwinger model without external magnetic field.

⁷ Recently chiral transition in strong magnetic field is studied in [25].

magnetic field is of order $10^{13} - 10^{15}$ Gauß (see [26] and the references therein). It is also relevant in the heavy ion experiments, where it is believed that the magnetic field in the center of gold-gold collision is $eB \sim 10^2 - 10^3$ MeV² or $B \sim 10^{16} - 10^{17}$ Gauß [27]. Defining further an efficiency factor $\eta \equiv 1 - u^{-1}$ for the IR and static approximation, we will be able to compare the IR limit with various static limits. According to our numerical results presented in IV.E, for a given value of the magnetic field, the IR limit seems to be more efficient in decreasing the critical temperature arising from one-loop effective potential. The maximum value of η in the IR limit $\sim 63\%$ for $B \approx 1.6 \times 10^{16}$ Gauß. Our results are summarized in Sect. V. In Appendix A, we will define the one-loop effective potential and the ring potential in the LLL at zero temperature. In Appendix B, the gap equation arising from one-loop effective potential and ring improved effective potential at zero temperature is derived. Appendix C generalizes the definition from Appendix B to finite temperature.

B. Technical details

QED ring potential at $T \neq 0$ and $B = 0$ in the static limit

In this section, we will review the results in [14] on QED ring potential at finite temperature using the static (zero momentum) limit. Eventually we will argue why an approximation beyond the zero momentum limit is necessary when we turn on a strong magnetic field.

Let us just start with the partition function of QED at finite temperature

$$Z = \int \mathcal{D}c \mathcal{D}\bar{c} \mathcal{D}A_\mu \mathcal{D}\psi \mathcal{D}\bar{\psi} \exp \left(\int_0^\beta d\tau \int d^3x \mathcal{L} \right), \quad (\text{I.2})$$

where $\mathcal{L} = \mathcal{L}_0 + \mathcal{L}_I$. Here, \mathcal{L}_0 is the free part of the Lagrangian

$$\mathcal{L}_0 = \bar{\psi} (i\gamma_\mu \partial^\mu - m) \psi - \frac{1}{4} F_{\mu\nu} F^{\mu\nu} - \frac{1}{2\xi} (\partial^\mu A_\mu)^2 + (\partial^\mu \bar{c}) (\partial_\mu c),$$

and \mathcal{L}_I the interaction Lagrangian

$$\mathcal{L}_I = -e\bar{\psi} A_\mu \gamma^\mu \psi.$$

Using the above Lagrangian the free photon propagator of the theory is given by

$$D_0^{\mu\nu} = \frac{1}{k^2} \left\{ g^{\mu\nu} - (1 - \xi) \frac{k^\mu k^\nu}{k^2} \right\}, \quad k_0 \equiv 2\pi i n T;$$

and $n \in]-\infty, +\infty[$ labels the Matsubara frequencies for the bosons. The photon-self energy at one-loop level is

$$\Pi_{\mu\nu} = \mathcal{D}_{\mu\nu}^{-1} - D_{0\mu\nu}^{-1}. \quad (\text{I.3})$$

Using the corresponding Ward identities arising from the gauge invariance of the theory

$$k_\mu \Pi^{\mu\nu} = 0, \quad k^\mu k^\nu \mathcal{D}_{\mu\nu} = \xi,$$

it is possible to determine the general structure of the photon propagator $\mathcal{D}_{\mu\nu}$ and the corresponding photon self-energy $\Pi_{\mu\nu}$ as a symmetric second-rank tensors. Here, ξ denotes the covariant gauge. At

finite temperature, the most general tensor of this type is a linear combination of $g_{\mu\nu}$, $k_\mu k_\nu$, $u_\mu u_\nu$, and $k_\mu u_\nu + k_\nu u_\mu$, where $u_\mu = (1, 0, 0, 0)$ specifies the rest frame of the many body system. Using the above properties $\mathcal{D}_{\mu\nu}$ and $\Pi_{\mu\nu}$ have the general form

$$\begin{aligned}\Pi^{\mu\nu} &= GP_T^{\mu\nu} + FP_L^{\mu\nu}, \\ \mathcal{D}^{\mu\nu} &= \frac{1}{G - k^2} P_T^{\mu\nu} + \frac{1}{F - k^2} P_L^{\mu\nu} + \frac{\xi}{k^2} \frac{k^\mu k^\nu}{k^2},\end{aligned}\quad (\text{I.4})$$

where F and G are scalar function of k^0 and $\omega \equiv |\mathbf{k}|$. They are of order e^2 in the QED coupling constant e . The projector operators P_T and P_L in (I.4) are given by

$$\begin{aligned}P_T^{00} &= P_T^{0i} = P_T^{i0} = 0, \\ P_T^{ij} &= \delta^{ij} - \frac{k^i k^j}{\mathbf{k}^2}, \\ P_L^{\mu\nu} &= \frac{k^\mu k^\nu}{k^2} - g^{\mu\nu} - P_T^{\mu\nu}.\end{aligned}\quad (\text{I.5})$$

They have the properties

$$\begin{aligned}P_L^{\mu\rho} P_{L\rho\nu} &= -P_{L\nu}^\mu, & P_T^{\mu\rho} P_{T\rho\nu} &= -P_{T\nu}^\mu, \\ k_\mu P_T^{\mu\nu} &= k_\mu P_L^{\mu\nu} = 0, & P_L^{\mu\rho} P_{T\rho\nu} &= 0, \\ P_{L\mu}^\mu &= -1, & P_{T\mu}^\mu &= -2.\end{aligned}\quad (\text{I.6})$$

As it is shown in [14], the lowest correction to the QED thermodynamic potential V_2 is of order e^2

$$\ln Z_2 = -\frac{1}{2} \left(\text{wavy line in a circle} \right) = -\frac{1}{2} \left(\text{sun-like diagram with } \Pi \text{ in the center} \right) \quad (\text{I.7})$$

Note that these two diagrams are equivalent [14]. As for the next correction to the thermodynamic effective potential, it is not of order e^4 as expected, but of order e^3 when $T > 0$. It arises from the set of ring diagrams shown in Fig. 1.⁸

$$\begin{aligned}V_{ring} &= -\frac{T}{2} \sum_{n=-\infty}^{+\infty} \int \frac{d^3 k}{(2\pi)^3} \sum_{N=2}^{\infty} \frac{(-1)^{N-1}}{N} \left[D_0^{\mu\rho}(n, \mathbf{k}) \Pi_{\rho\mu}(n, \mathbf{k}) \right]^N \\ &= -\frac{T}{2} \sum_{n=-\infty}^{+\infty} \int \frac{d^3 k}{(2\pi)^3} \left\{ \ln[1 + D_0^{\mu\rho}(n, \mathbf{k}) \Pi_{\rho\mu}(n, \mathbf{k})] - D_0^{\mu\rho}(n, \mathbf{k}) \Pi_{\rho\mu}(n, \mathbf{k}) \right\}.\end{aligned}\quad (\text{I.8})$$

Plugging $D_0^{\mu\nu}$ and $\Pi_{\mu\nu}$ in (I.8) and using the properties of the projection operators P_L and P_T from (I.5) and (I.6), (I.8) is given by

$$V_{ring} = -\frac{T}{2} \sum_{n=-\infty}^{+\infty} \int \frac{d^3 k}{(2\pi)^3} \left\{ 2 \left[\ln \left(1 - \frac{G(n, \omega)}{k^2} \right) + \frac{G(n, \omega)}{k^2} \right] + \ln \left(1 - \frac{F(n, \omega)}{k^2} \right) + \frac{F(n, \omega)}{k^2} \right\}. \quad (\text{I.9})$$

⁸ In some recent references, as in [7] and [10, 11, 12] the ring potential V_{ring} is defined by adding (I.7) to the expression in (I.8), which is given by the series of diagrams in Fig. 1. This means that the series over $D_0^{\mu\rho}(n, \mathbf{k}) \Pi_{\rho\mu}(n, \mathbf{k})$ on the first line of (I.8) starts in [7] and [10, 11, 12] from $N = 1$. In this paper, we will use in the latter definition, where the sum over N starts from $N = 1$ on the first line of (I.8) [see (III.9) for the definition of the ring potential in this paper].

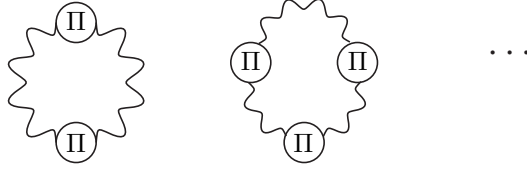


FIG. 1: Diagrams contributing to the ring potential (I.8). In the LLL approximation, the wavy lines are free photon propagators $D_0^{\mu\nu}$ and the circles indicate the insertion of vacuum polarization tensor $\Pi_{\mu\nu}$. In this approximation, $\Pi_{\mu\nu}$ are calculated using the free fermion propagator in the LLL.

Here, $-k^2 = \omega^2 + 4\pi^2 n^2 T^2$. To determine the next to leading order term in the effective potential, V_{ring} in the *static (zero momentum) limit*, an IR divergent term, V_{e^3} , is added to and subtracted from the ring potential (I.9) [14]. It is therefore given by

$$V_{ring} = V_{e^3} + V_{e^4},$$

where

$$V_{e^3} = -\frac{T}{2} \int \frac{d^3 k}{(2\pi)^3} \left\{ 2 \left[\ln \left(1 + \frac{G(0, \mathbf{0})}{\omega^2} \right) - \frac{G(0, \mathbf{0})}{\omega^2} \right] + \ln \left(1 + \frac{F(0, \mathbf{0})}{\omega^2} \right) - \frac{F(0, \mathbf{0})}{\omega^2} \right\}, \quad (\text{I.10})$$

and

$$V_{e^4} = -\frac{T}{2} \sum_{n=-\infty}^{+\infty} \int \frac{d^3 k}{(2\pi)^3} \left\{ 2 \left[\ln \left(1 - \frac{G(n, \omega)}{k^2} \right) + \frac{G(n, \omega)}{k^2} \right] + \ln \left(1 - \frac{F(n, \omega)}{k^2} \right) + \frac{F(n, \omega)}{k^2} \right\} \\ + \frac{T}{2} \int \frac{d^3 k}{(2\pi)^3} \left\{ 2 \left[\ln \left(1 + \frac{G(0, \mathbf{0})}{\omega^2} \right) - \frac{G(0, \mathbf{0})}{\omega^2} \right] + \ln \left(1 + \frac{F(0, \mathbf{0})}{\omega^2} \right) - \frac{F(0, \mathbf{0})}{\omega^2} \right\}. \quad (\text{I.11})$$

Carrying out the three-dimensional integration over \mathbf{k} , V_{e^3} is given by

$$V_{e^3} = \frac{T}{12\pi} \left[2G^{3/2}(0, \mathbf{0}) + F^{3/2}(0, \mathbf{0}) \right] = \frac{T}{12\pi} F^{3/2}(0, \mathbf{0}), \quad (\text{I.12})$$

where $G(0, \mathbf{0}) = 0$ is used. This is the well-known nonperturbative e^3 (or equivalently $\alpha^{3/2}$) contribution to the thermodynamic potential arising from the ring (plasmon) part of this potential. As for V_{e^4} from (I.11), it can now be expanded in the orders of e and is thus given by

$$V_{e^4} = \frac{T}{4} \int \frac{d^3 k}{(2\pi)^3} \left\{ \sum_{n \neq 0} \left[2 \left(\frac{G(n, \omega)}{k^2} \right)^2 + \left(\frac{F(n, \omega)}{k^2} \right)^2 \right] + \left[2 \left(\frac{G(0, \omega)}{\omega^2} \right)^2 + \left(\frac{F(0, \omega)}{\omega^2} \right)^2 \right] \right. \\ \left. - \left[2 \left(\frac{G(0, \mathbf{0})}{\omega^2} \right)^2 + \left(\frac{F(0, \mathbf{0})}{\omega^2} \right)^2 \right] \right\}, \quad (\text{I.13})$$

which is of order e^4 in the QED coupling constant. Note that expanding the logarithms in V_{e^4} in the orders of e , is only possible because it remains IR-finite. This is the case in QED but not in the confining gauge theories like QCD. The ring contribution to the effective potential of QCD is calculated in [19], where it is shown that, in particular $F(0, \omega)$ in (I.13) is a so called “dangerous” term containing a

logarithmically divergent part. To remove this term, it is necessary to go beyond the static limit. This is done in [19], where it is shown that the plasmon potential in QCD effective potential contains besides the g_s^3 -term a contribution of order $g_s^4 \ln g_s$ at any non-zero temperature. This contribution arises from the term $\Pi_{\mu\nu}(n=0, \mathbf{k} \neq \mathbf{0})$ in the IR limit.

In the present paper, we are in particular interested in the ring improved effective thermodynamic potential of QED in a *strong* magnetic field. It is believed that at weak coupling, the QED dynamics is dominated by the LLL. It is known that in the regime of LLL dominance the ordinary four dimensional QED is reduced to a two dimensional confining theory, like QCD, where the original chiral symmetry is broken by a dynamically generated fermion mass. Comparing to [19], we expect therefore to have some “dangerous” logarithmically divergent terms in the plasmon potential, if we use the static (zero momentum) limit ($n=0, \mathbf{k}=0$). To avoid these types of difficulties, we will determine, in the next section, the general structure of QED vacuum polarization tensor in the IR limit $n=0$ (or equivalently $k_0 \rightarrow 0$) as a function of finite three-momentum \mathbf{k} . To determine the ring potential in the limit of *weak* and *strong* magnetic field, we will use (I.8), where only $n=0$ is considered.

II. QED IN A CONSTANT MAGNETIC FIELD AT ZERO AND FINITE TEMPERATURE

In the first part of this section, we will briefly review the characteristics of QED in a constant magnetic field at zero temperature. In particular, we will consider the fermion and photon propagators in a *strong* magnetic field, where the QED dynamics is dominated by LLL. Then, in the second part, we will determine QED vacuum polarization tensor in a constant magnetic field at finite temperature and in a certain IR limit.

A. Fermions and photons in a strong magnetic field at zero and non-zero temperature

Let us start with QED Lagrangian density at zero temperature

$$\mathcal{L} = \bar{\psi} (i\gamma^\mu D_\mu^{ext.} - m) \psi - \frac{1}{4} F_{\mu\nu} F^{\mu\nu}, \quad (\text{II.1})$$

where $D_\mu^{ext.} \equiv \partial_\mu + ieA_\mu^{ext.}(x)$, with the gauge field $A_\mu \equiv A_\mu^{ext.}$ describing an external magnetic field. In this paper, we will choose the symmetric gauge

$$A_\mu^{ext.} = \frac{B}{2} (0, x_2, -x_1, 0),$$

that leads to a magnetic field in the x_3 direction. From now on, the longitudinal (x_0, x_3) components will be indicated as \mathbf{x}_\parallel and the transverse directions (x_1, x_2) components by \mathbf{x}_\perp . The free (bare) fermion propagator of a four dimensional QED in a constant magnetic field at zero temperature can be found using the Schwinger’s proper-time formalism [28] from $(i\gamma^\mu D_\mu^{ext.} - m)^{-1}$. In the above symmetric gauge, the free fermion propagator in a constant magnetic field is given by

$$\begin{aligned} S_F(x, y) &= \exp \left(\frac{ie}{2} (x-y)^\mu A_\mu^{ext.}(x+y) \right) S(x-y) \\ &= e^{\frac{ieB}{2} \epsilon^{ab} x_a y_b} S(x-y), \quad a, b = 1, 2. \end{aligned} \quad (\text{II.2})$$

Here, the first factor containing the external $A_\mu^{ext.}$ is the Schwinger line integral [28] and $S(x-y)$ is a translationally invariant part, whose Fourier transform is given by

$$\begin{aligned} \tilde{S}(k) = & i \int_0^\infty ds e^{-ism^2} \exp \left(is \left[k_\parallel^2 - \frac{k_\perp^2}{eBs \cot(eBs)} \right] \right) \\ & \times \left\{ \left(m + \gamma^\parallel \cdot \mathbf{k}_\parallel \right) \left(1 + \gamma^1 \gamma^2 \tan(eBs) \right) - \gamma^\perp \cdot \mathbf{k}_\perp \left(1 + \tan^2(eBs) \right) \right\}. \end{aligned} \quad (\text{II.3})$$

Here, $\mathbf{k}_\parallel = (k_0, k_3)$ and $\gamma_\parallel = (\gamma_0, \gamma_3)$ and $\mathbf{k}_\perp = (k_1, k_2)$ and $\gamma_\perp = (\gamma_1, \gamma_2)$. After performing the integral over s , $\tilde{S}(k)$ can be decomposed in Landau levels, that are labeled by n

$$\tilde{S}(k) = ie^{-\frac{\mathbf{k}_\perp^2}{|eB|}} \sum_{n=0}^\infty (-1)^n \frac{D_n(eB, k)}{k_\parallel^2 - m^2 - 2|eB|n}. \quad (\text{II.4})$$

Here, $D_n(eB, k)$ are expressed through the generalized Laguerre polynomials L_m^α as

$$D_n(eB, k) = (\gamma^\parallel \cdot \mathbf{k}_\parallel + m) \left\{ 2 \mathcal{O} \left[L_n(2\rho) - L_{n-1}(2\rho) \right] + 4\gamma^\perp \cdot \mathbf{k}_\perp L_{n-1}^{(1)}(2\rho) \right\}, \quad (\text{II.5})$$

where we have introduced $\rho \equiv \frac{k_\perp^2}{|eB|}$ and

$$\mathcal{O} \equiv \frac{1}{2} (1 - i\gamma^1 \gamma^2 \text{sign}(eB)).$$

Relation (II.5) suggests that in the IR region, with $|\mathbf{k}_\parallel|, |\mathbf{k}_\perp| \ll \sqrt{|eB|}$, all the higher Landau levels with $n \geq 1$ decouple and only the LLL with $n = 0$ is relevant. In strong magnetic field limit, the free fermion propagator (II.3) can therefore be decomposed into two independent transverse and longitudinal parts [20, 22]

$$\bar{S}_{\text{LLL}}(x, y) = \bar{S}_\parallel(\mathbf{x}_\parallel - \mathbf{y}_\parallel) P(\mathbf{x}_\perp, \mathbf{y}_\perp), \quad (\text{II.6})$$

with the longitudinal part

$$\bar{S}_\parallel(\mathbf{x}_\parallel - \mathbf{y}_\parallel) = \int \frac{d^2 k_\parallel}{(2\pi)^2} e^{i\mathbf{k}_\parallel \cdot (\mathbf{x} - \mathbf{y})^\parallel} \frac{i\mathcal{O}}{\gamma^\parallel \cdot \mathbf{k}_\parallel - m}, \quad (\text{II.7})$$

and the transverse part

$$P(\mathbf{x}_\perp, \mathbf{y}_\perp) = \frac{|eB|}{2\pi} \exp \left(\frac{ieB}{2} \epsilon^{ab} x^a y^b - \frac{|eB|}{4} (\mathbf{x}_\perp - \mathbf{y}_\perp)^2 \right), \quad a, b = 1, 2. \quad (\text{II.8})$$

As for the photon propagator $\mathcal{D}_{\mu\nu}$ of QED in an external constant magnetic field, it is calculated explicitly in [20, 22, 29] in the LLL at one-loop level. It is given by

$$i\mathcal{D}_{\mu\nu}(q) = \frac{g_{\mu\nu}^\perp}{q^2} + \frac{q_\mu^\parallel q_\nu^\parallel}{q^2 q_\parallel^2} + \frac{(g_{\mu\nu}^\parallel - q_\mu^\parallel q_\nu^\parallel / q_\parallel^2)}{q^2 + q_\parallel^2 \Pi(q_\perp^2, q_\parallel^2)} - \xi \frac{q_\mu q_\nu}{(q^2)^2}, \quad (\text{II.9})$$

where ξ is an arbitrary gauge parameter. Since the LLL fermions couple only to the longitudinal (0, 3) components of the photon fields, no polarization effects are present in the transverse (1, 2) components of

$\mathcal{D}_{\mu\nu}(q)$. Therefore, the photon propagator in the LLL approximation including the one-loop correction is given by the Feynman-like covariant propagator [20, 22]

$$i\tilde{\mathcal{D}}_{\mu\nu}(q) = \frac{g_{\mu\nu}^{\parallel}}{q^2 + \mathbf{q}_{\parallel}^2 \Pi(\mathbf{q}_{\parallel}^2, \mathbf{q}_{\perp}^2)}, \quad (\text{II.10})$$

with $\Pi(q_{\perp}^2, q_{\parallel}^2)$ having the form [30]

$$\Pi(q_{\perp}^2, q_{\parallel}^2) = \frac{2\alpha|eB|N_f}{\mathbf{q}_{\parallel}^2} e^{-\frac{q_{\parallel}^2}{2|eB|}} H\left(\frac{\mathbf{q}_{\parallel}^2}{4m_{dyn.}^2}\right), \quad (\text{II.11})$$

where N_f is the number of fermion flavors. Here, $H(z)$ is defined by

$$H(z) \equiv \frac{1}{2\sqrt{z(z-1)}} \ln\left(\frac{\sqrt{1-z} + \sqrt{-z}}{\sqrt{1-z} - \sqrt{-z}}\right) - 1. \quad (\text{II.12})$$

Expanding this expression for $|\mathbf{q}_{\parallel}^2| \ll m_{dyn.}^2 \ll |eB|$ and $m_{dyn.}^2 \ll |\mathbf{q}_{\parallel}^2| \ll |eB|$, we arrive at

$$\Pi(\mathbf{q}_{\perp}^2, \mathbf{q}_{\parallel}^2) \simeq +\frac{\alpha|eB|N_f}{3\pi m_{dyn.}^2} e^{-\frac{q_{\parallel}^2}{2|eB|}} \quad \text{for} \quad |\mathbf{q}_{\parallel}^2| \ll m_{dyn.}^2 \ll |eB|, \quad (\text{II.13})$$

$$\Pi(\mathbf{q}_{\perp}^2, \mathbf{q}_{\parallel}^2) \simeq -\frac{2\alpha|eB|N_f}{\pi \mathbf{q}_{\parallel}^2} e^{-\frac{q_{\parallel}^2}{2|eB|}} \quad \text{for} \quad m_{dyn.}^2 \ll |\mathbf{q}_{\parallel}^2| \ll |eB|. \quad (\text{II.14})$$

In [20, 22], it is shown that the kinematic region mostly responsible for generating the fermion mass is with the dynamical mass, $m_{dyn.}$, satisfying $m_{dyn.}^2 \ll |\mathbf{q}_{\parallel}^2| \ll |eB|$. Plugging (II.14) in the photon propagator (II.10) and assuming that $|\mathbf{q}_{\perp}^2| \ll |eB|$, we get

$$\tilde{\mathcal{D}}_{\mu\nu}(q) \approx -\frac{ig_{\mu\nu}^{\parallel}}{q^2 - M_{\gamma}^2}, \quad \text{with} \quad M_{\gamma}^2 = \frac{2\alpha|eB|N_f}{\pi}, \quad (\text{II.15})$$

where M_{γ} is the finite photon mass, whose appearance is the result of the dimensional reduction $3+1 \rightarrow 1+1$ in the presence of a constant magnetic field.

The dynamically generated fermion mass in the LLL approximation is determined in [20] by solving the ladder Bethe-Salpeter (BS) equation in the LLL approximation. It is given by

$$m_{dyn.}^{(1)} = C\sqrt{eB} \exp\left(-\sqrt{\frac{\pi}{\alpha}}\right), \quad (\text{II.16})$$

where the constant C is of order one. In [31], the same result is determined by solving the corresponding SD equation in the ladder LLL approximation. In both methods, to determine (II.16) in the ladder approximation, the free fermion propagator in the LLL approximation (II.6)-(II.8) with $m = m_{dyn.}$ is used. In this approximation, the full photon propagator are also replaced by free photon propagator in the covariant Feynman gauge

$$D_{\mu\nu}^{(0)}(q) = -\frac{ig_{\mu\nu}}{q^2} \quad (\text{II.17})$$

In [21] two-loop contribution to the corresponding SD equation arising from composite effective action à la Cornwall-Jackiw-Tomboulis [32] in LLL approximation is considered. Here, the full fermion propagator

in the LLL and the full photon propagator in a covariant and a non-covariant gauge is taken into account in the two-loop level. In the improved rainbow approximation, defined by the photon propagator in a non-covariant gauge, the expression for $m_{dyn.}$ takes the following form [21]

$$m_{dyn.} = \tilde{C} \sqrt{|eB|} F(\alpha) \exp \left(-\frac{\pi}{\alpha \ln(C_1/\alpha N_f)} \right), \quad (\text{II.18})$$

where $F(\alpha) \simeq (N_f \alpha)^{1/3}$, $C_1 \simeq 1.82 \pm 0.06$ and $\tilde{C} \sim O(1)$.

In this paper, we work with fermion and photon propagators at finite temperature. To find the free fermion propagator at finite temperature, we will turn into the Euclidean space by replacing $s \rightarrow -is$ and $k_0 \rightarrow i\hat{\omega}_\ell$ in (II.3) and find [16]

$$S_\ell(\vec{k}) = -i \int_0^\infty ds e^{-s(\hat{\omega}_\ell^2 + k_3^2 + \mathbf{k}_\perp^2 \frac{\tanh(|eB|s)}{|eB|s} + m^2)} \times [(-\hat{\omega}_\ell \gamma^4 - k^3 \gamma^3 + m)(1 - i\gamma^1 \gamma^2 \tanh(|eB|s)) - \gamma^\perp \cdot \mathbf{k}_\perp (1 - \tanh^2(|eB|s))]. \quad (\text{II.19})$$

In the following, we indicate the Matsubara frequencies in the fermionic case with $\hat{\omega}_\ell \equiv (2\ell + 1)\pi T$ and those in the bosonic case by $\omega_n \equiv 2n\pi T$. Next, the free photon propagator $D_{\mu\nu}^{(0)}(k)$ and the full photon propagator $\mathcal{D}_{\mu\nu}(k)$ in a constant magnetic field and at finite temperature are given by [15]

$$\begin{aligned} D_{\mu\nu}^{(0)}(k_0, \mathbf{k}) &= -\sum_{i=1}^4 \frac{1}{k_E^2} \frac{b_\mu^{(i)} b_\nu^{\star(i)}}{\left(b_\rho^{(i)} b^{\star\rho(i)}\right)}, \\ \mathcal{D}_{\mu\nu}(k_0, \mathbf{k}) &= -\sum_{i=1}^4 \frac{1}{(k_E^2 + \kappa_i(k_0, \mathbf{k}))} \frac{b_\mu^{(i)} b_\nu^{\star(i)}}{\left(b_\rho^{(i)} b^{\star\rho(i)}\right)}, \end{aligned} \quad (\text{II.20})$$

where κ_i and $b_\mu^{(i)}$ are eigenvalue and eigenfunctions of the vacuum polarization tensor $\Pi_{\mu\nu}$, *i.e.*

$$\Pi_{\mu\nu}(k) b_\nu^{(i)} = \kappa_i(k) b_\mu^{(i)}. \quad (\text{II.21})$$

In (II.20) k_E is the Euclidean four-momentum and $k_E^2 \equiv 4\pi^2 n^2 T^2 + \mathbf{k}^2$. In the next paragraph, we will determine $\kappa_i(k)$ in the IR limit *i.e.* for $k_0 \rightarrow 0$ ($n = 0$) but finite \mathbf{k} . Then, using the eigenfunctions $b_\mu^{(i)}$, QED vacuum polarization tensor $\Pi_{\mu\nu}(k_0, \mathbf{k})$ will be diagonalized and eventually determined in the IR limit.

B. QED vacuum polarization tensor in a constant magnetic field at finite temperature

In [15] it is shown that the vacuum polarization tensor $\Pi_{\mu\nu}$ in the presence of external magnetic field and at finite temperature can be diagonalized as

$$\Pi_{\mu\nu}(k_0, \mathbf{k}) = \sum_{i=1}^4 \kappa_i(k_0, \mathbf{k}) \frac{b_\mu^{(i)} b_\nu^{\star(i)}}{\left(b_\rho^{(i)} b^{\star\rho(i)}\right)}, \quad (\text{II.22})$$

where κ_i and $b_\mu^{(i)}$ are defined in (II.21). This relation can be proved by plugging it back in (II.21) and using the property $b_\mu^{(i)} b^{\star\mu(j)} = 0$, $\forall i \neq j$. According to the results in [15], the eigenvalues κ_i in the

Minkowski space are given by

$$\begin{aligned}\kappa_{1,2}(k_0, \mathbf{k}) &= \frac{1}{2} \left\{ P + S \pm [(P - S)^2 - 4Q^2]^{1/2} \right\}, \\ \kappa_3(k_0, \mathbf{k}) &= R, \quad \kappa_4(k_0, \mathbf{k}) = 0,\end{aligned}\tag{II.23}$$

with

$$\begin{aligned}P(k_0, \mathbf{k}) &\equiv k^2 \pi_1 + \left(k \cdot \tilde{F}^2 \cdot k \right) \pi_3 - \frac{(u \cdot k)^2 (k \cdot F^2 \cdot k)}{(k \cdot \tilde{F}^2 \cdot k)} \pi_4 \\ Q(k_0, \mathbf{k}) &\equiv \frac{(u \cdot k)(u \cdot \tilde{F} \cdot k)}{(k \cdot \tilde{F}^2 \cdot k)} \left(-\frac{k \cdot F^2 \cdot k}{k^2} \right)^{1/2} \pi_4 \\ S(k_0, \mathbf{k}) &\equiv k^2 \pi_1 - \frac{(u \cdot \tilde{F} \cdot k)^2}{(k \cdot \tilde{F}^2 \cdot k)} \pi_4 \\ R(k_0, \mathbf{k}) &\equiv k^2 \pi_1 - (k \cdot F^2 \cdot k) \pi_2 + 2 \mathcal{F} k^2 \pi_3,\end{aligned}\tag{II.24}$$

where the notation $a \cdot b \equiv a_\mu b^\mu$ is used. Here, $F_{\mu\nu}$ is the field strength tensor, $\tilde{F}_{\mu\nu}$ the dual tensor $\tilde{F}_{\mu\nu} \equiv \frac{1}{2} \epsilon_{\mu\nu\rho\sigma} F^{\rho\sigma}$, $u \equiv (1, 0, 0, 0)$ the rest frame vector in the Minkowski space, $k^2 \equiv k_0^2 - \mathbf{k}^2$ and $\mathcal{F} \equiv -\frac{1}{4} F_{\mu\rho} F^{\rho\mu}$. Assuming that there exists only a magnetic field $B_\ell = \frac{1}{2} \epsilon_{\ell mn} F^{mn}$ directed along the 3-axis (*i.e.* $\mathbf{B} = B \mathbf{e}_3$), we get $F_{12} = -F_{21} = B$. The other components of $F_{\mu\nu}$ vanish. For the dual tensor $\tilde{F}_{\mu\nu}$ only the components $\tilde{F}_{03} = -\tilde{F}_{30} = B$ survive.

Considering again (II.24), $\pi_i, i = 1, 2, 3, 4$, are the coefficients of the expansion of $\Pi_{\mu\nu}$ as a second rank tensor in certain basis $\Psi_{\mu\nu}^{(i)}$ [15]

$$\Pi_{\mu\nu}(k_0, \mathbf{k}) = \sum_{i=1}^4 \pi_i \left((u \cdot k)^2, k \cdot F^2 \cdot k, \mathcal{F}, k^2 \right) \Psi_{\mu\nu}^{(i)},\tag{II.25}$$

where the basis $\Psi_{\mu\nu}^{(i)}$ are second rank tensors, that are built up from four vectors $k_\mu, F_{\mu\rho} k^\rho, F_{\rho\mu} F^{\mu\nu} k_\nu$, and u_μ .⁹ They are given by

$$\begin{aligned}\Psi_{\mu\nu}^{(1)}(k_0, \mathbf{k}) &= k^2 g_{\mu\nu} - k_\mu k_\nu, \\ \Psi_{\mu\nu}^{(2)}(k_0, \mathbf{k}) &= F_{\mu\lambda} k^\lambda F_{\nu\sigma} k^\sigma, \\ \Psi_{\mu\nu}^{(3)}(k_0, \mathbf{k}) &= -k^2 \left(g_{\mu\lambda} - \frac{k_\mu k_\lambda}{k^2} \right) F_\rho^\lambda F^{\rho\eta} \left(g_{\eta\nu} - \frac{k_\eta k_\nu}{k^2} \right), \\ \Psi_{\mu\nu}^{(4)}(k_0, \mathbf{k}) &= \left(u_\mu - \frac{k_\mu (u \cdot k)}{k^2} \right) \left(u_\nu - \frac{k_\nu (u \cdot k)}{k^2} \right),\end{aligned}\tag{II.26}$$

where $\Psi_{\mu\nu}^{(i)}, i = 1, \dots, 4$ satisfy $\Psi_{\mu\nu}^{(i)} = \Psi_{\nu\mu}^{(i)}, \forall i$. It is the purpose of this section to determine P, Q, S and R from (II.24) and eventually $\kappa_i, i = 1, \dots, 4$ from (II.23) in the IR limit where k_0 is taken to zero but \mathbf{k} is nonvanishing. This will enable us to determine the ring contribution of the effective potential in the IR limit. To do this we have to determine $\pi_i, i = 1, \dots, 4$ from (II.25) explicitly. Multiplying (II.25) with $\Psi_{\nu\sigma}^{(j)}$ and adding over ν , we arrive at

$$\mathcal{P}^j = \sum_{i=1}^4 \mathcal{A}^{ji} \pi^i,\tag{II.27}$$

⁹ In Minkowskian space there are indeed 16 independent tensors $\Psi_{\mu\nu}^{(i)}$. But, as it is shown in [15], for zero chemical potential and due to symmetry properties only $\Psi_{\mu\nu}^{(i)}, i = 1, \dots, 4$ from (II.26) are nonvanishing.

where $\mathcal{P}^j \equiv \Pi^{\mu\nu} \Psi_{\nu\mu}^{(j)}$ and $\mathcal{A}^{ij} \equiv \Psi^{(i)\mu\nu} \Psi_{\nu\mu}^{(j)}$. To calculate π_i , we consider (II.27) first as a generic system of equations in terms of generic \mathcal{P}^j and \mathcal{A}^{ji} . Solving this system of equations π_i are given by

$$\begin{aligned}
\pi_1 &= \frac{\mathcal{P}_1}{Y} (A_{22}A_{34}^2 + A_{23}^2A_{44} - A_{22}A_{33}A_{44}) + \frac{\mathcal{P}_2}{Y} (A_{14}A_{23}A_{34} - A_{12}A_{34}^2 - A_{13}A_{23}A_{44} + A_{12}A_{33}A_{44}) \\
&\quad + \frac{\mathcal{P}_3}{Y} (-A_{22}(A_{14}A_{34} - A_{13}A_{44}) - A_{12}A_{23}A_{44}) + \frac{\mathcal{P}_4}{Y} (-A_{14}A_{23}^2 + A_{22}(A_{14}A_{33} - A_{13}A_{34}) + A_{12}A_{23}A_{34}), \\
\pi_2 &= \frac{\mathcal{P}_1}{Y} (-A_{14}A_{23}A_{34} + A_{13}A_{23}A_{44} + A_{12}(A_{34}^2 - A_{33}A_{44})) + \frac{\mathcal{P}_2}{Y} (-A_{14}(A_{14}A_{33} - 2A_{13}A_{34}) - A_{13}^2A_{44} \\
&\quad - A_{11}(A_{34}^2 - A_{33}A_{44})) + \frac{\mathcal{P}_3}{Y} (A_{14}^2A_{23} - A_{12}(A_{14}A_{34} - A_{13}A_{44}) - A_{11}A_{23}A_{44}) \\
&\quad + \frac{\mathcal{P}_4}{Y} (A_{12}A_{14}A_{33} + A_{11}A_{23}A_{34} - A_{13}(A_{14}A_{23} + A_{12}A_{34})), \\
\pi_3 &= \frac{\mathcal{P}_1}{Y} (A_{22}(A_{14}A_{34} - A_{13}A_{44}) + A_{12}A_{23}A_{44}) + \frac{\mathcal{P}_2}{Y} (A_{14}(A_{14}A_{23} - A_{12}A_{34}) + A_{44}(A_{12}A_{13} - A_{11}A_{23})) \\
&\quad - \frac{\mathcal{P}_3}{Y} (A_{14}^2A_{22} + A_{44}(A_{12}^2 - A_{11}A_{22})) + \frac{\mathcal{P}_4}{Y} (A_{14}(A_{13}A_{22} - A_{12}A_{23}) + A_{34}(A_{12}^2 - A_{11}A_{22})), \\
\pi_4 &= \frac{\mathcal{P}_1}{Y} (A_{14}(-A_{23}^2 + A_{22}A_{33}) + A_{34}(-A_{13}A_{22} + A_{12}A_{23})) + \frac{\mathcal{P}_2}{Y} (A_{14}(A_{13}A_{23} - A_{12}A_{33}) + \\
&\quad A_{34}(A_{12}A_{13} - A_{11}A_{23})) + \frac{\mathcal{P}_3}{Y} (A_{14}(-A_{13}A_{22} + A_{12}A_{23}) + A_{34}(-A_{12}^2 + A_{11}A_{22})) \\
&\quad + \frac{\mathcal{P}_4}{Y} (A_{13}^2A_{22} + A_{12}(-2A_{13}A_{23} + A_{12}A_{33}) + A_{11}(A_{23}^2 - A_{22}A_{33})), \tag{II.28}
\end{aligned}$$

with the denominator

$$\begin{aligned}
Y &= - \left[A_{14}^2 (A_{23}^2 - A_{22}A_{33}) + 2A_{14}A_{34} (A_{13}A_{22} - A_{12}A_{23}) - A_{11}A_{22}A_{34}^2 - A_{13}^2A_{22}A_{44} \right. \\
&\quad \left. + 2A_{12}A_{13}A_{23}A_{44} - A_{11}A_{23}^2A_{44} + A_{11}A_{22}A_{33}A_{44} + A_{12}^2 (A_{34}^2 - A_{33}A_{44}) \right].
\end{aligned}$$

As next we have to calculate \mathcal{A}^{ij} and \mathcal{P}^j from (II.27). Here, \mathcal{A}^{ij} can be determined using the $\Psi_{\mu\nu}^{(i)}$ from (II.26). They are given by

$$\begin{aligned}
\mathcal{A}^{11} &= 3(k^2)^2, \\
\mathcal{A}^{12} &= -k^2 (k \cdot F^2 \cdot k) = -B^2 k^2 \mathbf{k}_\perp^2, \\
\mathcal{A}^{13} &= -(k^2)^2 \text{tr}(F^2) + k^2 (k \cdot F^2 \cdot k) = B^2 k^2 (2k^2 + \mathbf{k}_\perp^2), \\
\mathcal{A}^{14} &= k^2 u^2 - (u \cdot k)^2 = -\mathbf{k}^2, \\
\mathcal{A}^{22} &= (k \cdot F^2 \cdot k)^2 = B^4 (\mathbf{k}_\perp^2)^2, \\
\mathcal{A}^{23} &= k^2 (k \cdot F^4 \cdot k) = -B^4 k^2 \mathbf{k}_\perp^2, \\
\mathcal{A}^{24} &= 0, \\
\mathcal{A}^{33} &= (k^2)^2 \text{tr}(F^4) - 2k^2 (k \cdot F^4 \cdot k) + (k \cdot F^2 \cdot k)^2 = B^4 (2(k^2)^2 + 2k^2 \mathbf{k}_\perp^2 + (\mathbf{k}_\perp^2)^2), \\
A^{34} &= -\frac{(k \cdot F^2 \cdot k)(u \cdot k)^2}{k^2} = -\frac{B^2 k_0^2 \mathbf{k}_\perp^2}{k^2}, \\
\mathcal{A}^{44} &= 1 - \frac{2(u \cdot k)^2}{k^2} + \frac{(u \cdot k)^4}{(k^2)^2} = 1 - \frac{2k_0^2}{k^2} + \frac{k_0^4}{(k^2)^2}, \tag{II.29}
\end{aligned}$$

where the rest frame constraint $u_\mu F^{\mu\nu} = 0$ and the following relations are used

$$k \cdot F \cdot k = 0, \quad k \cdot F^2 \cdot k = B^2 \mathbf{k}_\perp^2, \quad k \cdot F^4 \cdot k = -B^4 \mathbf{k}_\perp^2, \quad \text{tr}(F^2) = -2B^2, \quad \text{tr}(F^4) = 2B^4.$$

Other components of \mathcal{A}^{ij} are determined by the symmetry property $\mathcal{A}^{ji} = \mathcal{A}^{ij}$. To determine \mathcal{P}^j from (II.27), we use $\Psi_{\mu\nu}^{(i)}$ from (II.26) and $k_\mu \Pi^{\mu\nu} = 0$ to get

$$\begin{aligned}\mathcal{P}_1 &= k^2 \text{tr}(\Pi) = k^2 \left(\Pi_{00} - \sum_{i=1}^3 \Pi_{ii} \right), \\ \mathcal{P}_2 &= -k \cdot F \cdot \Pi \cdot F \cdot k = B^2 (-k_1 k_2 \Pi_{21} + k_1^2 \Pi_{22} + k_2^2 \Pi_{11} - k_1 k_2 \Pi_{12}), \\ \mathcal{P}_3 &= -k^2 \text{tr}(\Pi \cdot F^2) = -B^2 k^2 (\Pi_{11} + \Pi_{22}), \\ \mathcal{P}_4 &= u \cdot \Pi \cdot u = \Pi_{00}.\end{aligned}\tag{II.30}$$

The components of QED vacuum polarization tensor $\Pi_{\mu\nu}$ in a magnetic field at finite temperature are explicitly calculated in [16] using the Schwinger proper-time formalism [28].¹⁰ To determine \mathcal{P}^j we need only the components $\Pi_{\mu\mu}(n, \mathbf{k})$ with $\mu = 1, \dots, 4$, and $\Pi_{12}(n, \mathbf{k})$ of the vacuum polarization tensor. In the Euclidean space, they are given by

$$\begin{aligned}\Pi_{ii}(n, \mathbf{k}) &= \frac{-\alpha T e B}{\sqrt{\pi}} \int_{\frac{1}{\Lambda^2}}^{\infty} du \sqrt{u} \int_{-1}^{+1} dv \sum_{\ell=-\infty}^{\infty} e^{\phi_n(u, v; \ell)} \left[\omega_n W_{\ell n} \coth \bar{u} \frac{\sinh \bar{u} v}{\sinh \bar{u}} \right. \\ &\quad \left. + (k_\perp^2 - k_i^2) \frac{(\cosh \bar{u} - \cosh \bar{u} v)}{\sinh^3 \bar{u}} + \frac{(\omega_n^2 + k_3^2)}{2} \frac{(\cosh \bar{u} v - v \coth \bar{u} \sinh \bar{u} v)}{\sinh \bar{u}} \right], \quad i = 1, 2, \\ \Pi_{33}(n, \mathbf{k}) &= \frac{-\alpha T e B}{\sqrt{\pi}} \int_{\frac{1}{\Lambda^2}}^{\infty} du \sqrt{u} \int_{-1}^{+1} dv \sum_{\ell=-\infty}^{\infty} e^{\phi_n(u, v; \ell)} \\ &\quad \times \left[v \omega_n W_{\ell n} \coth \bar{u} + \frac{k_\perp^2}{2} \frac{(\cosh \bar{u} v - v \coth \bar{u} \sinh \bar{u} v)}{\sinh \bar{u}} + \omega_n^2 \frac{(1 - v^2)}{2} \coth \bar{u} \right], \\ \Pi_{44}(n, \mathbf{k}) &= -\frac{\alpha T e B}{\sqrt{\pi}} \int_{\frac{1}{\Lambda^2}}^{\infty} du \sqrt{u} \int_{-1}^{+1} dv \sum_{\ell=-\infty}^{+\infty} e^{\phi_n(u, v; \ell)} \\ &\quad \times \left[\frac{k_\perp^2}{2} \frac{(\cosh \bar{u} v - v \coth \bar{u} \sinh \bar{u} v)}{\sinh \bar{u}} - \coth \bar{u} \left(\frac{1}{u} - 2W_{\ell n}^2 + v \omega_n W_{\ell n} - \frac{(1 - v^2)}{2} k_3^2 \right) \right], \\ \Pi_{12}(n, \mathbf{k}) &= +\frac{\alpha T e B}{\sqrt{\pi}} \int_{\frac{1}{\Lambda^2}}^{\infty} du \sqrt{u} \int_{-1}^{+1} dv \sum_{\ell=-\infty}^{+\infty} e^{\phi_n(u, v; \ell)} k_1 k_2 \frac{(\cosh \bar{u} - \cosh \bar{u} v)}{\sinh^3 \bar{u}},\end{aligned}\tag{II.31}$$

where $\mathbf{k}_\perp \equiv (k_1, k_2)$, $\bar{u} \equiv ueB$ and $\phi_n(u, v; \ell)$ is defined by

$$\phi_n(u, v; \ell) \equiv -\frac{k_\perp^2}{eB} \frac{(\cosh \bar{u} - \cosh \bar{u} v)}{2 \sinh \bar{u}} - u \left[m^2 + W_{\ell n}^2 + \frac{(1 - v^2)}{4} (\omega_n^2 + k_3^2) \right].$$

In all the above expressions $W_{\ell n} \equiv \hat{\omega}_\ell - \frac{1-v}{2} \omega_n$, where $\hat{\omega}_\ell$ and ω_n are the Matsubara frequencies of the fermionic and bosonic fields, respectively.¹¹ In the IR limit $n = 0$ (or equivalently $k_0 \rightarrow 0$) they are given

¹⁰ To determine the vacuum polarization tensor $\Pi_{\mu\nu}$ in the Schwinger proper-time formalism, it is enough to replace the free fermion propagator in ordinary $\Pi_{\mu\nu}$ by the free fermion propagator in the constant background magnetic field arising from Schwinger proper-time formalism. At finite temperature, this is done in [16] to determine $\Pi_{\mu\nu}$.

¹¹ Note that compared to the results in [16], there are some temperature independent contact terms missing in the above expression. We will omit them here, keeping in mind that they are relevant only to cancel temperature independent imaginary terms in Sect. III.A.

by

$$\begin{aligned}
\Pi^{11}(n=0, \mathbf{k}) &= 2k_2^2 I_4 + k_3^2 I_1, \\
\Pi^{22}(n=0, \mathbf{k}) &= 2k_1^2 I_4 + k_3^2 I_1, \\
\Pi^{33}(n=0, \mathbf{k}) &= \mathbf{k}_\perp^2 I_1, \\
\Pi^{44}(n=0, \mathbf{k}) &= \mathbf{k}_\perp^2 I_1 + k_3^2 I_3 - I_2, \\
\Pi^{12}(n=0, \mathbf{k}) &= -2k_1 k_2 I_4,
\end{aligned} \tag{II.32}$$

where the integrals $I_i, i = 1, \dots, 4$ can be determined using (II.31) with $n = 0$. For future purposes, we will separate $I_i, i = 1, \dots, 4$ in a temperature independent part I_i^0 and a temperature dependent part I_i^T . This can be done using the Poisson resummation formula

$$\sum_{\ell=-\infty}^{\infty} e^{-a(\ell-z)^2} = \left(\frac{\pi}{a}\right)^{1/2} \sum_{\ell=-\infty}^{\infty} \exp\left(-\frac{\pi^2 \ell^2}{a} - 2i\pi z \ell\right),$$

that leads to

$$\sum_{\ell=-\infty}^{+\infty} e^{-u W_{\ell 0}^2} = \frac{1}{T\sqrt{\pi u}} \sum_{\ell \geq 1} (-1)^\ell e^{-\frac{\ell^2}{4uT^2}} + \frac{1}{2T\sqrt{\pi u}},$$

and

$$\sum_{\ell=-\infty}^{+\infty} \left(-2W_{\ell 0}^2 + \frac{1}{u}\right) e^{-u W_{\ell 0}^2} = \frac{1}{2T\sqrt{\pi}} \sum_{\ell \geq 1} (-1)^\ell \frac{1}{u^{5/2}} \frac{\ell^2}{T^2} e^{-\frac{\ell^2}{4uT^2}}.$$

We arrive therefore at $I_i = I_i^0 + I_i^T, i = 1, \dots, 4$ with¹²

$$\begin{aligned}
I_1^0 &= -\frac{\alpha e B}{4\pi} \int_{\frac{1}{\Lambda^2}}^{\infty} du \int_{-1}^{+1} dv e^{\phi(u,v)} \frac{(\cosh \bar{u} v - v \coth \bar{u} \sinh \bar{u} v)}{\sinh \bar{u}}, \\
I_1^T &= -\frac{\alpha e B}{2\pi} \int_0^{\infty} du \int_{-1}^{+1} dv e^{\phi(u,v)} \sum_{\ell=1}^{\infty} (-1)^\ell e^{-\frac{\ell^2}{4uT^2}} \frac{(\cosh \bar{u} v - v \coth \bar{u} \sinh \bar{u} v)}{\sinh \bar{u}}, \\
I_2^0 &= 0, \\
I_2^T &= -\frac{\alpha e B}{2\pi} \int_0^{\infty} du \int_{-1}^{+1} dv e^{\phi(u,v)} \sum_{\ell=1}^{\infty} (-1)^\ell \frac{\ell^2}{T^2} e^{-\frac{\ell^2}{4uT^2}} \frac{\coth \bar{u}}{u^2}, \\
I_3^0 &= -\frac{\alpha e B}{4\pi} \int_{\frac{1}{\Lambda^2}}^{\infty} du \int_{-1}^{+1} dv e^{\phi(u,v)} (1-v^2) \coth \bar{u}, \\
I_3^T &= -\frac{\alpha e B}{2\pi} \int_0^{\infty} du \int_{-1}^{+1} dv e^{\phi(u,v)} \sum_{\ell=1}^{\infty} (-1)^\ell e^{-\frac{\ell^2}{4uT^2}} (1-v^2) \coth \bar{u}, \\
I_4^0 &= -\frac{\alpha e B}{4\pi} \int_{\frac{1}{\Lambda^2}}^{\infty} du \int_{-1}^{+1} dv e^{\phi(u,v)} \frac{(\cosh \bar{u} - \cosh \bar{u} v)}{\sinh^3 \bar{u}}, \\
I_4^T &= -\frac{\alpha e B}{2\pi} \int_0^{\infty} du \int_{-1}^{+1} dv e^{\phi(u,v)} \sum_{\ell=1}^{\infty} (-1)^\ell e^{-\frac{\ell^2}{4uT^2}} \frac{(\cosh \bar{u} - \cosh \bar{u} v)}{\sinh^3 \bar{u}},
\end{aligned} \tag{II.33}$$

¹² In [16], a similar method is used to separate Π_{44} into a temperature dependent and a temperature independent part.

where $\phi(u, v) \equiv \phi_0(u, v; \ell) + uW_{\ell 0}^2$. Plugging now $\Pi^{\mu\nu}(n=0, \mathbf{k})$ from (II.32) in (II.30), $\mathcal{P}_i, i=1, \dots, 4$ in the IR limit are given by

$$\begin{aligned}\mathcal{P}_1(k_0 \rightarrow 0, \mathbf{k}) &= \mathbf{k}^2(2\mathbf{k}_\perp^2 I_1 + 2\mathbf{k}_\perp^2 I_4 + k_3^2 I_3 - I_2), \\ \mathcal{P}_2(k_0 \rightarrow 0, \mathbf{k}) &= B^2 \mathbf{k}_\perp^2 (2\mathbf{k}_\perp^2 I_4 + k_3^2 I_1), \\ \mathcal{P}_3(k_0 \rightarrow 0, \mathbf{k}) &= +B^2 \mathbf{k}^2 (2k_3^2 I_1 + 2\mathbf{k}_\perp^2 I_4), \\ \mathcal{P}_4(k_0 \rightarrow 0, \mathbf{k}) &= -\mathbf{k}_\perp^2 I_1 - k_3^2 I_3 + I_2.\end{aligned}\tag{II.34}$$

Plugging further \mathcal{A}^{ji} from (II.29) and \mathcal{P}^j from (II.34) in (II.28) and taking carefully the limit $k_0 \rightarrow 0$, $\pi_i, i=1, \dots, 4$ can be determined in the IR limit. They are given by

$$\begin{aligned}\pi_1 &= \frac{I_1(k_3^2 \mathbf{k}_\perp^2 + 3\mathbf{k}_\perp^4) + I_2(2k_3^2 - \mathbf{k}_\perp^2) + I_3(k_3^2 \mathbf{k}_\perp^2 - 2k_3^4) + 2I_4 \mathbf{k}_\perp^4}{2\mathbf{k}_\perp^2 \mathbf{k}^2}, \\ \pi_2 &= \frac{I_1(\mathbf{k}_\perp^4 - 3k_3^2 \mathbf{k}_\perp^2) + I_2(2k_3^2 - \mathbf{k}_\perp^2) + I_3(k_3^2 \mathbf{k}_\perp^2 - 2k_3^4) + I_4(4k_3^2 \mathbf{k}_\perp^2 + 2\mathbf{k}_\perp^4)}{2B^2 k_3^2 \mathbf{k}_\perp^2}, \\ \pi_3 &= \frac{I_1(k_3^2 \mathbf{k}_\perp^2 - \mathbf{k}_\perp^4) + I_2(\mathbf{k}_\perp^2 - 2k_3^2) + I_3(2k_3^4 - k_3^2 \mathbf{k}_\perp^2) - 2I_4 \mathbf{k}_\perp^4}{2B^2 k_3^2 \mathbf{k}_\perp^2}, \\ \pi_4 &= \frac{I_1(k_3^2 \mathbf{k}_\perp^2 + \mathbf{k}_\perp^4) + I_2(2k_3^2 + \mathbf{k}_\perp^2) - I_3(2k_3^4 + k_3^2 \mathbf{k}_\perp^2) + 2I_4 \mathbf{k}_\perp^4}{2\mathbf{k}_\perp^2},\end{aligned}\tag{II.35}$$

where $I_i = I_i^0 + I_i^T, i=1, \dots, 4$ are given in (II.33). The above information are enough to determine $\kappa_i, i=1, \dots, 4$ from (II.23) in the IR limit. To do this, let us replace $\pi_i, i=1, \dots, 4$ from (II.35) in (II.24) to get

$$\begin{aligned}P(k_0 \rightarrow 0, \mathbf{k}) &= -\mathbf{k}^2 \pi_1 - B^2 k_3^2 \pi_3 = -\mathbf{k}^2 I_1 \\ Q(k_0 \rightarrow 0, \mathbf{k}) &= 0 \\ S(k_0 \rightarrow 0, \mathbf{k}) &= -\mathbf{k}^2 \pi_1 + \pi_4 = -\mathbf{k}_\perp^2 I_1 + I_2 - k_3^2 I_3 \\ R(k_0 \rightarrow 0, \mathbf{k}) &= -\mathbf{k}^2 \pi_1 - B^2 \mathbf{k}^2 \pi_3 - B^2 \mathbf{k}_\perp^2 \pi_2 = -k_3^2 I_1 - 2\mathbf{k}_\perp^2 I_4.\end{aligned}\tag{II.36}$$

Thus, in the basis of $b_\mu^{(i)}$ from (II.21), QED vacuum polarization tensor in the IR limit $k_0 \rightarrow 0$ reads

$$\Pi_{\mu\nu}(k_0 \rightarrow 0, \mathbf{k}) = \sum_{i=1}^4 \kappa_i(k_0 \rightarrow 0, \mathbf{k}) \frac{b_\mu^{(i)} b_\nu^{\star(i)}}{\left(b_\mu^{(i)} b_\mu^{\star(i)}\right)},\tag{II.37}$$

where $\kappa_i(k_0 \rightarrow 0, \mathbf{k})$ are determined by plugging (II.36) in (II.23). They are given by

$$\begin{aligned}\kappa_1(k_0 \rightarrow 0, \mathbf{k}) &= P(k_0 \rightarrow 0, \mathbf{k}), \\ \kappa_2(k_0 \rightarrow 0, \mathbf{k}) &= S(k_0 \rightarrow 0, \mathbf{k}), \\ \kappa_3(k_0 \rightarrow 0, \mathbf{k}) &= R(k_0 \rightarrow 0, \mathbf{k}), \\ \kappa_4(k_0 \rightarrow 0, \mathbf{k}) &= 0.\end{aligned}\tag{II.38}$$

In the next section (II.36)-(II.38) will be used to determine the ring potential of QED in a constant magnetic field at finite temperature.

III. QED EFFECTIVE POTENTIAL FOR $T \neq 0$ AND $B \neq 0$ BEYOND THE STATIC LIMIT

In this section QED effective potential in a constant magnetic field at finite temperature will be determined in an approximation beyond the static limit. It receives contributions from the one-loop and ring (plasmon) potentials. Let us first look at the one-loop part of the effective potential, $V^{(1)}$, which is calculated in [33] for constant magnetic field and zero chemical potential.¹³ It is given by the following integral over the Schwinger parameter s

$$V^{(1)}(m, eB; T) = -\frac{2eB}{\beta} \int_0^\infty ds \frac{\Theta_2(0|is\frac{4\pi}{\beta^2})}{(4\pi s)^{\frac{3}{2}}} \coth(seB) e^{-sm^2}. \quad (\text{III.1})$$

Here, β is the inverse of temperature $\beta \equiv \frac{1}{T}$ and

$$\Theta_2(u|\tau) \equiv 2 \sum_{n=0}^{\infty} e^{i\pi\tau(n+\frac{1}{2})^2} \cos((2n+1)u), \quad (\text{III.2})$$

is the elliptic Θ -function of second kind. The above potential can be separated into a temperature independent part, $V_0^{(1)}$, and a temperature dependent part, $V_T^{(1)}$,

$$V^{(1)}(m, eB; T) = V_0^{(1)}(m, eB; \Lambda) + V_T^{(1)}(m, eB). \quad (\text{III.3})$$

To do this, we use the identity [37]

$$\Theta_2(u|\tau) = \left(\frac{i}{\tau}\right)^{1/2} e^{-\frac{iu^2}{\pi\tau}} \Theta_4\left(\frac{u}{\tau} \middle| -\frac{1}{\tau}\right), \quad (\text{III.4})$$

where

$$\Theta_4(u|\tau) = 1 + 2 \sum_{n=1}^{\infty} (-1)^n e^{i\pi n^2 \tau} \cos(2nu), \quad (\text{III.5})$$

is the fourth Jacobian Θ -function. Using the above identities and the series expansion

$$\coth t = 1 + 2 \sum_{m=1}^{\infty} e^{-2mt},$$

the temperature independent part is given by

$$\begin{aligned} V_0^{(1)}(m, eB; \Lambda) &= -\frac{eB}{8\pi^2} \int_{\frac{1}{\Lambda^2}}^{\infty} \frac{ds}{s^2} \left[e^{-sm^2} + 2 \sum_{\ell=1}^{\infty} e^{-s(m^2+2eB\ell)} \right], \\ &= -\frac{eB}{8\pi^2} \left[m^2 \Gamma\left(-1, \frac{m^2}{\Lambda^2}\right) + 2 \sum_{\ell=1}^{\infty} (m^2 + 2eB\ell) \Gamma\left(-1, \frac{(m^2 + 2eB\ell)}{\Lambda^2}\right) \right]. \end{aligned} \quad (\text{III.6})$$

¹³ There are different equivalent methods to determine the one-loop effective potential in the presence of constant magnetic field. One of these methods is to use the Schwinger proper-time formalism [20], where the one-loop effective potential is defined by $V^{(1)} = -i\Omega^{-1} \text{Tr} \ln S^{-1}$. Here, Ω is the 4-dimensional space-time volume, and S is the free propagator of massive fermions in a constant magnetic field with m (II.2)-(II.3) [for a definition of one-loop effective potential in LLL approximation see (A.4) in Appendix A]. The same one-loop effective potential is calculated in [33] using the worldline formalism [34]. Although this method is different from the well-known Schwinger proper-time formalism, but the final result for the one-loop effective potential is the same as in the Schwinger's method (see [35] and [36] for recent example on the equivalence between these two methods).

with Λ the ultraviolet (UV) cutoff, and $\Gamma(n, z) \equiv \int_z^\infty dt t^{n-1} e^{-t}$ the incomplete Γ -function. The temperature dependent part of the one-loop effective potential (III.1) reads

$$\begin{aligned} V_T^{(1)}(m, eB) &= -\frac{eB}{4\pi^2} \sum_{n=1}^{\infty} (-1)^n \left[\int_0^\infty \frac{ds}{s^2} e^{-\left(sm^2 + \frac{n^2 \beta^2}{4s}\right)} + 2 \sum_{\ell=1}^{\infty} \int_0^\infty \frac{ds}{s^2} e^{-\left(s(m^2 + 2eB\ell) + \frac{n^2 \beta^2}{4s}\right)} \right] \\ &= -\frac{eB}{\pi^2} \sum_{n=1}^{\infty} (-1)^n \left[\frac{m}{n\beta} K_1(n\beta m) + 2 \sum_{\ell=1}^{\infty} \frac{\sqrt{(m^2 + 2eB\ell)}}{n\beta} K_1\left(n\beta \sqrt{(m^2 + 2eB\ell)}\right) \right], \end{aligned} \quad (\text{III.7})$$

where $K_n(z)$ is the modified Bessel-function of the second kind defined by

$$\int_0^\infty dx x^{\nu-1} \exp\left(-\frac{\beta}{x} - \gamma x\right) = 2 \left(\frac{\beta}{\gamma}\right)^{\frac{\nu}{2}} K_\nu\left(2\sqrt{\beta\gamma}\right). \quad (\text{III.8})$$

Next, we will focus on the ring contribution to QED effective potential, that will be determined in the IR limit. The general structure of the ring diagram is given by

$$\begin{aligned} V_{ring} &= \frac{T}{2} \sum_{n=-\infty}^{+\infty} \int \frac{d^3 k}{(2\pi)^3} \sum_{N=1}^{\infty} \frac{(-1)^N}{N} \left[D_{\mu\rho}^{(0)}(n, \mathbf{k}) \Pi^{\rho\mu}(n, \mathbf{k}) \right]^N \\ &= -\frac{T}{2} \sum_{n=-\infty}^{+\infty} \int \frac{d^3 k}{(2\pi)^3} \ln[1 + D_{\mu\rho}^{(0)}(n, \mathbf{k}) \Pi^{\rho\mu}(n, \mathbf{k})]. \end{aligned} \quad (\text{III.9})$$

To simplify this potential we use the definition of the free photon propagator $D_{\mu\nu}^{(0)}(k)$ from (II.20) and the vacuum polarization tensor $\Pi_{\mu\nu}(k)$ from (II.22), and arrive at¹⁴

$$V_{ring}(m, eB; T) = -\frac{T}{2} \sum_{n=-\infty}^{+\infty} \int \frac{d^3 k}{(2\pi)^3} \sum_{i=1}^4 \ln \left(1 - \frac{\kappa_i(k_0, \mathbf{k})}{k_E^2} \right), \quad (\text{III.10})$$

where for Euclidean four-momentum k_E , we have $k_E^2 = \mathbf{k}^2 + 4\pi^2 n^2 T^2$. Here, the orthogonality of the eigenfunctions $b_\mu^{(i)}$ from (II.21) and the relation $b_\mu^{(i)} b_\mu^{\star(j)} = 0, \forall i \neq j$ are used. To take the IR limit of this potential, we set $n = 0$ or equivalently $k_0 \rightarrow 0$ in $\kappa_i(k_0, \mathbf{k})$ as well as in k_E^2 . We arrive therefore at

$$V_{ring}^{\text{IR limit}}(m, eB; T) = -\frac{T}{2} \int \frac{d^3 k}{(2\pi)^3} \sum_{i=1}^4 \ln \left(1 - \frac{\kappa_i(k_0 \rightarrow 0, \mathbf{k})}{\mathbf{k}^2} \right), \quad (\text{III.11})$$

where $\kappa_i(k_0 \rightarrow 0, \mathbf{k})$ are given in (II.38). To compare this result with the result (I.1) from [10, 11], let us consider the static (zero momentum) limit $\mathbf{k} \rightarrow 0$ in (III.11). Using the (II.38) and (II.36) and taking $\mathbf{k} \rightarrow 0$, we have

$$\kappa_i(0, \mathbf{0}) = 0, \quad \text{for} \quad i = 1, 3, 4 \quad \text{and} \quad \kappa_2(0, \mathbf{0}) = S(0, \mathbf{0}) = I_2. \quad (\text{III.12})$$

¹⁴ To build the ring potential, we have used the free (bare) photon propagator $D_{\mu\nu}^{(0)}(k)$ to be consistent with the result from our one-loop effective potential throughout this paper. Note that the fermion propagator that are used to determine the polarization tensor $\Pi_{\mu\nu}$ in the ring potential, are free propagator of massive fermions in the LLL approximation. This is also consistent with the approximations used in this paper.

Further, using (II.32), $\kappa_2(0, \mathbf{0}) = I_2 = -\Pi_{44}(0, \mathbf{0})$. Continuing into the Minkowski space we have $\kappa_2^{\text{Mink.}} \equiv -\Pi_{00} = \Pi_{44} = -\kappa_2$. Plugging this result in (III.11), the ring contribution to QED effective potential in the *static limit* reads

$$\begin{aligned} V_{ring}^{\text{static limit}}(m, eB; T) &= -\frac{T}{2} \int \frac{d^3k}{(2\pi)^3} \sum_{i=1}^4 \ln \left(1 - \frac{\kappa_i^{\text{Mink.}}(0, \mathbf{0})}{\mathbf{k}^2} \right) = -\frac{T}{2} \int \frac{d^3k}{(2\pi)^3} \ln \left(1 + \frac{\Pi_{00}(0, \mathbf{0})}{\mathbf{k}^2} \right) \\ &= -\frac{T}{4\pi^2} \int_0^\Lambda \mathbf{k}^2 d\mathbf{k} \ln \left(1 + \frac{\Pi_{00}(0, \mathbf{0})}{\mathbf{k}^2} \right) = \frac{T}{12\pi} \left[\Pi_{00}(0, \mathbf{0}) \right]^{3/2} + \Lambda \text{ dependent terms.} \end{aligned} \quad (\text{III.13})$$

Taking the Higgs mass $m(v) = 0$, this result indeed coincides with (I.1) from [10, 11].

The ring improved effective potential for QED in a constant magnetic field at finite temperature is therefore given by adding the one-loop effective potential (III.6)-(III.7) and the ring (plasmon) potential (III.10)

$$\begin{aligned} V_{\text{eff}}(m, eB; T, \Lambda) &= -\frac{eB}{8\pi^2} \left[m^2 \Gamma \left(-1, \frac{m^2}{\Lambda^2} \right) + 2 \sum_{\ell=1}^{\infty} (m^2 + 2eB\ell) \Gamma \left(-1, \frac{(m^2 + 2eB\ell)}{\Lambda^2} \right) \right] \\ &\quad - \frac{eB}{\pi^2} \sum_{n=1}^{\infty} (-1)^n \left[\frac{m}{n\beta} K_1(n\beta m) + 2 \sum_{\ell=1}^{\infty} \frac{\sqrt{(m^2 + 2eB\ell)}}{n\beta} K_1 \left(n\beta \sqrt{(m^2 + 2eB\ell)} \right) \right] \\ &\quad - \frac{T}{2} \sum_{n=-\infty}^{+\infty} \int \frac{d^3k}{(2\pi)^3} \sum_{i=1}^4 \ln \left(1 - \frac{\kappa_i(k_0, \mathbf{k})}{\mathbf{k}^2} \right). \end{aligned} \quad (\text{III.14})$$

In the following two paragraphs, we will determine QED effective potential V_{eff} in the limit of weak and strong magnetic field.

A. QED effective potential in the limit of weak magnetic field

The weak magnetic field limit is characterized by $eB \ll m^2 \ll T^2$. To determine the effective potential in this limit, let us first consider the one-loop effective potential (III.1). Expanding $\coth(eBs)$ on the right hand side (r.h.s.) of (III.1) in the orders of eB up to second order, we get

$$V^{(1)}(m, eB; T) = -\frac{2}{\beta} \int_{\mathcal{S}} \frac{ds}{(4\pi s)^{3/2}} \Theta_2 \left(0 \middle| i s \frac{4\pi}{\beta^2} \right) \left(\frac{1}{s} + \frac{s(eB)^2}{3} + \dots \right) e^{-sm^2}. \quad (\text{III.15})$$

To separate (III.15) into a temperature independent and a temperature dependent part, we use (III.4) and (III.5) and arrive first at

$$V^{(1)}(m, eB; T) = -\frac{1}{8\pi^2} \int_{\mathcal{S}} \frac{ds}{s^2} \left(\frac{1}{s} + \frac{s(eB)^2}{3} \right) e^{-sm^2} \left(1 + 2 \sum_{n=1}^{\infty} (-1)^n e^{-\frac{n^2 \beta^2}{4s}} \right) + \dots \quad (\text{III.16})$$

Here, the integration region \mathcal{S} spans over $s \in [\frac{1}{\Lambda^2}, \infty[$ for the temperature independent part, and over $s \in [0, \infty[$ for the temperature dependent part. Using the definition of the incomplete Γ -function, $\Gamma(n, z) = \int_z^\infty dt t^{n-1} e^{-t}$, as well as (III.8), the one-loop effective potential can be determined in the

limit of weak magnetic field up to second order in eB

$$V^{(1)/\text{weak}}(m, eB; T) = -\frac{1}{8\pi^2} \left\{ m^4 \Gamma\left(-2, \frac{m^2}{\Lambda^2}\right) + \frac{(eB)^2}{3} \Gamma\left(0, \frac{m^2}{\Lambda^2}\right) + 4 \sum_{n=1}^{\infty} (-1)^n \left(\frac{4m^2}{n^2 \beta^2} K_2(nm\beta) + \frac{(eB)^2}{3} K_0(nm\beta) \right) \right\}. \quad (\text{III.17})$$

To determine the ring contribution to the effective potential in the limit of weak magnetic field, let us consider (III.11), where $\kappa_i(0, \mathbf{k}), i = 1, \dots, 4$ are given in (II.38). To determine κ_i in limit of weak magnetic field, we have to evaluate P, S and R from (II.36), and consequently the functions $I_i, i = 1, \dots, 4$ from (II.33) in this limit. To do this we expand I_i up to second order in eB . Assuming $\mathbf{k}_\perp^2 \ll eB \ll k_3^2$ and neglecting therefore the terms proportional to $\mathbf{k}_\perp^2 (eB)^2$ [38], we arrive first at¹⁵

$$\begin{aligned} \tilde{I}_1^0 &= -\frac{\alpha}{4\pi} \int_{\frac{1}{\Lambda^2}}^{\infty} du \int_{-1}^{+1} dv e^{-u(m^2 + \frac{1-v^2}{4}\mathbf{k}^2)} \left[\frac{1-v^2}{u} - \frac{(eB)^2}{6} u (1-v^2)^2 \right], \\ \tilde{I}_1^T &= -\frac{\alpha}{2\pi} \int_0^{\infty} du \int_{-1}^{+1} dv e^{-u(m^2 + \frac{1-v^2}{4}\mathbf{k}^2)} \sum_{\ell=1}^{\infty} (-1)^\ell e^{-\frac{\ell^2}{4uT^2}} \left[\frac{1-v^2}{u} - \frac{(eB)^2}{6} u (1-v^2)^2 \right], \\ \tilde{I}_2^0 &= 0 \\ \tilde{I}_2^T &= -\frac{\alpha}{2\pi} \int_0^{\infty} du \int_{-1}^{+1} dv e^{-u(m^2 + \frac{1-v^2}{4}\mathbf{k}^2)} \sum_{\ell=1}^{\infty} (-1)^\ell e^{-\frac{\ell^2}{4uT^2}} \frac{\ell^2}{T^2} \left[\frac{1}{u^3} + \frac{(eB)^2}{3u} \right], \\ \tilde{I}_3^0 &= -\frac{\alpha}{4\pi} \int_{\frac{1}{\Lambda^2}}^{\infty} du \int_{-1}^{+1} dv e^{-u(m^2 + \frac{1-v^2}{4}\mathbf{k}^2)} \left[\frac{1-v^2}{u} + \frac{(eB)^2}{3} u (1-v^2) \right], \\ \tilde{I}_3^T &= -\frac{\alpha}{2\pi} \int_0^{\infty} du \int_{-1}^{+1} dv e^{-u(m^2 + \frac{1-v^2}{4}\mathbf{k}^2)} \sum_{\ell=1}^{\infty} (-1)^\ell e^{-\frac{\ell^2}{4uT^2}} \left[\frac{1-v^2}{u} + \frac{(eB)^2}{3} u (1-v^2) \right]. \end{aligned} \quad (\text{III.18})$$

To perform then the integrations over u and v , we expand the above expressions in the order of $\frac{\mathbf{k}^2}{m^2}$. We get the following general structure

$$\tilde{I}_i^0 = a_i^0 + \frac{\mathbf{k}^2}{m^2} b_i^0 \quad \text{for} \quad i = 1, 3, \quad \text{as well as} \quad \tilde{I}_i^T = a_i^T + \frac{\mathbf{k}^2}{m^2} b_i^T, \quad \text{for} \quad i = 1, 2, 3, \quad (\text{III.19})$$

where, the temperature independent parts are¹⁶

$$\begin{aligned} a_1^0 &= +\frac{2\alpha}{45\pi} \frac{(eB)^2}{m^4}, & b_1^0 &= +\frac{\alpha}{15\pi} - \frac{2\alpha}{105\pi} \frac{(eB)^2}{m^4}, \\ a_3^0 &= -\frac{\alpha}{9\pi} \frac{(eB)^2}{m^4}, & b_3^0 &= +\frac{\alpha}{15\pi} + \frac{2\alpha}{45\pi} \frac{(eB)^2}{m^4}, \end{aligned} \quad (\text{III.20})$$

¹⁵ In the following, I_4 will be skipped since, as it turns out, the ring potential in the limit of weak magnetic field is determined only by $I_i, i = 1, 2, 3$ [See (III.22)].

¹⁶ Note that the temperature independent part consists of imaginary terms. These terms cancel the contact terms in (II.31) [see footnote 11].

and the temperature dependent parts are

$$\begin{aligned}
a_1^T &= \sum_{\ell=1}^{\infty} (-1)^\ell \left[-\frac{4\alpha}{3\pi} K_0(\ell m\beta) + \frac{2\alpha}{45\pi} \frac{(eB)^2}{m^4} (\ell m\beta)^2 K_2(\ell m\beta) \right], \\
b_1^T &= \sum_{\ell=1}^{\infty} (-1)^\ell \left[\frac{2\alpha}{15\pi} (\ell m\beta) K_1(\ell m\beta) - \frac{\alpha}{210\pi} \frac{(eB)^2}{m^4} (\ell m\beta)^3 K_3(\ell m\beta) \right], \\
a_2^T &= \sum_{\ell=1}^{\infty} (-1)^\ell \left[-\frac{8\alpha}{\pi} m^2 K_2(\ell m\beta) - \frac{2\alpha}{3\pi} \frac{(eB)^2}{m^2} (\ell m\beta)^2 K_0(\ell m\beta) \right], \\
b_2^T &= \sum_{\ell=1}^{\infty} (-1)^\ell \left[\frac{2\alpha}{3\pi} m^2 (\ell m\beta) K_1(\ell m\beta) + \frac{\alpha}{18\pi} \frac{(eB)^2}{m^2} (\ell m\beta)^3 K_1(\ell m\beta) \right], \\
a_3^T &= \sum_{\ell=1}^{\infty} (-1)^\ell \left[-\frac{4\alpha}{3\pi} K_0(\ell m\beta) - \frac{\alpha}{9\pi} \frac{(eB)^2}{m^4} (\ell m\beta)^2 K_2(\ell m\beta) \right], \\
b_3^T &= \sum_{\ell=1}^{\infty} (-1)^\ell \left[\frac{2\alpha}{15\pi} (\ell m\beta) K_1(\ell m\beta) + \frac{\alpha}{90\pi} \frac{(eB)^2}{m^4} (\ell m\beta)^3 K_3(\ell m\beta) \right]. \tag{III.21}
\end{aligned}$$

To evaluate P, S and R from (II.36) in the limit of weak eB , we use again $\mathbf{k}_\perp^2 \ll eB \ll k_3^2$ [38]. The most dominant terms in $\kappa_i(0, \mathbf{k})$ are therefore given by

$$\begin{aligned}
\kappa_1(k_0 \rightarrow 0, \mathbf{k}) &= -k_3^2 \tilde{I}_1 + \mathcal{O}\left(\frac{k_\perp^2}{eB}\right) \\
\kappa_2(k_0 \rightarrow 0, \mathbf{k}) &= -k_3^2 \tilde{I}_3 + \tilde{I}_2 + \mathcal{O}\left(\frac{k_\perp^2}{eB}\right) \\
\kappa_3(k_0 \rightarrow 0, \mathbf{k}) &= -k_3^2 \tilde{I}_1 + \mathcal{O}\left(\frac{k_\perp^2}{eB}\right) \\
\kappa_4(k_0 \rightarrow 0, \mathbf{k}) &= 0. \tag{III.22}
\end{aligned}$$

Plugging as next these expressions in (III.11), the ring potential in the limit of weak magnetic field is given by

$$\begin{aligned}
V_{ring}^{\text{IR limit/weak}} &\approx -\frac{T}{2} \int \frac{d^3 k}{(2\pi)^3} \left[2 \ln \left(1 + \frac{k_3^2}{\mathbf{k}^2} (a_1^0 + a_1^T) + \frac{k_3^2}{m^2} (b_1^0 + b_1^T) \right) \right. \\
&\quad \left. + \ln \left(1 + \frac{k_3^2}{\mathbf{k}^2} (a_3^0 + a_3^T) + \frac{k_3^2}{m^2} (b_3^0 + b_3^T) - \left(\frac{a_2^T}{\mathbf{k}^2} + \frac{b_2^T}{m^2} \right) \right) \right]. \tag{III.23}
\end{aligned}$$

To perform the integration over three-momentum \mathbf{k} , we will use the same procedure as was discussed in part B of the Introduction. Adding and subtracting an appropriate integral to the ring potential (III.23), whose integrand is independent of k_3^2 , we arrive at

$$V_{ring}^{\text{IR limit/weak}} = V_{ring}^{(f)} + V_{ring}^\Lambda, \tag{III.24}$$

where the finite part is

$$V_{ring}^{(f)} = -\frac{T}{2} \int \frac{d^3 k}{(2\pi)^3} \ln \left(1 - \left(\frac{a_2^T}{\mathbf{k}^2} + \frac{b_2^T}{m^2} \right) \right), \tag{III.25}$$

and the cutoff (Λ) dependent part

$$V_{ring}^\Lambda = -\frac{T}{2} \int \frac{d^3k}{(2\pi)^3} \left[2 \ln \left(1 + \frac{k_3^2}{\mathbf{k}^2} (a_1^0 + a_1^T) + \frac{k_3^2}{m^2} (b_1^0 + b_1^T) \right) \right. \\ \left. + \ln \left(1 + \frac{k_3^2}{\mathbf{k}^2} (a_3^0 + a_3^T) + \frac{k_3^2}{m^2} (b_3^0 + b_3^T) - \left(\frac{a_2^T}{\mathbf{k}^2} + \frac{b_2^T}{m^2} \right) \right) \right] - \frac{T}{2} \int \frac{d^3k}{(2\pi)^3} \ln \left(1 - \left(\frac{a_2^T}{\mathbf{k}^2} + \frac{b_2^T}{m^2} \right) \right). \quad (\text{III.26})$$

Performing the integration over \mathbf{k} in $V_{ring}^{(f)}$ we get

$$V_{ring}^{(f)} \approx T \frac{(a_2^T)^{3/2}}{\left(1 - \frac{b_2^T}{m^2}\right)^{3/2}} + \text{Cutoff dependent terms}, \quad (\text{III.27})$$

whereas for V_{ring}^Λ we have

$$V_{ring}^\Lambda \approx \alpha T \mathcal{O}(\Lambda^3). \quad (\text{III.28})$$

Note that V_{ring}^Λ can be derived by expanding the logarithms in (III.26) and performing the three dimensional integration over k using a momentum cutoff Λ . Neglecting now the cutoff dependent terms, we arrive at

$$V_{ring}^{\text{IR limit/weak}} = \mathcal{C} T \frac{(a_2^T)^{3/2}}{\left(1 - \frac{b_2^T}{m^2}\right)^{3/2}} \\ = \mathcal{C} m^3 T \left\{ \frac{\frac{8\alpha}{\pi} \sum_{\ell=1}^{\infty} (-1)^{\ell+1} K_2(\ell m \beta)}{1 - \frac{2\alpha}{3\pi} \sum_{\ell=1}^{\infty} (-1)^\ell (\ell m \beta) K_1(\ell m \beta)} \right\}^{3/2} + \mathcal{O} \left(\left(\frac{eB}{m^2} \right)^2 \right). \quad (\text{III.29})$$

Here, the proportionality constant $\mathcal{C} = \mathcal{O}(1)$. To compare this result with the ring potential in the leading *static limit*, (III.29) will be evaluated in the high temperature expansion $m\beta \rightarrow 0$. This can be determined from the behavior of Bessel functions in this limit

$$K_\nu(x) \xrightarrow{x \rightarrow 0} \frac{1}{2} \Gamma(\nu) \left(\frac{2}{x} \right)^\nu, \quad (\text{III.30})$$

and the Bessel function identities [39, 40]

$$\sum_{\ell=1}^{\infty} K_0(\ell z) \cos(\ell \phi) = \frac{1}{2} \left(\gamma + \ln \frac{z}{4\pi} \right) + C_0(z, \phi). \quad (\text{III.31})$$

Here, $\gamma \simeq 0.577$ is the Euler-Mascheroni constant and $C_0(z, \phi)$ is given by

$$C_0(z, \phi) \equiv \frac{\pi}{2} \sum_{\ell}' \left(\frac{1}{\sqrt{z^2 + (\phi - 2\pi\ell)^2}} - \frac{1}{2\pi|\ell|} \right), \quad (\text{III.32})$$

where the notation \sum_{ℓ}' indicates that singular terms are omitted when $\ell = 0$ [39]. Deriving (III.31) with respect to $\ln z$ and reminding the fact that $\frac{\partial K_0(z)}{\partial \ln z} = -z K_1(z)$, we get

$$\sum_{\ell=1}^{\infty} (\ell z) K_1(\ell z) \cos(\ell \phi) = -\frac{1}{2} + C_1(z, \phi), \quad (\text{III.33})$$

with

$$C_1(z, \phi) \equiv -\frac{\partial C_0(z, \phi)}{\partial \ln z} = \frac{\pi}{2} \sum_{\ell=-\infty}^{\infty} \frac{z^2}{\left(z^2 + (\phi - 2\pi\ell)^2\right)^{3/2}}. \quad (\text{III.34})$$

Choosing now $\nu = 2$ as well as $x \equiv \ell m\beta$ in (III.30) and $z \equiv m\beta$ as well as $\phi \equiv \pi$ in (III.31)-(III.34), and plugging (III.30) in the numerator and (III.33) in the denominator of (III.29), we arrive first at

$$V_{ring}^{\text{IR limit/weak}} \longrightarrow c \frac{8\pi}{3} \sqrt{\frac{\pi}{3}} \frac{T^4 \alpha^{3/2}}{\left(1 + \frac{\alpha}{3\pi} - \frac{2\alpha}{3\pi} C_1(m\beta, \pi)\right)^{3/2}}. \quad (\text{III.35})$$

Here, we have used $\sum_{\ell=1}^{\infty} \frac{(-1)^{\ell+1}}{\ell^2} = \frac{\pi^2}{12}$. Expanding now $C_1(m\beta, \pi)$ in the denominator of (III.35) in the orders of $m\beta$ and using $C_1(m\beta, \pi) = \frac{7(m\beta)^2 \zeta(3)}{8\pi^2} + \mathcal{O}((m\beta)^3)$, we arrive for $\alpha \rightarrow 0$ at

$$\begin{aligned} V_{ring}^{\text{IR limit/weak}} &= \frac{8\pi}{3} \sqrt{\frac{\pi}{3}} c T^4 \left(\frac{\alpha}{1 + \frac{\alpha}{2\pi}}\right)^{3/2} \left[1 - \frac{7\zeta(3)}{8\pi^3} \frac{\alpha}{\left(1 + \frac{\alpha}{2\pi}\right)} (m\beta)^2\right] + \mathcal{O}((m\beta)^3), \\ &= \frac{8\pi}{3} \sqrt{\frac{\pi}{3}} c T^4 \alpha^{3/2} \left[1 - \frac{\alpha}{2\pi} \left(1 - \frac{7\zeta(3)}{4\pi^2} (m\beta)^2\right)\right] + \mathcal{O}(\alpha^{7/2}, (m\beta)^3). \end{aligned} \quad (\text{III.36})$$

The first term is the usual $\alpha^{3/2}$ contribution to the ring potential from the *static limit* [10, 11, 14] [see also part B of the Introduction and in particular (I.12)]. The second term, however, arises only in the *IR limit*. It is a consequence of the additional b_2^T term in the denominator of V_{ring} from (III.29). The above result (III.29) can be viewed as a nonperturbative correction of QED effective potential in addition to the perturbative loop corrections to this potential. Note that in QCD at finite temperature and zero magnetic fields $\alpha_s^{3/2}$ and $\alpha_s^{5/2}$ terms are calculated using Hard Thermal Loop expansion (see [17, 18] and references therein). The above result are relevant in studying the standard electroweak phase transition in the presence of weak external magnetic field [12].

B. QED effective potential in the limit of strong magnetic field

The strong magnetic field is characterized by $m^2 \ll T^2 \ll eB$. To determine QED effective potential in the limit of strong magnetic field, let us consider first the one-loop effective potential (III.1). For $eB \rightarrow \infty$ (III.1) is given by

$$V^{(1)}(m, eB; T) = -\frac{2eB}{\beta} \int_0^\infty ds \frac{\Theta_2\left(0 \middle| i s \frac{4\pi}{\beta^2}\right)}{(4\pi s)^{\frac{3}{2}}} e^{-sm^2}, \quad (\text{III.37})$$

where $\coth(eBs) \approx 1$ is used. To separate (III.37) into a temperature dependent and a temperature independent part, we use (III.4) and (III.5) and arrive first at

$$V^{(1)}(m, eB; T) = -\frac{eB}{8\pi^2} \int_{\mathcal{S}} \frac{ds}{s^2} \left(1 + 2 \sum_{n=1}^{\infty} (-1)^n e^{-\frac{n^2 \beta^2}{4s}}\right) e^{-sm^2}, \quad (\text{III.38})$$

where the integration region \mathcal{S} spans over $s \in [\frac{1}{\Lambda^2}, \infty[$ for the temperature independent part, and over $s \in [0, \infty[$ for the temperature dependent part. Using the definition of the incomplete Γ -function as well

as (III.8), the one-loop effective potential in the limit of strong magnetic field is given by

$$V^{(1)/\text{strong}}(m, eB; \Lambda, T) = -\frac{eB}{8\pi^2} \left\{ m^2 \Gamma\left(-1, \frac{m^2}{\Lambda^2}\right) + \frac{8m}{\beta} \sum_{n=1}^{\infty} \frac{(-1)^n}{n} K_{-1}(nm\beta) \right\}. \quad (\text{III.39})$$

To determine the ring contribution to QED effective potential in the limit of strong magnetic field, let us consider (III.11) with $\kappa_i(0, \mathbf{k}), i = 0, \dots, 4$ from (II.38). To determine $\kappa_i, i = 1, \dots, 4$ in the limit of strong magnetic field, we have to evaluate P, S and R from (II.36), and consequently the functions $I_i, i = 1, \dots, 4$ from (II.33) in this limit. Note that in a strong magnetic field at finite temperature, as in the zero temperature case, QED dynamics is dominated by LLL, where the chiral symmetry is dynamically broken as a consequence of the external magnetic field. As we have mentioned in Sect. II.A, the LLL is characterized by $k_3^2, \mathbf{k}_\perp^2 \ll eB$ and a small dynamical mass $m^2 \ll eB$ [20, 22]. Keeping these facts in mind, it is easy to determine the most dominant I_i among $I_i, i = 1, \dots, 4$ in the limit of strong magnetic field. A simple calculation shows that in the limit $eB \rightarrow \infty$ only I_2 and I_3 survive. They are given by

$$\begin{aligned} I_2^T &\approx -\frac{\alpha eB}{2\pi} \int_0^\infty \frac{du}{u^2} \int_{-1}^1 dv e^\phi \sum_{\ell=1}^{\infty} (-1)^\ell \frac{\ell^2}{T^2} e^{-\frac{\ell^2}{4uT^2}}, \\ I_3^0 &\approx -\frac{\alpha eB}{4\pi} \int_0^\infty du \int_{-1}^1 dv e^\phi (1-v^2), \\ I_3^T &\approx -\frac{\alpha eB}{2\pi} \int_0^\infty du \int_{-1}^1 dv e^\phi \sum_{\ell=1}^{\infty} (-1)^\ell e^{-\frac{\ell^2}{4uT^2}} (1-v^2), \end{aligned} \quad (\text{III.40})$$

where

$$\phi \approx -\frac{\mathbf{k}_\perp^2}{2eB} - u \left[m^2 + \frac{(1-v^2)}{4} k_3^2 \right]. \quad (\text{III.41})$$

Plugging (III.40) in (II.36), we get

$$P, R \xrightarrow{eB \rightarrow \infty} 0, \quad \text{and} \quad S \xrightarrow{eB \rightarrow \infty} -k_3^2 (I_3^0 + I_3^T) + I_2^T. \quad (\text{III.42})$$

Using now the relations (II.38), only $\kappa_2(k_0 \rightarrow 0, \mathbf{k}) = S$ survives in (III.11). The ring potential is thus given by

$$\begin{aligned} V_{ring}^{\text{IR limit/strong}} &= -\frac{T}{2} \int \frac{d^3 k}{(2\pi)^3} \ln \left(1 - \frac{\kappa_2(k_0 \rightarrow 0, \mathbf{k})}{\mathbf{k}^2} \right) \\ &\approx -\frac{T}{8\pi^2} \int_0^\infty d(\mathbf{k}_\perp^2) \int_0^\infty dk_3 \ln \left(1 + \frac{k_3^2 (I_3^0 + I_3^T) - I_2^T}{(k_3^2 + \mathbf{k}_\perp^2)} \right). \end{aligned} \quad (\text{III.43})$$

As next the integration over k_3 will be evaluated separately in two different regimes of dynamical mass in the LLL. These two regimes will be indicated by $k_3^2 \ll m^2 \ll eB$ and $m^2 \ll k_3^2 \ll eB$ [see Sect. II.A and in particular (II.13) and (II.14)]. To do this we use the relation¹⁷

$$\int_0^\infty dk_3 = \int_0^m dk_3 + \int_m^\infty dk_3,$$

¹⁷ The same method is also used in [20]. Here, we have matched the asymptotics at $k_3 = m$.

where the first integral $\int_0^m dk_3$ corresponds to the first regime $k_3^2 \ll m^2 \ll eB$ and the second integral $\int_m^\infty dk_3$ to the second regime $m^2 \ll k_3^2 \ll eB$ in the LLL. As for the integration (III.43) only the phase ϕ from (III.41) is different in these two regimes. Thus taking

$$\phi \approx -\frac{\mathbf{k}_\perp^2}{2eB} - um^2 \quad \text{for} \quad k_3^2 \ll m^2 \ll eB, \quad (\text{III.44})$$

$$\phi \approx -\frac{\mathbf{k}_\perp^2}{2eB} - \frac{(1-v^2)}{4} uk_3^2 \quad \text{for} \quad m^2 \ll k_3^2 \ll eB, \quad (\text{III.45})$$

in I_2^T, I_3^0 and I_3^T the integration over u and v can be easily performed. As next, we will determine the corresponding ring contribution to the effective potential for these two regimes separately. The results will be added eventually.

i) Ring potential in the first regime $k_3^2 \ll m^2 \ll eB$ of LLL

To determine the ring potential in the $k_3^2 \ll m^2 \ll eB$ regime in the LLL, we have to calculate first the integrals I_2^T, I_3^0 and I_3^T from (III.40) in this regime. Using the phase ϕ from (III.44) we get

$$\begin{aligned} I_2^T &\approx -\frac{\alpha eB}{2\pi} e^{-\frac{\mathbf{k}_\perp^2}{2eB}} \int_{-1}^1 dv \sum_{\ell=1}^{\infty} (-1)^\ell (\ell\beta)^2 \int_0^\infty \frac{du}{u^2} e^{-um^2 - \frac{\ell^2}{4uT^2}} \equiv e^{-\frac{\mathbf{k}_\perp^2}{2eB}} A_2^T, \\ I_3^0 &\approx -\frac{\alpha eB}{4\pi} e^{-\frac{\mathbf{k}_\perp^2}{2eB}} \int_{-1}^1 dv (1-v^2) \int_0^\infty du e^{-um^2} \equiv e^{-\frac{\mathbf{k}_\perp^2}{2eB}} A_3^0, \\ I_3^T &\approx -\frac{\alpha eB}{2\pi} e^{-\frac{\mathbf{k}_\perp^2}{2eB}} \int_{-1}^1 dv (1-v^2) \sum_{\ell=1}^{\infty} (-1)^\ell \int_0^\infty du e^{-um^2 - \frac{\ell^2}{4uT^2}} \equiv e^{-\frac{\mathbf{k}_\perp^2}{2eB}} A_3^T. \end{aligned} \quad (\text{III.46})$$

Here, using the notation $M_\gamma^2 \equiv \frac{2\alpha eB}{\pi}$, we have $A_3^0 \equiv -\frac{M_\gamma^2}{6m^2}$ and

$$A_2^T \equiv -2M_\gamma^2 \sum_{\ell=1}^{\infty} (-1)^\ell (\ell m\beta) K_1(\ell m\beta), \quad A_3^T \equiv -\frac{M_\gamma^2}{3m^2} \sum_{\ell=1}^{\infty} (-1)^\ell (\ell m\beta) K_1(\ell m\beta). \quad (\text{III.47})$$

The ring potential (III.43) corresponding to the first regime $k_3^2 \ll m^2 \ll eB$ in LLL reads therefore

$$V_{ring}^{\text{IR limit/strong}} \Big|_{k_3^2 \ll m^2 \ll eB} \approx -\frac{T}{8\pi^2} \int_0^\infty d(\mathbf{k}_\perp^2) \int_0^m dk_3 \ln \left(1 + \frac{e^{-\frac{\mathbf{k}_\perp^2}{2eB}} (k_3^2 A_3 - A_2^T)}{(k_3^2 + \mathbf{k}_\perp^2)} \right), \quad (\text{III.48})$$

where $A_3 \equiv A_3^0 + A_3^T$. Using the expression (III.33), A_3 and A_2^T can be simplified

$$A_3 = -\frac{M_\gamma^2}{3m^2} C_1(m\beta, \pi), \quad \text{and} \quad A_2^T = M_\gamma^2 (1 - 2C_1(m\beta, \pi)), \quad (\text{III.49})$$

where $C_1(z, \phi)$ is defined in (III.34). Performing now the integration over $k_3 \in [0, m]$, we get first

$$V_{ring}^{\text{IR limit/strong}} \Big|_{k_3^2 \ll m^2 \ll eB} \approx -\frac{mT}{8\pi^2} \int_0^\infty d(\mathbf{k}_\perp^2) \ln \left(1 - \frac{e^{-\frac{\mathbf{k}_\perp^2}{2eB}} (A_2^T - m^2 A_3)}{\mathbf{k}_\perp^2 + m^2} \right) + J, \quad (\text{III.50})$$

where

$$J \equiv +\frac{T}{4\pi^2} \int_0^\infty d(\mathbf{k}_\perp^2) \sqrt{\mathbf{k}_\perp^2} \arctan \left(\frac{m}{\sqrt{\mathbf{k}_\perp^2}} \right) + \mathcal{O} \left(\frac{m}{\sqrt{eB}} \right). \quad (\text{III.51})$$

Here, an expansion in the orders of $\frac{m}{\sqrt{eB}}$ is performed, as we are in a regime where $m^2 \ll eB$. To perform the integration over the first term in (III.50), we use the identity

$$\int_0^\infty dy \ln \left(1 - \frac{e^{-\frac{y}{x}}}{y+z} \right) = x \operatorname{Li}_2 \left(-\frac{1}{z} \right), \quad (\text{III.52})$$

where the dilogarithm is defined by

$$\operatorname{Li}_2(z) \equiv - \int_0^z \frac{\ln(1-z)}{z} dz = - \int_0^z \ln(1-z) \frac{d}{dz} \ln z dz.$$

Choosing now $y(A_2^T - m^2 A_3) \equiv \mathbf{k}_\perp^2$, $x(A_2^T - m^2 A_3) \equiv 2eB$ and $z(A_2^T - m^2 A_3) \equiv m^2$ in (III.52), the ring contribution in the first regime $k_3^2 \ll m^2 \ll eB$ in the LLL reads

$$V_{ring}^{\text{IR limit/strong}} \Big|_{k_3^2 \ll m^2 \ll eB} \approx -\frac{mTeB}{4\pi^2} \operatorname{Li}_2 \left(-\frac{(A_2^T - m^2 A_3)}{m^2} \right) + J, \quad (\text{III.53})$$

where $A_2^T - m^2 A_3$ can be simplified using (III.49) and reads

$$A_2^T - m^2 A_3 = M_\gamma^2 \left(1 - \frac{5}{3} C_1(m\beta, \pi) \right). \quad (\text{III.54})$$

As it turns out, the second term on the r.h.s. of (III.53) vanishes with the ring potential corresponding to the second regime $m^2 \ll k_3^2 \ll eB$ in the LLL.

ii) Ring potential in the second regime $m^2 \ll k_3^2 \ll eB$ of LLL

As for the second regime $m^2 \ll k_3^2 \ll eB$, we have to determine I_2^T, I_3^0 and I_3^T from (III.40). Taking ϕ from (III.45), we get

$$\begin{aligned} I_2^T &\approx -\frac{\alpha eB}{2\pi} e^{-\frac{\mathbf{k}_\perp^2}{2eB}} \int_{-1}^1 dv \sum_{\ell=1}^{\infty} (-1)^\ell (\ell\beta)^2 \int_0^\infty \frac{du}{u^2} e^{-\frac{(1-v^2)}{4} uk_3^2 - \frac{\ell^2}{4uT^2}} \equiv e^{-\frac{\mathbf{k}_\perp^2}{2eB}} B_2^T \\ I_3^0 &\approx -\frac{\alpha eB}{4\pi} e^{-\frac{\mathbf{k}_\perp^2}{2eB}} \int_{-1}^1 dv (1-v^2) \int_0^\infty du e^{-\frac{(1-v^2)}{4} uk_3^2} = -\frac{2\alpha eB}{\pi k_3^2} e^{-\frac{\mathbf{k}_\perp^2}{2eB}} \equiv -e^{-\frac{\mathbf{k}_\perp^2}{2eB}} \frac{M_\gamma^2}{k_3^2}, \\ I_3^T &\approx -\frac{\alpha eB}{2\pi} e^{-\frac{\mathbf{k}_\perp^2}{2eB}} \int_{-1}^1 dv (1-v^2) \sum_{\ell=1}^{\infty} (-1)^\ell \int_0^\infty du e^{-\frac{(1-v^2)}{4} uk_3^2 - \frac{\ell^2}{4uT^2}} \equiv e^{-\frac{\mathbf{k}_\perp^2}{2eB}} \frac{B_3^T}{k_3^2}, \end{aligned} \quad (\text{III.55})$$

where $M_\gamma^2 \equiv \frac{2\alpha eB}{\pi}$, and

$$B_2^T = B_3^T \equiv -M_\gamma^2 \int_{-1}^{+1} dv \sum_{\ell=1}^{\infty} (-1)^\ell \left(\frac{\ell\beta k_3}{2} \sqrt{1-v^2} \right) K_1 \left(\frac{\ell\beta k_3}{2} \sqrt{1-v^2} \right). \quad (\text{III.56})$$

Plugging (III.55) in (III.43), the contribution from B_2^T and B_3^T cancel and we are left with

$$V_{ring}^{\text{IR limit/strong}} \Big|_{m^2 \ll k_3^2 \ll eB} \approx -\frac{T}{8\pi^2} \int_0^\infty d(\mathbf{k}_\perp^2) \int_m^\infty dk_3 \ln \left(1 - \frac{e^{-\frac{\mathbf{k}_\perp^2}{2eB}} M_\gamma^2}{(k_3^2 + \mathbf{k}_\perp^2)} \right). \quad (\text{III.57})$$

Here, the integration over k_3 can be performed and we arrive first at

$$V_{ring}^{\text{IR limit/strong}} \Big|_{m^2 \ll k_3^2 \ll eB} \approx W_{ring}^{\text{IR/nonpert.}} + V_{ring}^{\text{IR/pert.}} - J, \quad (\text{III.58})$$

where $W_{ring}^{\text{IR/nonpert.}}$ is the nonperturbative, $V_{ring}^{\text{IR/pert.}}$ is the perturbative part of $V_{ring}^{\text{IR limit/strong}}$ and J is given in (III.50). The nonperturbative part of the ring potential $W_{ring}^{\text{IR/nonpert.}}$ is given by

$$W_{ring}^{\text{IR/nonpert.}} = \frac{mT}{8\pi^2} \int_0^\infty d(\mathbf{k}_\perp^2) \ln \left(1 - \frac{e^{-\frac{k_\perp^2}{2eB}} M_\gamma^2}{(\mathbf{k}_\perp^2 + m^2)} \right) = \frac{mTeB}{4\pi^2} \text{Li}_2 \left(-\frac{M_\gamma^2}{m^2} \right). \quad (\text{III.59})$$

To evaluate this integral we have used (III.52) with $yM_\gamma^2 \equiv \mathbf{k}_\perp^2$, $xM_\gamma^2 \equiv 2eB$ and $zM_\gamma^2 \equiv m^2$. As for the perturbative part of the ring potential, $V_{ring}^{\text{IR/pert.}}$, it is given by the substitution $z \equiv \frac{\mathbf{k}_\perp^2}{eB}$. It reads

$$V_{ring}^{\text{IR/pert.}} \equiv \frac{TeB\sqrt{eB}}{8\pi} \int_0^\infty \left(\sqrt{z} - \sqrt{z - \frac{2\alpha}{\pi} e^{-\frac{z}{2}}} \right) dz = \frac{\alpha TeB\sqrt{2eB}}{8\pi^{3/2}} + \mathcal{O}(\alpha^2). \quad (\text{III.60})$$

Here, we have expanded the integrand in the orders of α and performed eventually the integration over z .

iii) QED Ring potential in the LLL; the IR limit

At this stage we are able to give the ring potential in the limit of strong magnetic field at finite temperature. It is determined by adding the contribution from the first regime (III.53) with the contribution from the second regime (III.58). It consists of a perturbative and a nonperturbative part

$$V_{ring}^{\text{IR limit/strong}} = V_{ring}^{\text{IR/pert.}} + V_{ring}^{\text{IR/nonpert.}}. \quad (\text{III.61})$$

The perturbative part, $V_{ring}^{\text{IR/pert.}}$, is given by (III.60) and the nonperturbative part, $V_{ring}^{\text{IR/nonpert.}}$, is given by adding up the ring contribution (III.53) and (III.59) from the first and second regime of LLL, respectively. It is given by

$$V_{ring}^{\text{IR/nonpert.}} = -\frac{mTeB}{4\pi^2} \left(\text{Li}_2 \left(-\frac{M_\gamma^2}{m^2} \left(1 - \frac{5}{3} C_1(m\beta, \pi) \right) \right) - \text{Li}_2 \left(-\frac{M_\gamma^2}{m^2} \right) \right). \quad (\text{III.62})$$

Here, we have replaced $A_2^T - m^2 A_3$ in (III.53) by its value from (III.54). It is interesting to examine the behavior of the ring potential in the high temperature limit. To do this we use the asymptotic expansion of the dilogarithm

$$\text{Li}_2(-x) \xrightarrow{x \rightarrow \infty} -\frac{\pi^2}{6} - \frac{1}{2} (\ln(x))^2 + \frac{1}{x} + \mathcal{O}\left(\frac{1}{x^2}\right), \quad (\text{III.63})$$

and expand (III.62) in the orders of $x \equiv \frac{eB}{m^2}$ and then in the orders of $t \equiv m\beta$ to get

$$V_{ring}^{\text{IR/nonpert.}} \Big|_{\frac{eB}{m^2} \rightarrow \infty, m\beta \rightarrow 0} \approx -\frac{35m^4 \zeta(3)}{192\pi^3 \alpha} \left[1 + \frac{2\alpha}{\pi} \frac{eB}{m^2} \ln \left(\frac{2\alpha}{\pi} \frac{eB}{m^2} \right) \right] (m\beta) + \mathcal{O}\left(\frac{m^4}{(eB)^2}, (m\beta)^2\right), \quad (\text{III.64})$$

where $C_1(t, \pi) = \frac{7t^2\zeta(3)}{8\pi^2} + \mathcal{O}(t^4)$ is also used. Together with the perturbative contribution to the effective potential, (III.60), the most dominant part of the ring potential in the limit $\frac{eB}{m^2} \rightarrow \infty$ is given by

$$V_{ring}^{\text{IR limit/strong}} \approx -\frac{35m^4\zeta(3)}{192\pi^3\alpha} \left[1 + \frac{2\alpha}{\pi} \frac{eB}{m^2} \ln \left(\frac{2\alpha}{\pi} \frac{eB}{m^2} \right) \right] (m\beta) + \frac{\alpha T e B \sqrt{2eB}}{8\pi^{3/2}} + \mathcal{O} \left(\frac{m^4}{(eB)^2}, \alpha^2, (m\beta)^2 \right). \quad (\text{III.65})$$

The same result will arise when we keep $\frac{eB}{m^2}$ in (III.62) fixed and after replacing $m \rightarrow \frac{t}{\beta}$ expand the resulting expression in the orders of t . This means that the two limits $eB \rightarrow \infty, m\beta \rightarrow 0$ and $m\beta \rightarrow 0$ and $eB \rightarrow \infty$ yield the same result.

C. Ring potential of QED in the LLL in the static limit; A comparison with the IR limit

Let us now compare the above results in the IR limit ($k_0 \rightarrow 0$) with the ring potential in the static limit ($k_0 \rightarrow 0$ and $\mathbf{k} \rightarrow \mathbf{0}$). In this case, the ring potential (III.43) is only determined by $\kappa_2(0, \mathbf{0}) = I_2^T(0, \mathbf{0})$

$$V_{ring}^{\text{static limit}} = -\frac{T}{2} \int \frac{d^3k}{(2\pi)^3} \ln \left(1 - \frac{\kappa_2(0, \mathbf{0})}{k_3^2 + \mathbf{k}_\perp^2} \right) = -\frac{T}{8\pi^2} \int_0^\infty d(k_\perp^2) \int_0^\infty dk_3 \ln \left(1 - \frac{I_2^T(0, \mathbf{0})}{k_3^2 + \mathbf{k}_\perp^2} \right). \quad (\text{III.66})$$

As we have seen in the previous paragraphs, in the limit of strong magnetic field the integration over k_3 must be separated into a regime where $k_3^2 \ll m^2 \ll eB$ and a regime with $m^2 \ll k_3^2 \ll eB$. As for I_2^T in the first regime $k_3^2 \ll m^2 \ll eB$, it is given in (III.46) with A_2^T from (III.49)

$$\begin{aligned} I_2^T(0, \mathbf{0}) \Big|_{k_3^2 \ll m^2 \ll eB} &= -\frac{\alpha e B}{2\pi} \int_{-1}^1 dv \sum_{\ell=1}^{\infty} (-1)^\ell (\ell\beta)^2 \int_0^\infty \frac{du}{u^2} e^{-um^2 - \frac{\ell^2}{4uT^2}} \\ &= A_2^T = M_\gamma^2 (1 - 2C_1(m\beta, \pi)). \end{aligned} \quad (\text{III.67})$$

Note that the only difference between the static and the previous IR limit is a factor $e^{-\frac{\mathbf{k}_\perp^2}{2eB}}$ that appears in $I_2^T(0, \mathbf{k} \neq \mathbf{0})$ in (III.46). This factor vanishes in the static limit where we take the limit $k_0 \rightarrow 0$ and $\mathbf{k} \rightarrow \mathbf{0}$. In the second regime $m^2 \ll k_3^2 \ll eB$, $I_2^T(0, \mathbf{k} \neq \mathbf{0})$ is given in (III.55) with B_2^T from (III.56). In the static limit for $\mathbf{k} \rightarrow \mathbf{0}$, it is, however, given by

$$I_2^T(0, \mathbf{0}) \Big|_{m^2 \ll k_3^2 \ll eB} = -\lim_{\varepsilon \rightarrow 0} \frac{\alpha e B}{2\pi} \int_{-1}^1 dv \sum_{\ell=1}^{\infty} (-1)^\ell (\ell\beta)^2 \int_0^\infty \frac{du}{u^2} e^{-u\varepsilon - \frac{\ell^2}{4uT^2}}, \quad (\text{III.68})$$

where ε is an IR cutoff. Using now the definition of the Bessel function (III.8), we get

$$I_2^T(0, \mathbf{0}) \Big|_{m^2 \ll k_3^2 \ll eB} = -\lim_{\varepsilon \rightarrow 0} 2M_\gamma^2 \sum_{\ell=1}^{\infty} (-1)^\ell (\ell\sqrt{\varepsilon}\beta) K_1(\ell\sqrt{\varepsilon}\beta) = M_\gamma^2. \quad (\text{III.69})$$

Here, we have used (III.33) and the fact that $C_1(\sqrt{\varepsilon}, \pi)$ from (III.34) vanishes for $\varepsilon \rightarrow 0$. Plugging now (III.67) and (III.69) in (III.66), the ring potential in the static limit and in the presence of strong

magnetic field is given by

$$\begin{aligned}
V_{ring}^{\text{static limit/strong}} &= \\
&= -\frac{T}{8\pi^2} \int_0^\infty d(\mathbf{k}_\perp^2) \left[\int_0^m dk_3 \ln \left(1 - \frac{I_2^T(0, \mathbf{0})|_{k_3^2 \ll m^2 \ll eB}}{k_3^2 + \mathbf{k}_\perp^2} \right) + \int_m^\infty dk_3 \ln \left(1 - \frac{I_2^T(0, \mathbf{0})|_{m^2 \ll k_3^2 \ll eB}}{k_3^2 + \mathbf{k}_\perp^2} \right) \right] \\
&= -\frac{T}{8\pi^2} \int_0^\infty d(\mathbf{k}_\perp^2) \left[\int_0^m dk_3 \ln \left(1 - \frac{M_\gamma^2 (1 - 2C_1(m\beta, \pi))}{k_3^2 + \mathbf{k}_\perp^2} \right) + \int_m^\infty dk_3 \ln \left(1 - \frac{M_\gamma^2}{k_3^2 + \mathbf{k}_\perp^2} \right) \right]. \quad (\text{III.70})
\end{aligned}$$

Following now the same steps as in the previous paragraph, the ring potential in the static limit can be decomposed into a perturbative and a nonperturbative part

$$V_{ring}^{\text{static limit/strong}} = V_{ring}^{\text{static/pert.}} + V_{ring}^{\text{static/nonpert.}} + \text{cutoff dependent terms.} \quad (\text{III.71})$$

The perturbative part is given, as in the previous case, by the substitution $z = \frac{\mathbf{k}_\perp^2}{eB}$. It reads

$$V_{ring}^{\text{static/pert.}} = \frac{TeB\sqrt{eB}}{8\pi} \int_0^\Lambda dz \left(\sqrt{z} - \sqrt{z - \frac{2\alpha}{\pi}} \right) = \frac{\alpha TeB\sqrt{eB}}{4\pi} \sqrt{\Lambda} + \mathcal{O}(\alpha^2). \quad (\text{III.72})$$

Here, we have first expanded the integrand in the orders of α and then performed the integration over z . Comparing to the perturbative part in the IR limit (III.60), $V_{ring}^{\text{static/pert.}}$ diverges for $\Lambda \rightarrow \infty$. This is due to the lack of a factor $e^{-\frac{z}{2}}$ in the second term of the integrand. This factor arises only in the IR limit where $\mathbf{k} \neq \mathbf{0}$ and damps the integral. The perturbative part (III.60) in the IR approximation remains therefore convergent and yields a finite contribution to the perturbative loop potential.

As for the nonperturbative part of $V_{ring}^{\text{static/strong}}$ (III.71), it is given by

$$V_{ring}^{\text{static/nonpert.}} = \frac{mT}{8\pi^2} \left[(m^2 - M_\gamma^2) \ln \left(1 + \frac{2M_\gamma^2 C_1}{m^2 - M_\gamma^2} \right) - 2C_1 M_\gamma^2 \right] + \text{cutoff dependent terms.} \quad (\text{III.73})$$

In the high temperature expansion $m\beta \rightarrow 0$, the most dominant term of the potential (III.73) for $\frac{eB}{m^2} \rightarrow \infty$ is given by

$$V_{ring}^{\text{static/nonpert.}} \Big|_{m\beta \rightarrow 0, \frac{eB}{m^2} \rightarrow \infty} = \frac{49m^4(\zeta(3))^2}{256\pi^6} \left(1 + \frac{2\alpha}{\pi} \frac{eB}{m^2} \right) (m\beta)^3 + \mathcal{O} \left(\frac{m^4}{(eB)^2}, (m\beta)^4 \right). \quad (\text{III.74})$$

The same result will arise if we expand (III.73) first in the orders of $\frac{eB}{m^2} \rightarrow \infty$ for fixed $m\beta$ and then take the limit $m\beta \rightarrow 0$. Together with the perturbative contribution to the effective potential, (III.72), the most dominant part of the ring potential in the limit $\frac{eB}{m^2} \rightarrow \infty$ is given by

$$V_{ring}^{\text{static limit/strong}} \approx \frac{49m^4(\zeta(3))^2}{256\pi^6} \left(1 + \frac{2\alpha}{\pi} \frac{eB}{m^2} \right) (m\beta)^3 + \text{cutoff dependent terms.} \quad (\text{III.75})$$

This result can be compared with (III.65) where, in the order $m\beta$, a novel term proportional to $\frac{2}{\pi} \frac{eB}{m^2} \ln(\frac{2\alpha}{\pi} \frac{eB}{m^2})$ appears.

D. A second possibility to determine the ring potential in the static limit; The strong limit

In III.C, we have determined the ring potential in the static limit using I_2 from (III.40), where we have first taken the limit $eB \rightarrow \infty$. This means that a transition to the LLL is occurred before the ring potential is calculated. Once we are in the LLL, it is necessary to distinguish between two different dynamical regimes in the LLL: $k_3^2 \ll m^2 \ll eB$ and $m^2 \ll k_3^2 \ll eB$, and separate consequently the k_3 integration interval $k_3 \in [0, \infty[$ into two parts, $k_3 \in [0, m]$ and $k_3 \in [m, \infty]$. As we have seen in (III.70) the integrands are also different in these two dynamical regimes. Mathematically, in the LLL, the three-dimensional integration over $\mathbf{k} = (k_1, k_2, k_3)$ in (III.66) and (III.70) are separated into two integrals over k_3 and a symmetric integral over k_1 - k_2 plane, which is perpendicular to the direction of external magnetic field.¹⁸ Physically, this can be viewed as a consequence of the dimensional reduction which is one of the well-known properties of the LLL dynamics [20].

In this section, we will point out that a second approach is also possible to determine the static ring potential in the limit $eB \rightarrow \infty$. In this approach, one starts directly from the ring potential (III.13) and take the limit $eB \rightarrow \infty$ afterwards.¹⁹ Doing this, one arrives at

$$V_{ring}^{\text{strong limit}} = \frac{T}{12\pi} (\Pi_{00}(0, \mathbf{0}))^{3/2} = \frac{T}{12\pi} (I_2^T(0, \mathbf{0}))^{3/2} \xrightarrow{eB \rightarrow \infty} \frac{T}{12\pi} \left[M_\gamma^2 (1 - 2C_1(m\beta, \pi)) \right]^{3/2}, \quad (\text{III.76})$$

where $\Pi_{00}(0, \mathbf{0}) = -\Pi_{44}(0, \mathbf{0}) = I_2^T(0, \mathbf{0})$ from (II.33) and

$$\begin{aligned} I_2^T(0, \mathbf{0}) &= A_2^T = -2M_\gamma^2 \sum_{\ell=1}^{\infty} (-1)^\ell (\ell m\beta) K_1(\ell m\beta) \\ &= M_\gamma^2 (1 - 2C_1(m\beta, \pi)), \end{aligned}$$

from (III.47) are used. In the next section, the ring potential (III.62), (III.73) and (III.76) will be used to study the dynamical chiral symmetry breaking of QED in the LLL.

IV. DYNAMICAL CHIRAL SYMMETRY BREAKING OF QED IN THE LLL

For a given one-loop effective potential $V^{(1)}$, the gap equation is given by [see Appendix B for the derivation of the gap equation at $T = 0$ and Appendix C for a generalization to $T \neq 0$ case]

$$\frac{\partial V^{(1)}(m, eB; T)}{\partial \langle \bar{\psi} \psi \rangle} = Gm, \quad (\text{IV.1})$$

where G is an appropriate coupling and m is the dynamical mass.²⁰ Using the identity $\langle \bar{\psi} \psi \rangle \equiv \frac{\partial V^{(1)}}{\partial m}$, the above equation is given by

$$\frac{\partial V^{(1)}(m, eB; T)}{\partial m} = Gm \frac{\partial^2 V^{(1)}(m, eB; T)}{\partial m^2}. \quad (\text{IV.2})$$

¹⁸ In other words, the integrations over $\mathbf{k} = (k_1, k_2, k_3)$ in (III.66) and (III.70) are to be performed over a cylinder with the basis in k_1 - k_2 plane and the height in the k_3 direction.

¹⁹ Note that mathematically in (III.13), there is no difference between k_3 and $\mathbf{k}_\perp = (k_1, k_2)$ integration. Both the integrand and the integration interval are spherical symmetric over a three-sphere, once we introduce a sharp momentum cutoff Λ to calculate the integral.

²⁰ In this section, we will omit the subscript *dyn* in m_{dyn} . from Appendices A-C.

In this section, we will use (IV.2) to determine the dynamical mass and critical temperature of the dynamical chiral symmetry breaking of QED at finite temperature and in the presence of *strong* magnetic field. To determine the gap equation of this theory, the ring improved effective potential including the one-loop and the ring contributions will be considered. To fix our notations and at the same time to check our procedure, we will first determine in Sect. IV.A, the dynamical mass $m(T)$ and the critical temperature T_c arising from (III.39), the one-loop effective potential of the theory.²¹ In the limit of strong magnetic field $eB \gg m^2$ and in the high temperature limit $m\beta \rightarrow 0$, our results indeed coincide with the results from [31, 41].²²

In the rest of this section, we will examine the possible effects of the ring contribution to the ring improved (one-loop) effective potential on the dynamical mass and critical temperature of QED at finite temperature and in the LLL. To this purpose, we will use the ring potentials in the IR, static and strong magnetic field limits that are calculated in the previous sections. As it is mentioned before, the ring potential arises only in the finite temperature field theory and reflects the infrared behavior of the theory at $T \neq 0$ [see Sect. I.A]. Its contribution to the one-loop effective potential has various effects. In [6], for instance, the phase transition of a simple scalar field theory is considered using the *ring improved* effective potential, including the one-loop *and* the ring contributions. It is shown that the addition of the ring to the one-loop effective potential has indeed two effects: First, in the ring contributions there are terms that cancel certain imaginary terms arising from the one-loop effective potential, and second, the order of phase transition changes from second to first order. The same effect happens also in [7], where in particular, it is shown that after adding the ring contribution to the one-loop effective potential of the electroweak Standard Model (SM), the critical temperature of electroweak symmetry breaking decreases from its value arising from the one-loop effective potential of the theory. It is the purpose of this section to show that the critical temperature of the dynamical chiral symmetry breaking of QED at finite temperature and in the LLL approximation is indeed affected by the contribution from the ring potential. To show this, we will consider in Sect. IV.B the ring potential in the improved IR limit, (III.62), and calculate the dynamical mass and the critical temperature in the strong magnetic field limit $eB \gg m^2$ and high temperature limit $m\beta \rightarrow 0$. Then, in Sect. IV.C and IV.D, the ring potential in the static limit, (III.73), and the strong limit, (III.76), will be considered separately and the corresponding dynamical mass and critical temperature will be determined. Whereas adding the ring potential in the improved IR and strong limits to the one-loop effective potential decreases the critical temperature arising from one-loop effective potential, the ring potential in the static limit does not change $T_c^{(1)}$. In Sect. IV.E, we will finally consider the ratio $T_c^{(1)}/\mathcal{T}_c$, where \mathcal{T}_c is the ring improved critical temperature

²¹ Note that (III.39) is determined using the worldline formalism [34], which is supposed to lead to the same one-loop effective potential arising from the well-known Schwinger proper-time formalism [20, 22, 28]. For the exact definition of the one-loop effective potential in the LLL approximation see Appendix A.

²² In [41] the dynamical mass and the critical temperature of an effective Nambu-Jona Lasinio (NJL) model at finite temperature are determined using the one-loop effective potential of the theory in the presence of an external chromomagnetic field. In [31], the same quantities are determined by solving the SD equation of QED in the presence of a strong magnetic field using a ladder approximation. The common result in these two papers is the well-known relation $T_c^{(1)} = \mathcal{C}m^{(1)}(T=0)$, where $T_c^{(1)}$ is the critical temperature arising from one-loop effective potential/solution of SD equation in the ladder approximation and $m^{(1)}(T=0)$ is the corresponding dynamical mass at zero temperature, and \mathcal{C} is a numerical factor. This relation seems to be model independent. In this section, using the one-loop effective potential of QED in the presence of strong magnetic field, (III.39), and following the procedure described in Sect. IV.A, we arrive at the same result $T_c^{(1)} \approx m^{(1)}(T=0)$ [see (IV.11)].

arising from the *ring improved* effective potential including the one-loop and the ring potential. Further, we will define an efficiency factor $\eta = 1 - u^{-1}$. In this way we will be able to compare numerically the effect of the ring potential in the IR limit with effect of the ring potential in the strong limit in changing $T_c^{(1)}$. As it turns out, compared to the strong limit, the IR limit is more efficient in decreasing the critical temperature arising from one-loop effective potential. This is indeed a promising result in view of the baryogenesis problem in the electroweak SM, when the ring potential in the improved IR limit is considered to calculate the critical temperature of the electroweak SM in the presence of strong magnetic field.²³

A. Dynamical mass and critical temperature arising from QED one-loop effective potential

Let us start from QED one-loop effective potential $V^{(1)/\text{strong}}(m, eB; \Lambda, T)$ in the limit of strong magnetic field (III.39). It consists of a temperature dependent and a temperature independent part. Whereas the temperature dependent part is renormalization free, the temperature independent part depends explicitly on a sharp momentum cutoff Λ .²⁴ In the limit of strong magnetic field, where QED dynamics is described by an effective field theory in the LLL, the momentum cutoff Λ can be replaced by $\Lambda_B \equiv \sqrt{eB}$. In this section, using (III.39) with $\Lambda \rightarrow \Lambda_B$, we will determine the dynamical mass and the critical temperature of the dynamical chiral phase transition arising from QED one-loop effective potential. The results will then be compared with the corresponding results in [31] and [41]. We will show that in the limit of strong magnetic field, $m^2 \ll eB$, and in the high temperature limit, $m\beta \rightarrow 0$, our results coincides with the results from [31, 41].

To start, let us replace the potential V in (IV.2) by (III.39) which is given by

$$V^{(1)/\text{strong}}(m, eB; T) = -\frac{eB}{8\pi^2} \left\{ m^2 \Gamma \left(-1, \frac{m^2}{\Lambda_B^2} \right) + \frac{8m}{\beta} \sum_{n=1}^{\infty} \frac{(-1)^n}{n} K_{-1}(nm\beta) \right\}.$$

We arrive first at

$$\begin{aligned} \frac{\partial V^{(1)/\text{strong}}}{\partial m} - Gm \frac{\partial^2 V^{(1)/\text{strong}}}{\partial m^2} &= \frac{eBm}{4\pi^2} \left[(1-G) \Gamma \left(0, \frac{m^2}{\Lambda_B^2} \right) + 2G \Gamma \left(1, \frac{m^2}{\Lambda_B^2} \right) \right. \\ &\quad \left. + 4(1-G) \sum_{n=0}^{\infty} (-1)^n K_0(nm\beta) + 4G \sum_{n=1}^{\infty} (-1)^n (nm\beta) K_1(nm\beta) \right] = 0. \end{aligned} \quad (\text{IV.3})$$

The above equation will be simplified as follows. First, we take the high temperature limit $m\beta \rightarrow 0$ in the temperature dependent part of (IV.3) which is given in the second line of the above expression. Using (III.31) and (III.33), it turns out that the term proportional to $(nm\beta)K_1(nm\beta)$ behaves as $\approx \mathcal{O}(1)$, whereas the term proportional to $K_0(nm\beta)$ is proportional to $\sim \ln(m\beta)$. Keeping only the logarithmic divergent terms in the limit $m\beta \rightarrow 0$, the term proportional to $(nm\beta)K_1(nm\beta)$ can therefore be

²³ In [10, 11] the standard electroweak symmetry breaking is considered in the presence of a strong hypermagnetic field. To determine the ring potential in the strong magnetic field limit, first the ring integral is calculated and then $eB \rightarrow \infty$ limit is taken, as in (III.76). Our calculation shows that the results in [10, 11] may be improved, if in place of the strong limit, the improved IR limit is used [42].

²⁴ The temperature independent part of the one-loop effective potential is also called "the renormalized effective potential" [33].

neglected in this limit. Next, in the temperature independent part of (IV.3) which is given in the first line of the above expression, we take the strong magnetic field limit, $z \equiv \frac{m^2}{eB} \ll 1$. Using the relation

$$\Gamma(0, z) \xrightarrow{z \rightarrow 0} -\gamma - \ln z, \quad \text{and} \quad \Gamma(1, z) \xrightarrow{z \rightarrow 0} 1,$$

where γ is the Euler-Mascheroni constant, we arrive therefore at the gap equation

$$\ln \frac{m}{\Lambda_B} = -\frac{\gamma}{2} + \frac{G}{1-G} + 2 \sum_{n=1}^{\infty} (-1)^n K_0(nm\beta), \quad (\text{IV.4})$$

where $m \equiv m(G; T)$ is the temperature dependent dynamical mass, which is given by

$$m(G; T) = \Lambda_B \exp \left(-\frac{\gamma}{2} + \frac{G}{1-G} + 2 \sum_{n=1}^{\infty} (-1)^n K_0(nm\beta) \right). \quad (\text{IV.5})$$

At $T = 0$ we have

$$m(G_0; T = 0) = \Lambda_B \exp \left(-\frac{\gamma}{2} + \frac{G_0}{1-G_0} \right). \quad (\text{IV.6})$$

This is a general structure for the dynamical mass as a function of the effective coupling G_0 at zero temperature (see Appendices B and C for an exact definition of G_0 at zero temperature as well as G at finite temperature). As it is shown in (B.5), in the lowest order of α correction, $G_0^{(1)}$ receives contribution from diagrams shown in Fig. 3 (Appendix A) of order α (only the $T = 0$ part of these diagrams are relevant for $G_0^{(1)}$). In higher orders of α expansion G_0 receives contribution from the temperature independents parts of all diagrams shown in Fig. 1 and (I.7) (ring diagrams) at zero temperature.

As we have mentioned in Sect. II.A, the dynamically generated fermion mass in the lowest order of α correction at zero temperature is calculated in [20] and [31] in the ladder LLL approximation.²⁵ It is given by (II.16). Comparing to the exact result, $m(G_0, T = 0)$ from (IV.6), this first correction to the dynamical mass can be indicated as: $m_{dyn}^{(1)} \equiv m^{(1)}(G_0^{(1)}; T = 0)$. As it is shown in Appendix B, the result from (IV.6) is indeed comparable with the dynamical mass $m^{(1)}(G_0^{(1)}; T = 0)$ (II.16), provided $G_0^{(1)}$ in this lowest order of α correction is fixed as in (B.12) *i.e.* by $G_0^{(1)} = 1/(1 - \sqrt{\frac{\alpha}{\pi}}) \approx 1 + \sqrt{\frac{\alpha}{\pi}}$. Plugging this result in (IV.6), we get

$$m^{(1)}(G_0^{(1)}; T = 0) = \mathcal{C}_m \Lambda_B \exp \left(-\sqrt{\frac{\pi}{\alpha}} \right), \quad \mathcal{C}_m = e^{-\gamma/2} = 0.749306. \quad (\text{IV.7})$$

As next, let us determine the critical temperature of chiral symmetry breaking of QED in the LLL approximation. To do this we use the gap equation (IV.4), and replace [see (III.31)]

$$\sum_{n=1}^{\infty} (-1)^n K_0(nm\beta) \rightarrow \frac{1}{2} \left(\gamma + \ln \frac{m\beta}{4\pi} \right) + C_0(m\beta, \pi).$$

²⁵ Note that in [31] apart from the ladder approximation, a constant mass approximation (CMA) is also used. In this approximation, one neglects the fermion mass structure in the solution of the corresponding SD equation [43]. In other words momentum dependence of self-energy in the gap equation are neglected in this approximation. As it is shown in [44] this turns out to be a reliable approximation in QED (with only one coupling constant) in the presence of a strong magnetic field limit, although there is no general principle that guarantees the validity of this approximation for the whole range of physical coupling. In other theories with more than one coupling constant, due to the richness of parameter space, the reliability of CMA is questionable and should be investigated in detail (see Elizalde *et al.* in [43]).

The critical temperature arising from one-loop effective potential (III.39), $T_c(G; T)$, can now be determined from the condition $m(T_c) = 0$. It is given as a function of G by [see Appendix C for an exact definition of G]

$$T_c(G; T) = \Lambda_B \exp \left(\frac{\gamma}{2} + \frac{G}{1-G} + 2 \ln 2 \right). \quad (\text{IV.8})$$

Here, we have used the expansion of $C_0(t, \pi)$

$$C_0(t, \pi) = \ln 2 - \frac{7t^2 \zeta(3)}{16\pi^2} + \mathcal{O}(t^4), \quad (\text{IV.9})$$

at $t = 0$. The critical temperature as it is given in (IV.8) includes all orders of α correction through definition of G from (C.6). All diagrams contributing to G are to be considered at finite temperature. In the lowest order of α correction, $G^{(1)}$ receives contributions from diagrams shown in Fig. 3 of order α . This fact allows us to compare (IV.8) in the lowest order of α correction, *i.e.* $T_c^{(1)}$, with the critical temperature arising from the SD equation including the contributions from the same two diagrams in Fig. 3, that are relevant in determining $m^{(1)}(G_0^{(1)}; T = 0)$ [31]. Doing this $G^{(1)}$ is again fixed to be $G^{(1)} = G_0^{(1)} = 1/(1 - \sqrt{\frac{\alpha}{\pi}}) \approx 1 + \sqrt{\frac{\alpha}{\pi}}$. Plugging this expression in (IV.8), we arrive at

$$T_c^{(1)}(G^{(1)}; T) = \mathcal{C}_T \Lambda_B \exp \left(-\sqrt{\frac{\pi}{\alpha}} \right), \quad \mathcal{C}_T = \pi^{-1} e^{\gamma/2} = 0.156277, \quad (\text{IV.10})$$

which is comparable with the result from [31]. Comparing to $m^{(1)}(0)$ from (IV.7), we arrive at the well-known relation

$$T_c^{(1)} = \pi^{-1} e^{\gamma} m^{(1)}(0) = 0.424806 m^{(1)}(0). \quad (\text{IV.11})$$

The same relation arises in [41] between the critical temperature $T_c^{(1)}$ and the dynamical mass $m^{(1)}(T = 0)$ in the effective NJL model in the presence of constant chromomagnetic field. Note that in higher orders of α correction, the critical temperature $T_c(G; T)$ receive contribution from higher loop diagrams through the definition of G from (C.6).

As next, we will determine the gap equation, the dynamical mass and the critical temperature for the *ring improved* effective potential including the one-loop effective potential (III.39) and the ring potential in the IR, static and strong limits [see (III.62), (III.73) and (III.76), respectively].

B. Full dynamical mass and critical temperature of QED in the IR limit

Full dynamical mass in the IR limit

As in (IV.2), the general structure of the gap equation corresponding to the *ring improved* effective potential (see Appendix C for more details), $\tilde{V} \equiv V^{(1)} + V_{ring}$, is given by

$$\frac{\partial \tilde{V}}{\partial \tilde{m}} = \tilde{G} \tilde{m} \frac{\partial^2 \tilde{V}}{\partial \tilde{m}^2}. \quad (\text{IV.12})$$

In \tilde{V} , $V^{(1)}$ and V_{ring} denote the one-loop effective potential and the ring contribution to the effective potential, respectively. Here, comparing to the effective coupling G in (IV.1), the modified coupling \tilde{G} is

given by²⁶

$$G = \tilde{G} - \frac{1}{\tilde{m}} \frac{\partial V_{ring}(\tilde{m}, eB; T)}{\partial \langle \bar{\psi} \psi \rangle}.$$

Using the gap equation arising from ring improved effective potential including the one-loop effective potential and the ring potential and following the same procedure as was described in Sect. IV.A, the *full* dynamical mass $\tilde{m}(\tilde{G}, T)$ reads

$$\tilde{m}(\tilde{G}; T) = m(\tilde{G}; T) \exp \left(+ \frac{2\pi^2}{eB\tilde{m}(1-\tilde{G})} \left[\frac{\partial V_{ring}}{\partial \tilde{m}} - \tilde{G}\tilde{m} \frac{\partial^2 V_{ring}}{\partial \tilde{m}^2} \right] \right). \quad (\text{IV.13})$$

On the r.h.s. of this expression $m(G; T)$ is given by the dynamical mass arising from one-loop effective potential (IV.5) with G replaced by \tilde{G} . Here, to determine the full dynamical mass in the IR limit, \tilde{m}^{IR} , we will replace V_{ring} on the r.h.s. of (IV.13) by the ring contribution of the LLL ring potential in the IR limit (III.62),²⁷ and arrive first at

$$\begin{aligned} & \frac{2\pi^2}{eB\tilde{m}(1-\tilde{G})} \left[\frac{\partial V_{ring}^{\text{IR/nonpert.}}}{\partial \tilde{m}} - \tilde{G}\tilde{m} \frac{\partial^2 V_{ring}^{\text{IR/nonpert.}}}{\partial \tilde{m}^2} \right] = \\ & = + \frac{2}{\tilde{m}\beta(1-\tilde{G})} \left\{ \frac{\tilde{G}z^2}{(1+z^2)} - \frac{\tilde{G}z^2 \left(6 - 10C_1 + 5\tilde{m}\beta C_1'\right)^2}{36 \left(1 - \frac{5}{3}C_1\right) \left(1 + z^2 \left(1 - \frac{5}{3}C_1\right)\right)} \right. \\ & \quad + \frac{(1-\tilde{G})}{2} \left[\ln(1+z^2) - \ln \left(1 + z^2 \left(1 - \frac{5}{3}C_1\right)\right) \right] + \frac{1}{4} \left[\text{Li}_2(-z^2) - \text{Li}_2 \left(-z^2 \left(1 - \frac{5}{3}C_1\right)\right) \right] \\ & \quad \left. - \frac{5\tilde{m}\beta \left(\left(1 - 2\tilde{G}\right) (3 - 5C_1) C_1' - 5\tilde{G}\tilde{m}\beta C_1'^2 - \tilde{G}\tilde{m}\beta (3 - 5C_1) C_1'' \right)}{36 \left(1 - \frac{5}{3}C_1\right)^2} \ln \left(1 + z^2 \left(1 - \frac{5}{3}C_1\right)\right) \right\}. \end{aligned} \quad (\text{IV.14})$$

Here, $\tilde{G} = \tilde{G}^{\text{IR}}$ and $\tilde{m} = \tilde{m}^{\text{IR}}$.²⁸ Further, $z^2(\tilde{m}) \equiv \frac{M_2^2}{\tilde{m}^2} = \frac{2\alpha}{\pi} \frac{eB}{\tilde{m}^2}$. Using (IV.9), the expansion of $C_0(t, \pi)$ in the orders of $t \equiv \tilde{m}\beta$, and the relations

$$\begin{aligned} C_1(t, \pi) &= \frac{7t^2\zeta(3)}{4\pi^2} + \mathcal{O}(t^3), \\ C_1'(t, \pi) &= \frac{7t\zeta(3)}{4\pi^2} + \mathcal{O}(t^3), \\ C_1''(t, \pi) &= \frac{7\zeta(3)}{4\pi^2} - \frac{279t^2\zeta(5)}{16\pi^4} + \mathcal{O}(t^3), \end{aligned} \quad (\text{IV.15})$$

the full dynamical mass in the IR limit is given by

$$\tilde{m}^{\text{IR}}(\tilde{G}^{\text{IR}}; T) \approx m(\tilde{G}^{\text{IR}}; T) (1 + (\tilde{m}^{\text{IR}}\beta)\mathcal{E}^{\text{IR}}), \quad (\text{IV.16})$$

²⁶ See Appendix C.3 for an exact definition of \tilde{G} .

²⁷ The perturbative part of the ring potential in the IR limit from (III.60) is mass independent and has therefore no contribution to the gap equation, the dynamical mass and the critical temperature. We will therefore omit this mass independent contribution in this section.

²⁸ See (C.14) in Appendix C for the difference between \tilde{G} and \tilde{G}^{IR} .

where

$$\mathcal{E}^{\text{IR}} \equiv +\frac{35\zeta(3)}{24\pi^2} \frac{(1-5\tilde{G}^{\text{IR}})}{(1-\tilde{G}^{\text{IR}})} \left(1 - \frac{3}{2} \frac{(1-2\tilde{G}^{\text{IR}})}{(1-5\tilde{G}^{\text{IR}})} \ln \left(\frac{2\alpha}{\pi} \frac{eB}{\tilde{m}_{\text{IR}}^2} \right) \right) + \mathcal{O} \left(\frac{\tilde{m}_{\text{IR}}^4}{(eB)^2} \right). \quad (\text{IV.17})$$

Full critical temperature in the IR limit

Using the gap equation (IV.12) with the ring improved effective potential \tilde{V} , and following the same procedure described in Sect. IV.A to determine the critical temperature arising from the one-loop effective potential, we arrive first at the following general expression for the *full* critical temperature

$$\tilde{T}_c(\tilde{G}; T) = T_c(\tilde{G}; T) \exp \left(+\frac{2\pi^2}{eB\tilde{m}(1-\tilde{G})} \left[\frac{\partial V_{\text{ring}}}{\partial \tilde{m}} - \tilde{G}\tilde{m} \frac{\partial^2 V_{\text{ring}}}{\partial \tilde{m}^2} \right] \right) \Big|_{\tilde{m}(T_c)=0}. \quad (\text{IV.18})$$

Here, $T_c(\tilde{G}; T)$ is given in (IV.8) by replacing G by \tilde{G} . To determine the full critical temperature \tilde{T}_c of dynamical chiral symmetry restoration in the IR limit, we have to recalculate the ring potential, (III.43), for a fixed, temperature independent mass cutoff m_0 ²⁹. To do this we separate the integral over $k_3 \in [0, \infty]$ in (III.43) into two regimes $[0, m_0]$ and $[m_0, \infty]$ and follow the same procedure which led from (III.43) to (III.62). We arrive at the relevant nonperturbative part of ring potential in the IR limit

$$V_{\text{ring}}^{\text{IR}}(eB, m_0; T) = -\frac{m_0 T e B}{4\pi^2} \left\{ \text{Li}_2 \left(-\frac{M_\gamma^2}{m_0^2} \left(1 - \frac{5}{3} C_1(m\beta, \pi) \right) \right) - \text{Li}_2 \left(-\frac{M_\gamma^2}{m_0^2} \right) \right\}. \quad (\text{IV.19})$$

Replacing (IV.19) on the r.h.s. of (IV.18), we get first

$$\begin{aligned} & \frac{2\pi^2}{eB\tilde{m}(1-\tilde{G})} \left[\frac{\partial V_{\text{ring}}}{\partial \tilde{m}} - \tilde{G}\tilde{m} \frac{\partial^2 V_{\text{ring}}}{\partial \tilde{m}^2} \right] = \\ & = -\frac{5m_0\beta}{6(1-\frac{5}{3}C_1)(1-\tilde{G})} \left\{ \frac{5}{3} C_1'^2 \tilde{G} \left[\frac{z_0^2}{(1+z_0^2(1-\frac{5}{3}C_1))} - \frac{\ln(1+z_0^2(1-\frac{5}{3}C_1))}{1-\frac{5}{3}C_1} \right] \right. \\ & \quad \left. + \left[\left(\frac{C_1'}{\tilde{m}\beta} - C_1'' \tilde{G} \right) \ln \left(1 + z_0^2 \left(1 - \frac{5}{3} C_1 \right) \right) \right] \right\}. \end{aligned} \quad (\text{IV.20})$$

Here, $\tilde{G} = \tilde{G}^{\text{IR}}$ and $\tilde{m} = \tilde{m}^{\text{IR}}$. Further, $z_0^2 \equiv z^2(m_0) = \frac{M_\gamma^2}{m_0^2} = \frac{2\alpha}{\pi} \frac{eB}{m_0^2}$. Using now the definition $m(T_c) = 0$ and using (IV.9) as well as (IV.15) to determine $C_i, i = 0, 1$, C_1' and C_1'' at $m = 0$, we arrive at the full critical temperature of QED in the IR limit

$$\tilde{T}_c^{\text{IR}}(\tilde{G}^{\text{IR}}; T) = T_c(\tilde{G}^{\text{IR}}; T) \exp \left(-\frac{35\zeta(3)}{24\pi^2} (m_0 \tilde{\beta}_c^{\text{IR}}) \ln(1+z_0^2) \right). \quad (\text{IV.21})$$

Here, $T_c^{(1)}$ is given in (IV.8) and $\tilde{\beta}_c^{\text{IR}} \equiv 1/\tilde{T}_c^{\text{IR}}$.

²⁹ m_0 plays the role of an IR regulator.

C. Full dynamical mass and critical temperature of QED in the static limit

In Sect. III.C and III.D, we have presented two different approaches leading to the ring contribution to the effective potential in the static limit $(k_0, \mathbf{k}) = (0, \mathbf{0})$ for strong magnetic field. First using the method presented in III.C, we arrived at the nonperturbative part of the ring potential (III.73). In a second approach in III.D, we just started from the ring potential (III.13) and took the limit $eB \rightarrow \infty$. This leads to the ring potential (III.76). Although it seems that these two approaches are physically equivalent, but according to our arguments in Sect. III.D, they are indeed different.³⁰ In this section, we will determine the full dynamical mass and critical temperature using the ring potential in the static limit. In the next section, these quantities are calculated using the ring potential in the strong limit.³¹

Full dynamical mass in the static limit

Let us consider first the nonperturbative part of the LLL ring potential in the static limit (III.73)

$$V_{ring}^{\text{st./nonpert.}} = \frac{mT}{8\pi^2} \left[(m^2 - M_\gamma^2) \ln \left(1 + \frac{2M_\gamma^2 C_1}{m^2 - M_\gamma^2} \right) - 2C_1 M_\gamma^2 \right], \quad (\text{IV.22})$$

where we have omitted the irrelevant mass independent terms. The *full* dynamical mass $\tilde{m}(\tilde{G}; T)$, arising from one-loop and ring contribution to the effective potential is given in (IV.13), where V_{ring} is to be replaced by (IV.22). Doing this, we arrive first at

$$\begin{aligned} & \frac{2\pi^2}{eB\tilde{m}(1-\tilde{G})} \left[\frac{\partial V_{ring}^{\text{static/nonpert.}}}{\partial \tilde{m}} - \tilde{G}\tilde{m} \frac{\partial^2 V_{ring}^{\text{static/nonpert.}}}{\partial \tilde{m}^2} \right] = \\ & = -\frac{\tilde{m}T}{4eB(1-\tilde{G})} \left\{ 2z^2 \left[\tilde{m}\beta \left((1-2\tilde{G})C_1' - \tilde{m}\beta\tilde{G}C_1'' \right) + C_1 \right] - \frac{4z^4 \left(2C_1 - \tilde{m}\beta(1-z^2)C_1' \right)^2}{(1-z^2)(1-z^2+2z^2C_1)^2} \right. \\ & \quad - [3(1-2\tilde{G}) - z^2] \ln \left(1 + \frac{2z^2C_1}{1-z^2} \right) \\ & \quad \left. + \frac{2z^2 \left[2(1-3\tilde{G})C_1 - \tilde{m}\beta(1-z^2) \left((1-2\tilde{G})C_1' - \tilde{m}\beta\tilde{G}C_1'' \right) \right]}{(1-z^2+2z^2C_1)} \right\}. \end{aligned} \quad (\text{IV.23})$$

Here, $\tilde{G} = \tilde{G}^{\text{st.}}$ and $\tilde{m} = \tilde{m}^{\text{st.}}$. Using (IV.9) and (IV.15) to expand $C_i, i = 0, 1$ as well as C_1' and C_1'' in the order of $m\beta$, the full dynamical mass in the static limit is given by

$$\tilde{m}^{\text{st.}}(\tilde{G}^{\text{st.}}; T) \approx m(\tilde{G}^{\text{st.}}; T) \left(1 + (\tilde{m}^{\text{st.}}\beta)^3 \mathcal{E}^{\text{st.}} \right), \quad (\text{IV.24})$$

³⁰ In the first approach, we take first the limit $eB \rightarrow \infty$ and then calculate the ring integral. In the second approach, however, we calculate first the ring integral and then take the limit $eB \rightarrow \infty$. As it turns out, the limit $eB \rightarrow \infty$ and the integration over k_3 in the LLL are not commutative. Physically, this can be viewed as a direct consequence of dimensional reduction, which is one of the well-known properties of the LLL dynamics.

³¹ Although we believe that in the LLL the first approach (static limit) is more reliable, we will present the results corresponding to the strong limit in Sect. IV.D. This is just to compare them with the result from IR limit in Set. IV.B.

where $m^{(1)}(T)$ is given in (IV.5) and

$$\mathcal{E}^{\text{st.}} \equiv +\frac{245\alpha(\zeta(3))^2}{64\pi^5} \frac{(1 - 4\tilde{G}^{\text{st.}})}{(1 - \tilde{G}^{\text{st.}})} + \mathcal{O}\left(\frac{(\tilde{m}^{\text{st.}})^4}{(eB)^2}\right). \quad (\text{IV.25})$$

This result can be compared with (IV.16)-(IV.17) from the improved IR limit. Whereas \tilde{m}^{IR} in (IV.17) consists of a $\ln \alpha$ in the leading order of $eB \rightarrow \infty$ and $m\beta \rightarrow 0$ limits, $\tilde{m}^{\text{st.}}$ in (IV.24)-(IV.25) has no contribution in the order $\tilde{m}\beta$. Thus, in the high temperature limit $m\beta \rightarrow 0$, we have practically $\tilde{m}^{\text{st.}} \approx \tilde{m}$. As it will be shown below, the ring potential in the static limit does not change the full critical temperature in this limit too.

Full critical temperature in the static limit

Here, as in the previous part, the critical temperature of dynamical chiral symmetry breaking can be determined only after recalculating the ring potential (III.66) for a fixed, temperature independent mass cutoff m_0 . We separate the interval $[0, \infty]$ of the integration over k_3 in (III.66) into two intervals $[0, m_0]$ and $[m_0, \infty]$ and follow the same steps leading from (III.66) to (III.73) as the relevant nonperturbative part of the ring potential. We arrive therefore at

$$V_{ring}^{\text{static limit}}(eB, m_0; T) = \frac{m_0^3 T (1 - z_0^2)}{8\pi^2} \ln \left(1 + \frac{2C_1 z_0^2}{1 - z_0^2} \right) - \frac{m_0^3 z_0^2 T C_1}{4\pi^2}. \quad (\text{IV.26})$$

Replacing (IV.26) on the r.h.s. of (IV.18) we get first

$$\begin{aligned} & \frac{2\pi^2}{eB\tilde{m}(1 - \tilde{G})} \left[\frac{\partial V_{ring}^{\text{IR}}}{\partial \tilde{m}} - \tilde{G}\tilde{m} \frac{\partial^2 V_{ring}^{\text{IR}}}{\partial \tilde{m}^2} \right] = \\ & = -\frac{M_\gamma^2 m_0 \beta}{2eB(1 - \tilde{G})} \left\{ \left(\frac{C_1'}{\tilde{m}\beta} - C_1'' \tilde{G} \right) \left(1 - \frac{(1 - z_0^2)}{(1 - z_0^2(1 - 2C_1))} \right) - 2\tilde{G}C_1'^2 z_0^2 \left(\frac{(1 - z_0^2)}{(1 - z_0^2(1 - 2C_1))^2} \right) \right\}. \end{aligned} \quad (\text{IV.27})$$

Here, $\tilde{G} = \tilde{G}^{\text{st.}}$ and $\tilde{m} = \tilde{m}^{\text{st.}}$. Using now the definition $m(T_c) = 0$ and (IV.9) as well as (IV.15) to determine $C_i, i = 0, 1$, C_1' and C_1'' at $m = 0$, it turns out that full critical temperature of QED receives no contribution from the ring potential in the static limit, *i.e.*

$$\tilde{T}_c^{\text{st.}}(\tilde{G}^{\text{st.}}; T) = T_c(\tilde{G}^{\text{st.}}; T), \quad (\text{IV.28})$$

where $T_c(\tilde{G}^{\text{st.}}; T)$ can be read from (IV.8) by replacing G with $\tilde{G}^{\text{st.}}$.

D. Full dynamical mass and critical temperature of QED in the strong limit

Full dynamical mass in the strong limit

To determine the *full* dynamical mass in the strong limit, we use (IV.13) and replace V_{ring} by (III.76)

$$V_{ring}^{\text{strong}} = \frac{T}{12\pi} \left[M_\gamma^2 (1 - 2C_1(m\beta, \pi)) \right]^{3/2}. \quad (\text{IV.29})$$

Here, we have neglected the cutoff dependent terms. The full dynamical mass $\tilde{m}(T)$, arising from one-loop effective potential (III.39) and the ring contribution to the effective potential is given in (IV.13), where V_{ring} is to be replaced by (IV.29). Doing this, we arrive first at

$$\frac{2\pi^2}{eB\tilde{m}(1-\tilde{G})} \left[\frac{\partial V_{ring}^{strong}}{\partial \tilde{m}} - \tilde{G}\tilde{m} \frac{\partial^2 V_{ring}^{strong}}{\partial \tilde{m}^2} \right] = -\frac{M_\gamma^3 \pi \beta (1-2C_1)^{1/2}}{2eB(1-\tilde{G})} \left(\frac{C_1'}{\tilde{m}\beta} - C_1''\tilde{G} + \frac{\tilde{G}C_1^2}{(1-2C_1)} \right). \quad (IV.30)$$

Here, $\tilde{G} = \tilde{G}^{str.}$ and $\tilde{m} = \tilde{m}^{str.}$. In the high temperature limit $m\beta \rightarrow 0$ and for the strong magnetic field, the dynamical mass behaves as

$$\tilde{m}^{str.}(T) \approx m(1 + (\tilde{m}^{str.}\beta)\mathcal{E}^{strong}), \quad \text{with} \quad \mathcal{E}^{strong} \equiv -\frac{7\zeta(3)\alpha}{2\pi^2} \left(\frac{2\alpha}{\pi} \frac{eB}{(\tilde{m}^{str.})^2} \right)^{1/2}. \quad (IV.31)$$

This result is in contrast to \mathcal{E}^{IR} from (IV.16)-(IV.17), where a novel term proportional to $\ln \alpha$ appears. Besides it is in contrast to (IV.24)-(IV.25), where the first nonvanishing coefficient in the $m\beta \rightarrow 0$ expansion is of order $(m\beta)^3$ and can be practically neglected in the very high temperature.

Full critical temperature in the strong limit

To determine the critical temperature corresponding to the ring improved effective potential, (IV.18) has to be used. Replacing (IV.29) in the exponent of (IV.18), we arrive, as it is shown above, at (IV.30).³² Setting $m = 0$ in (IV.30) and using (IV.9) as well as (IV.15), we arrive at

$$\tilde{T}_c^{strong}(\tilde{G}^{strong}; T) = T_c(\tilde{G}^{strong}; T) \exp \left(-\frac{7\zeta(3)\alpha}{4\pi^2} (m_0 \tilde{\beta}_c^{strong}) z_0 \right). \quad (IV.32)$$

Here, the temperature independent mass m_0 is introduced by hand. This enables us to compare this result with the previous results from the IR limit (IV.21) and the static limit (IV.28).

In the next section, we study the effect of ring contribution to the effective potential in decreasing the critical temperature arising only from the one-loop effective potential.³³ To this purpose, we compare numerically the critical temperature of chiral symmetry restoration in three different approximation: T_c from (IV.21) in the IR limit, T_c from (IV.28) in the static limit and finally T_c from (IV.32) in the strong limit.

E. Numerical analysis of T_c

In Sect. IV.B - IV.D, we have determined the ring improved critical temperature of QED in the LLL using the ring potential from IR, static and strong limits. They are given in (IV.21), (IV.28) and (IV.32), respectively. Note that, according to our arguments in Appendix C, these results are indeed exact (full in quantum corrections). They include all quantum correction through the coupling $\tilde{G}^{\{IR, st., strong\}}$

³² Note that here, in contrast to the previous two cases, no constant mass cutoff m_0 is necessary to calculate the ring potential leading to the critical temperature.

³³ As it is known from [7], the ring contribution to the effective potential of Standard Model without magnetic field decreases the critical temperature arising from one-loop effective potential. The same phenomenon is shown to be true in the presence of magnetic field [10, 11] in the static limit $(k_0, \mathbf{k}) = (0, \mathbf{0})$.

[see (C.13) for a mathematically rigorous definition of \tilde{G}^{\aleph} , $\aleph = \{\text{IR}, \text{st.}, \text{strong}\}$]. In this section, we will study the effect of the ring diagram in decreasing the critical temperature that arises from the lowest order of α -correction (ladder approximation), *i.e.* $T_c^{(1)}(G^{(1)}; T)$ from (IV.10).³⁴ To do this let us consider $T_c(\tilde{G}^{\{\text{IR}, \text{st.}, \text{strong}\}}; T)$, the factors behind the ring contribution on the r.h.s. of (IV.21), (IV.28) and (IV.32). Now consider $T_c(\tilde{G}^{\{\text{IR}, \text{st.}, \text{strong}\}}; T)$, only in the lowest order of α correction and denote the resulting expression by $T_c(\tilde{G}^{(1)/\{\text{IR}, \text{st.}, \text{strong}\}}; T)$. Next, use the following approximation, which is only reliable in the high temperature limit $m\beta \rightarrow 0$ and for $eB \gg m^2$,³⁵

$$T_c(\tilde{G}^{(1)/\text{IR}}; T) \approx T_c(\tilde{G}^{(1)/\text{st.}}; T) \approx T_c(\tilde{G}^{(1)/\text{strong}}; T) \approx T_c^{(1)}(G^{(1)}; T). \quad (\text{IV.33})$$

Using this approximation, we will be now able to compare the effect of ring potential in different limits, the IR, the static and the strong limits in decreasing $T_c^{(1)}$. To do this, let us first define the ring improved critical temperature by

$$\mathcal{T}_c \equiv T_c^{(1)} \exp\left(-\frac{m_0 \kappa}{\mathcal{T}_c}\right). \quad (\text{IV.34})$$

The argument in the exponent is the nonperturbative contribution from ring potential. Comparing (IV.34) with the critical temperature arising from ring potential in IR, static and strong limit from (IV.21), (IV.28) and (IV.32), respectively, and using the approximation (IV.33), we get

$$\kappa^{\text{IR}} = \frac{35\zeta(3)}{24\pi^2} \ln(1 + z_0^2), \quad (\text{IV.35})$$

for the IR limit,

$$\kappa^{\text{static}} = 0, \quad (\text{IV.36})$$

for the static limit, and

$$\kappa^{\text{strong}} = \frac{7\zeta(3)\alpha}{4\pi^2} z_0, \quad (\text{IV.37})$$

for the strong limit. Then, solving (IV.34) as a function of \mathcal{T}_c , the ring improved critical temperature \mathcal{T}_c in all three cases can be determined as a function of the one-loop critical temperature in the ladder approximation, $T_c^{(1)}$, the temperature independent mass, m_0 , and the parameter κ . Doing this, we get

$$\mathcal{T}_c = -\frac{m_0 \kappa}{W\left(-\frac{m_0}{T_c^{(1)}} \kappa\right)}, \quad (\text{IV.38})$$

³⁴ Ring contributions lead to nonperturbative correction to the critical temperature $T_c^{(1)}$.

³⁵ Note that according to our descriptions in Appendix C.4, for different approaches to the ring potential $\aleph = \{\text{IR}, \text{static}, \text{strong}\}$, the quantity $\Delta T_c^{\aleph} = T_c^{\aleph}(\tilde{G}^{(1)/\aleph}; T) - T_c^{(1)}(G^{(1)}; T)$ vanishes only in the limit of high temperature ($m\beta \rightarrow 0$) and strong magnetic field ($eB \gg m^2$). Thus the above approximation (IV.33) is only reliable in these limits. To check this for the IR limit, for instance, let us consider $G^{(1)}$ and $\tilde{G}^{(1)/\text{IR}}$ from (C.6) and (C.17), respectively. In the lowest order of α correction $G^{(1)} - \tilde{G}^{(1)/\text{IR}} = -\frac{1}{m_{dyn.} \Omega} \frac{\partial}{\partial \langle \psi \psi \rangle} \left(\alpha \mathcal{R}_{N=1}^{(n=0)} \right)$. This is a term that arises from the two-loop diagram (a) in Fig. 3 ($N = 1$) and includes only zero Matsubara frequencies ($n = 0$). As it turns out, in the limit of $eB \gg m^2$, this term leads to a term proportional to $(m\beta)^{-1}$. Adding this contribution to the gap equation arising from one-loop effective potential (IV.3), this contribution can indeed be neglected in the high temperature limit $m\beta \rightarrow 0$ comparing to logarithmic divergent term including in $K_0(nm\beta)$ in $m\beta \rightarrow 0$ limit [see our descriptions in the paragraph following (IV.3)].

where the Lambert-function $W(z)$, is a function that satisfies [45]

$$W(z)e^{W(z)} = z.$$

To have a quantitative first estimate on the effect of the ring potential on decreasing the one-loop critical temperature $T_c^{(1)}$, we define further

$$u \equiv \frac{T_c^{(1)}}{\mathcal{T}_c} = \frac{W(-a\kappa)}{-a\kappa} \quad \text{with} \quad a \equiv \frac{m_0}{T_c^{(1)}}, \quad (\text{IV.39})$$

using (IV.38) and the efficiency factor

$$\eta \equiv 1 - \frac{1}{u}. \quad (\text{IV.40})$$

In Table I the values of u and η for various choices of $eB \in [10^{-8}, 1]$ GeV² and for fixed $a = 2$ are listed.

eB in GeV ²	B in Gauß	u^{IR}	η^{IR} in %	u^{static}	η^{static} in %	u^{strong}	η^{strong} in %
10^{-8}	1.7×10^{12}	1.00007	0.01%	1.	0%	1.00004	0.004%
10^{-7}	1.7×10^{13}	1.00066	0.07%	1.	0%	1.0001	0.01%
10^{-6}	1.7×10^{14}	1.01	0.65%	1.	0%	1.0004	0.04%
10^{-5}	1.7×10^{15}	1.07	6.26%	1.	0%	1.0013	0.13%
3.2×10^{-5}	5.3×10^{15}	1.22	18.19%	1.	0%	1.0024	0.24%
5.0×10^{-5}	8.5×10^{15}	1.38	27.60%	1.	0%	1.0030	0.30%
7.9×10^{-5}	1.3×10^{16}	1.77	43.39%	1.	0%	1.0038	0.38%
8.9×10^{-5}	1.5×10^{16}	2.07	50.17%	1.	0%	1.0040	0.40%
9.8×10^{-5}	1.6×10^{16}	2.67	62.62%	1.	0%	1.0042	0.42%
10^{-4}	1.7×10^{16}	$2.65 - 0.45i$	—	1.	0%	1.0043	0.43%
10^{-1}	1.7×10^{19}	$-0.14 - 0.7i$	—	1.	0%	1.1699	14.53%
1	1.7×10^{20}	$-0.16 - 0.5i$	—	1.	0%	$2.13 - 1.24i$	—

TABLE I: The values of u and the efficiency factor η for different values of eB and different limits (IR, static and strong limit). Here a , the proportionality factor between m_0 and $T_c^{(1)}$ is chosen to be $a = 2$. The efficiency factor η increases by increasing the strength of magnetic field. For a given value of eB , the IR limit is more efficient in decreasing the critical temperature from its value arising from one-loop effective potential $T_c^{(1)}$.

The results are also drawn in the graphs of Fig. 2. Here, eB is in GeV² (1 GeV=10⁹ eV) which is equivalent to $B = 1.691 \times 10^{20}$ in Gauß.³⁶ The above range corresponds therefore to $B \in [1.7 \times 10^{12}, 1.7 \times 10^{20}]$ Gauß, which is phenomenologically relevant in the astrophysics of neutron stars, where it is believed that the strength of the magnetic field is of the order $10^{13} - 10^{15}$ Gauß. It is also relevant in the heavy ion experiments, for example in RHIC, where it is believed that the magnetic field in the center of gold-gold collision is $10^2 - 10^3$ MeV² corresponding to $B \sim 10^{16} - 10^{17}$ Gauß (Here, the center

³⁶ In this paper, we have worked in Planck units, where $\hbar = c = 1$. In these units eB has the dimension of energy, *i.e.* Joule (J) and will be denoted eB as $[eB]_J$. To get a relation between $[eB]_J$ and B in Gauß, we have to convert eB into SI units, where we get $eB = \frac{[eB]_J}{\hbar c^2}$. Having in mind that $\hbar = 1.054 \times 10^{-34}$ Js, $e = 1.602 \times 10^{-19}$ C and $c = 2.998 \times 10^8$ m/s, we get $B = 6.589 \times 10^{35} ([eB]_J)^2$ Tesla = $6.589 \times 10^{39} ([eB]_J)^2$ in Gauß, providing $[eB]_J$ is in Joule. Choosing, for instance, $eB = 1$ GeV², which is equivalent to $([eB]_J)^2 = 2.567 \times 10^{-20}$ J², we get $B = 1.691 \times 10^{20}$ in Gauß. Here, we have used $1\text{J}=6.241 \times 10^9$ GeV.

of mass energy is ~ 200 GeV per nucleon pair) [27]. Defining further m_0 as the zero temperature mass, *i.e.* $m_0 \equiv m(0)$, the above choices for a are indeed justified by the fact that the dynamical mass at zero temperature $m(0)$ is proportional to the critical temperature $T_c^{(1)}$ with a proportionality factor $a = \mathcal{O}(1)$ [31, 41]. To determine $z_0^2 = \frac{2\alpha}{\pi} \frac{eB}{m_0^2}$, we have fixed $\alpha = \frac{1}{137}$ and chosen $m_0 = 0.5$ MeV, the electron mass at zero temperature.

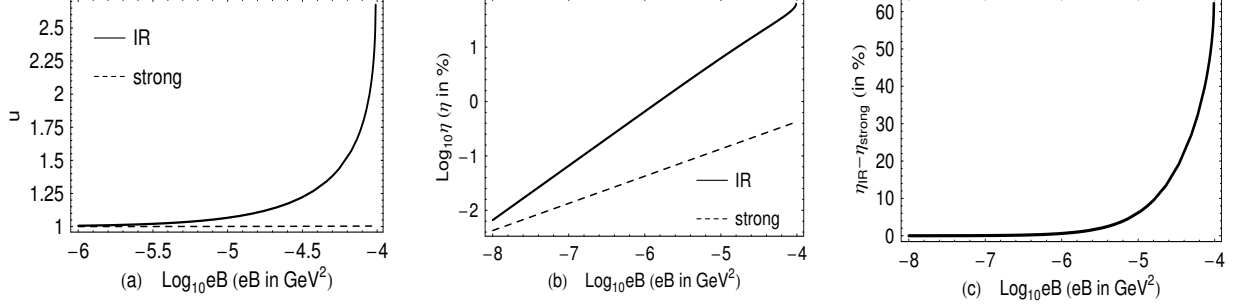


FIG. 2: (a) Fixing $a = 2$, the ratio $u \equiv T_c^{(1)}/T_c$ for the IR and strong limit is considered versus $\text{Log}_{10} eB$ (eB in GeV^2). The effect of the ring potential in the strong limit in decreasing $T_c^{(1)}$ is minimal comparing to the effect of the ring potential in the IR limit. (b) For η the efficiency factor, $\log_{10} \eta$ is considered versus $\log_{10} eB$ for the improved IR and the strong limit. The efficiency factor η increases with increasing eB . (c) The difference of the efficiency factor between the improved IR and strong limits, $\Delta\eta \equiv \eta^{\text{IR}} - \eta^{\text{strong}}$, is considered versus $\text{Log}_{10} eB$. $\Delta\eta$ increases with increasing eB . The maximum $\Delta\eta_{\star} \approx 62\%$ for $B \approx 1.6 \times 10^{16}$ Gauß. Note that u for the static limit is $u^{\text{static}} = 1$.

As it can be seen in Table I, for every given values of m_0 and a , there is always a certain value of $(eB)_{\star}$, for which u is imaginary and η cannot be defined. This is due to the fact that the Lambert W -function, $W(z)$ in (IV.39), has a branch cut discontinuity in the complex z plane running from $z = -\infty$ to $z = -1/e$. Here, e is the Euler number. Using (IV.39), this threshold can be determined for the IR and the strong limits as

$$(eB)_{\star}^{\text{IR limit}} = \frac{\pi m_0^2}{2\alpha} \left(-1 + \exp \left(\frac{24\pi^2}{35ae\zeta(3)} \right) \right), \quad (eB)_{\star}^{\text{strong limit}} = \frac{8\pi^5 m_0^2}{49a^2 e^2 \alpha^3 (\zeta(3))^2}. \quad (\text{IV.41})$$

For $a = 2$ and $m_0 = 0.5$ MeV, we get therefore

$$(eB)_{\star}^{\text{IR limit}} = 9.77 \times 10^{-5} \text{ GeV}^2 \quad \text{or} \quad B_{\star}^{\text{IR limit}} = 1.65 \times 10^{16} \text{ Gauß}. \quad (\text{IV.42})$$

The corresponding efficiency factor $\eta_{\star}^{\text{IR}} \equiv \eta^{\text{IR}}((eB)_{\star}) = 63.21\%$. This means a variation from the corresponding efficiency factor in the strong limit $\Delta\eta \equiv \eta^{\text{IR}} - \eta^{\text{strong}} = 62.79\%$. We conclude therefore, that the IR limit, compared to the static and the strong limit, leads to maximum efficiency factor η for a given value of eB (see Fig. 2).

V. CONCLUSION

In the first part of this paper, using the vacuum polarization tensor $\Pi_{\mu\nu}(k_0, \mathbf{k})$ in the IR limit $k_0 \rightarrow 0$, the general structure of the plasmon (ring) potential of QED is determined in a constant magnetic

field B . Then, taking the limit of weak and strong magnetic field, the ring improved effective potential including the one-loop and the ring potentials is determined. In the weak magnetic field limit, the effective potential consists of a $T^4\alpha^{5/2}$ term, in addition to the expected $T^4\alpha^{3/2}$ contribution arising in the static ($k_0 \rightarrow 0, \mathbf{k} \rightarrow \mathbf{0}$) limit. The additional corrections are potentially relevant for the study of electroweak phase transition in the presence of weak magnetic field limit [12]. Note that similar terms of order $\alpha_s^{3/2}$ and $\alpha_s^{5/2}$ appear also in QCD effective potential at finite temperature and without magnetic field. They are calculated using the Hard Thermal Loop expansion [17] (see also [18] and the references therein). It would be interesting to develop the same program for QED and QCD at finite temperature and in the presence of weak/strong magnetic field.

Next, QED ring potential is calculated in the strong magnetic field limit. In this limit, QED dynamics is dominated by LLL and the chiral symmetry of the theory is broken as a result of a dynamically generated fermion mass. To study this well-known phenomenon of magnetic catalysis for QED at finite temperature in the LLL, the ring improved effective potential of the theory is determined in strong magnetic field limit. In particular, the ring potential is determined in the IR, $k_0 \rightarrow 0$, as well as the static limit, ($k_0 \rightarrow 0, \mathbf{k} \rightarrow \mathbf{0}$). In the IR limit, it includes a novel term consisting of a dilogarithmic function $(eB)\text{Li}_2\left(-\frac{2\alpha}{\pi}\frac{eB}{m^2}\right)$. Similar term in the form $g_s^4 \ln g_s$ appears also in QCD ring potential at finite temperature and zero magnetic field [19]. As for the static limit in the presence of strong magnetic field, there are indeed two different approaches leading to different ring potentials in this limit [see III.C and III.D for more details. Here, these two limits are indicated by static and strong limits]. Physically, the difference between these two results lies in the dimensional reduction as one of the consequences of LLL dynamics.

In the second part of this paper, using the ring improved effective potential in the IR, static and strong limits, the gap equation, the dynamical mass and critical temperature T_c of chiral symmetry restoration of QED are determined. Note that the critical temperature could only be determined by choosing a temperature independent IR cutoff m_0 in the integrals leading to the ring potential. Concerning the two different ring potentials in the static and strong limits, we note that according to our arguments in Sect. III.C and III.D, once we consider QED in the LLL at finite temperature, we have to determine the full dynamical mass and critical temperature using the ring potential in the static limit. We have presented nevertheless the results arising from ring potential in strong limit in Sect. IV.D and compared the results from Sect. IV.B - IV.D in Sect. IV.E.

To have an estimate on the efficiency of the IR limit in decreasing the critical temperature from its value arising from the one-loop effective potential, $T_c^{(1)}$, we have numerically determined $u = T_c^{(1)}/\mathcal{T}_c$ for various magnetic fields and as a function of m_0 . Here, \mathcal{T}_c is the ring improved critical temperature defined in (IV.33). Further, to compare the IR limit with the static and strong limit, we have defined an efficiency factor $\eta = 1 - u^{-1}$ for the IR, static and strong limits. As it turns out, for a given values of eB , the IR limit, compared to the static and the strong limits, is more efficient in decreasing the critical temperature $T_c^{(1)}$. The maximum efficiency factor in the IR limit is $\eta^{\text{IR}} \approx 63\%$ for $B \approx 1.6 \times 10^{16}$ Gauß.

Apart from its importance in the framework of magnetic catalysis, the above conclusion can be regarded as a promising result concerning the problem of electroweak phase transition (EWPT) in the electroweak SM in the presence of strong hypermagnetic field. There, one is looking for a possibility to decrease the critical temperature of EWPT in order to improve the baryogenesis condition $\frac{\langle v \rangle}{T_c} > 1 - 1.5$, where $\langle v \rangle$ is the Higgs mass [8, 12]. Note that the existence of baryon number violation in the SM is

realized by means of its vacuum structure through sphaleron mediated processes. The sphaleron transition between different topological distinct vacua is associated to baryon number $n_B - n_{\bar{B}}$ violation and can either induce or wash out a baryon asymmetry. In order to satisfy the baryon asymmetry condition during the baryogenesis process the rate of baryon violating transitions between different topological vacua must be suppressed in the broken phase, when the universe returns to thermal equilibrium. In other words, the sphaleron transition must be slower than the expansion of the universe and this in turn translates into the condition $\frac{\langle v \rangle}{T_c} > 1 - 1.5$ [12]. Using the improved ring potential in the IR limit in determining the critical temperature of EWPT in SM may improve the results of [10]-[13] as one of the possible solutions of baryon asymmetry problem within the minimal SM [42].

VI. ACKNOWLEDGMENT

We would like to thank the referee of this paper for instructive questions and comments, that have led, in particular, to a considerable improvement of the results in Sect. IV.

APPENDIX A: RING IMPROVED EFFECTIVE POTENTIAL OF QED IN LLL AT $T = 0$

In this appendix, using the composite effective action based on CJT (Cornwall-Jackiw-Tomboulis) approach [32], we will define the ring improved effective potential of QED at zero temperature in the LLL approximation. This fixes at the same time the notations used in the following appendices, where the gap equation of QED at zero and nonzero temperature are derived. The latter is used in Sect. IV to determine the dynamical mass and critical temperature of QED in the LLL approximation.

Let us start with the composite effective action of QED (see [32] and [46] for more details)

$$\Gamma[\mathcal{G}, \mathcal{D}_{\mu\nu}] = -i\text{Tr} \ln \mathcal{G}^{-1} - i\text{Tr} (S^{-1} \mathcal{G}) + \Gamma_2(\mathcal{G}, \mathcal{D}_{\mu\nu}) + \mathcal{F}[\mathcal{D}_{\mu\nu}]. \quad (\text{A.1})$$

Here, S is the free propagator of massless fermions. Further, \mathcal{G} is the full fermion and $\mathcal{D}_{\mu\nu}$ is the full photon propagator. As it is described in [32], the composite effective action (A.1) includes the sum of two- and higher-loop two-particle irreducible (2PI) diagrams. Note that Γ_2 on the r.h.s. of (A.1) includes the contribution of diagrams which are two-particle irreducible with respect to fermion lines only. In two loop order, the diagrams included in Γ_2 are shown in Fig. 3.

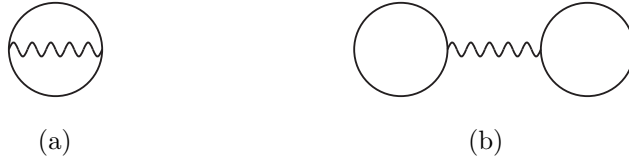


FIG. 3: Two-loop diagrams contributing to Γ_2 in (A.1). In the ladder LLL approximation, solid lines correspond to free fermion propagator in the LLL with $m = m_{dyn.}$ from (II.6)-(II.8), and wavy lines correspond to free photon propagator $\mathcal{D}_{\mu\nu}^{(0)}$ from (II.17). Diagram (a) is the same diagram appearing in (I.7) and can be regarded as the diagram corresponding to $N = 1$ in the ring potential (III.9) at zero and nonzero temperature. It is denoted by $\alpha\mathcal{R}_1$ in (A.6) and as $\sum_n \alpha\mathcal{R}_1^{(n)}$ in (C.4).

Replacing the full fermion propagator \mathcal{G} in (A.1) by the fermion propagator \bar{S}_{LLL} of massive fermions in the LLL approximation with mass $m = m_{\text{dyn.}}$, from (II.6)-(II.9), and, the full photon propagator, $\mathcal{D}_{\mu\nu}$ by the free photon propagator $D_{\mu\nu}^{(0)}$ from (II.17), the composite effective action $\bar{\Gamma}_{\text{LLL}} \equiv \Gamma[\bar{S}_{\text{LLL}}, D_{\mu\nu}^{(0)}]$ in the ladder LLL approximation reads³⁷

$$\bar{\Gamma}_{\text{LLL}} \simeq \Omega \tilde{V}(m_{\text{dyn.}}, eB; T=0) - i\text{Tr} (S_{\text{LLL}}^{-1} \bar{S}_{\text{LLL}}) + \tilde{\Gamma}_2^{(\infty)}[\bar{S}_{\text{LLL}}, D_{\mu\nu}^{(0)}] + \mathcal{F}[D_{\mu\nu}^{(0)}]. \quad (\text{A.2})$$

Here, the free fermion propagator of massless fermions S_{LLL} is given in (II.6)-(II.8) with $m = 0$. In (A.2), the ring improved (one-loop) effective potential $\tilde{V}(m_{\text{dyn.}}, eB; T=0)$ in the ladder LLL approximation is introduced. It is defined by the one-loop effective potential $V^{(1)}(m_{\text{dyn.}}, eB; T=0)$ and the ring potential $V_{\text{ring}}(m_{\text{dyn.}}, eB; T=0)$,

$$\tilde{V}(m_{\text{dyn.}}, eB; T=0) \equiv V^{(1)}(m_{\text{dyn.}}, eB; T=0) + V_{\text{ring}}(m_{\text{dyn.}}, eB; T=0). \quad (\text{A.3})$$

The one-loop effective potential in the LLL approximation is defined by the first term in (A.1) with \mathcal{G} replaced by \bar{S}_{LLL} ,

$$V^{(1)}(m_{\text{dyn.}}, eB; T=0) \equiv -i\Omega^{-1} \text{Tr} \ln \bar{S}_{\text{LLL}}^{-1}. \quad (\text{A.4})$$

In a constant magnetic field, (A.4) is calculated in [33] using the method of worldline formalism. In the LLL approximation, it is given by

$$\begin{aligned} V^{(1)}(m, eB; T=0) &= -\frac{eB}{8\pi^2} \int_{\frac{1}{\Lambda^2}}^{\infty} \frac{ds}{s^2} e^{-sm^2} \\ &= -\frac{eBm^2}{8\pi^2} \Gamma\left(-1, \frac{m^2}{\Lambda^2}\right) \xrightarrow{\Lambda \rightarrow \infty} \frac{eBm^2}{8\pi^2} \left(\ln \frac{m^2}{\Lambda^2} + \mathcal{O}(m^0) \right), \end{aligned} \quad (\text{A.5})$$

[see also (III.38) for $T \neq 0$ case]. Here m is a general nonvanishing mass. On the last line of (A.5), $\Gamma(0, z) \xrightarrow{z \rightarrow 0} -\ln z - \gamma$ is used. Here, γ is the Euler-Mascheroni constant.

As for the ring potential, V_{ring} from (A.3), it receives contribution from the ring diagrams in (I.7) and Fig. 1. These diagrams are already included in Γ_2 from (A.1).³⁸ At zero temperature, the ring potential of QED is given by

$$\begin{aligned} V_{\text{ring}}(m_{\text{dyn.}}, eB; T=0) &\equiv \Omega^{-1} \sum_{N=1}^{\infty} \alpha^N \mathcal{R}_N[\bar{S}_{\text{LLL}}, D_{\mu\nu}^{(0)}] \\ &= -\frac{1}{2} \int \frac{d^4 k}{(2\pi)^4} \sum_{N=1}^{\infty} \frac{(-1)^N}{N} \left[D_{\mu\rho}^{(0)}(k) \Pi^{\rho\mu}(k) \right]^N, \\ &= -\frac{1}{2} \int \frac{d^4 k}{(2\pi)^4} \ln \left(1 + D_{\mu\rho}^{(0)}(k) \Pi^{\rho\mu}(k) \right). \end{aligned} \quad (\text{A.6})$$

³⁷ In the definition of effective potential we have used $\Gamma = \Omega V$, where Γ is the effective action, V is the effective potential and Ω is the four-dimensional space-time volume.

³⁸ Using the fermion gap equation $\frac{\delta \Gamma[\bar{S}_{\text{LLL}}, S_{\text{LLL}}, D_{\mu\nu}^{(0)}]}{\delta S_{\text{LLL}}} = 0$, it can be shown that $\alpha^N \mathcal{R}_N[\bar{S}_{\text{LLL}}, D_{\mu\nu}^{(0)}]$ from (A.2) leads, up to a constant factor, to the same α^N correction in the resulting SD equation, that arises from $\frac{\delta \Gamma[\mathcal{G}_{\text{LLL}}, S_{\text{LLL}}, \mathcal{D}_{\text{LLL}}]}{\delta \mathcal{G}_{\text{LLL}}} = 0$ where full photon propagator $\mathcal{D}_{\mu\nu}$ is used. In this sense, ring diagrams are already included in a composite effective action, where instead of free photon propagators, as in (A.2), full photon propagators are used. Other α^N corrections arising from quantum corrections of full fermion propagator in the LLL, \mathcal{G}_{LLL} , are included in $\bar{\Gamma}_2^{(\infty)}$ in (A.2).

[see also (III.9) for $T \neq 0$ case]. Here, \mathcal{R}_N denotes the contribution of the N -th diagram in the ring series in Fig. 1, where N vacuum polarization tensor $\Pi_{\mu\nu}$ are inserted in a photon loop. Note that in the LLL ladder (rainbow) approximation, the vacuum polarization tensor in (A.6) is determined using *free* propagator \bar{S}_{LLL} of *massive* fermions in LLL approximation with mass $m = m_{\text{dyn.}}$ from (II.6)-(II.8).³⁹ As we have mentioned above, ring diagrams are already included in Γ_2 from (A.1). Thus $\Gamma_2^{(\infty)}$ is (A.2) is defined by

$$\tilde{\Gamma}_2^{(\infty)}[\bar{S}_{\text{LLL}}, D_{\mu\nu}^{(0)}] \equiv \Gamma_2[\bar{S}_{\text{LLL}}, D_{\mu\nu}^{(0)}] - \Omega V_{\text{ring}}(m_{\text{dyn.}}, eB; T = 0). \quad (\text{A.7})$$

Here, the subscript ∞ in $\Gamma_2^{(\infty)}$ means that infinitely many ring diagrams are subtracted from Γ_2 in (A.1).

APPENDIX B: GAP EQUATION OF QED AT ZERO TEMPERATURE

1. Gap equation from one-loop effective potential at zero temperature

In the LLL, once the dynamical mass is generated via the mechanism of magnetic catalysis, the chiral symmetry of the originally massless QED breaks spontaneously. This leads to the formation of a chiral condensate $\langle \bar{\psi}\psi \rangle$. For a nonvanishing fermion mass, m , the nonvanishing chiral condensate can be most easily calculated by (see [28] and Eq. (19) in [20] for more details)

$$\langle \bar{\psi}\psi \rangle \equiv - \lim_{x \rightarrow y} \text{tr} (\bar{S}_{\text{LLL}}(x, y; m)) \simeq \frac{eBm}{4\pi^2} \left(\ln \frac{m^2}{\Lambda^2} + \mathcal{O}(m^0) \right). \quad (\text{B.1})$$

Here, Λ is a large momentum cutoff. Comparing now the value of the chiral condensate (B.1) with the one-loop effective potential (A.5), we arrive at⁴⁰

$$\langle \bar{\psi}\psi \rangle = \frac{\partial V^{(1)}(m, eB; T = 0)}{\partial m}. \quad (\text{B.2})$$

The above chiral condensate can be used to determine the gap equation of QED from composite effective action. To do this in the LLL approximation, let us consider the composite effective action $\bar{\Gamma}_{\text{LLL}}$ from (A.2) and use the fermion gap equation $\delta \bar{\Gamma}_{\text{LLL}} / \delta \bar{S}_{\text{LLL}} = 0$, to arrive at

$$\frac{\delta \bar{\Gamma}_{\text{LLL}}}{\delta \langle \bar{\psi}\psi \rangle} = \int d^4x \text{tr} \left(\frac{\delta \bar{\Gamma}_{\text{LLL}}}{\delta \bar{S}_{\text{LLL}}(x)} \frac{\partial \bar{S}_{\text{LLL}}(x)}{\partial \langle \bar{\psi}\psi \rangle} \right) = 0. \quad (\text{B.3})$$

Using now the gap equation $\frac{\delta \bar{\Gamma}_{\text{LLL}}}{\delta \langle \bar{\psi}\psi \rangle} = 0$ and the definition of $\bar{\Gamma}_{\text{LLL}}$ from (A.2), we arrive at the gap equation of QED arising from one-loop effective potential (A.4) [see also (IV.1)]

$$\frac{\partial V^{(1)}(m_{\text{dyn.}}, eB; T = 0)}{\partial \langle \bar{\psi}\psi \rangle} \equiv G_0 m_{\text{dyn.}}. \quad (\text{B.4})$$

Here, the “effective coupling” of QED in the LLL dominant regime, G_0 , is defined by

$$G_0 \equiv - \frac{1}{m_{\text{dyn.}} \Omega} \frac{\partial}{\partial \langle \bar{\psi}\psi \rangle} \left(-i \text{Tr} (S_{\text{LLL}}^{-1} \bar{S}_{\text{LLL}}) + \alpha \mathcal{R}_1[\bar{S}_{\text{LLL}}, D_{\mu\nu}^{(0)}] + \tilde{\Gamma}_2^{(1)}[\bar{S}_{\text{LLL}}, D_{\mu\nu}^{(0)}] + \mathcal{F}[D_{\mu\nu}^{(0)}] \right), \quad (\text{B.5})$$

³⁹ The ring potential V_{ring} from (A.6) for zero external magnetic field and in the static limit, *i.e.* for $\Pi_{\rho\nu} \equiv \Pi_{\rho\nu}(k = 0)$ in (A.6), is previously calculated by Akhiezer *et al.* [47]. It leads apart from cutoff dependent terms to nonperturbative $\alpha^2 \log \alpha$ corrections to the effective action.

⁴⁰ Relation (B.2) can generally be derived for $eB = 0$ using the definition of one-loop effective action [41].

where the definition of $\bar{\Gamma}_{\text{LLL}}$ from (A.2) is used. In general G_0 is a complicated function of α (see below). It can be determined order by order in α by computing the r.h.s. of (B.5). In the lowest order of α correction, for instance, it receives contribution from $\alpha\mathcal{R}_1$ [diagram (a) in Fig. 3], and diagram (b) in Fig 3, which is included in $\tilde{\Gamma}_2^{(1)}$. To determine G_0 in the lowest order of α correction, let us first give the gap equation (B.4) in a more appropriate form by making use of the identity

$$\frac{\partial}{\partial \langle \bar{\psi}\psi \rangle} = \left(\frac{\partial^2 V^{(1)}}{\partial m_{\text{dyn.}}^2} \right)^{-1} \frac{\partial}{\partial m_{\text{dyn.}}}, \quad (\text{B.6})$$

that can be derived from $\frac{\partial V^{(1)}}{\partial m} = \langle \bar{\psi}\psi \rangle$. As for the gap equation (B.4), it is given by

$$\frac{\partial V^{(1)}(eB, m_{\text{dyn.}}; T=0)}{\partial m_{\text{dyn.}}} = G_0 m_{\text{dyn.}} \frac{\partial^2 V^{(1)}(eB, m_{\text{dyn.}}; T=0)}{\partial m^2}. \quad (\text{B.7})$$

The above gap equation (B.7) can now be used to “fix” G_0 order by order as a function in α . To show this, let us consider the one-loop effective potential from (A.5) with $m = m_{\text{dyn.}}$ and plug it into (B.7). We arrive at

$$(1 - G_0) \Gamma \left(0, \frac{m_{\text{dyn.}}^2}{\Lambda^2} \right) + 2G_0 \Gamma \left(1, \frac{m_{\text{dyn.}}^2}{\Lambda^2} \right) = 0. \quad (\text{B.8})$$

Setting $\Lambda = \Lambda_B \equiv \sqrt{eB}$ and assuming that $m_{\text{dyn.}} \ll \Lambda_B$, the Γ -functions on the r.h.s. of (B.8) can be expanded as

$$\Gamma(0, z) \xrightarrow{z \rightarrow 0} -\gamma - \ln z, \quad \text{and} \quad \Gamma(1, z) \xrightarrow{z \rightarrow 0} 1. \quad (\text{B.9})$$

Plugging these relations into (B.8), we arrive at the following gap equation

$$\ln \frac{m_{\text{dyn.}}}{\Lambda_B} = -\frac{\gamma}{2} + \frac{G_0}{1 - G_0}, \quad (\text{B.10})$$

that leads to

$$m_{\text{dyn.}}(G_0; T=0) = \mathcal{C} \Lambda_B \exp \left(\frac{G_0}{1 - G_0} \right), \quad \text{with} \quad \mathcal{C} = e^{-\gamma/2}. \quad (\text{B.11})$$

This is indeed a general structure of the dynamical mass as a function of G_0 . The latter includes all higher loop contributions through its definition from (B.5). To determine G_0 in the lowest order of α correction, we use the result of the dynamical mass $m_{\text{dyn.}}^{(1)}$ in ladder approximation from (II.16) and compare (B.11) with it. Thus, the “effective coupling of QED in the LLL”, G_0 , can be “fixed” in this lowest order of α correction as

$$G_0^{(1)} \equiv \frac{1}{1 - \sqrt{\frac{\alpha}{\pi}}} \approx 1 + \sqrt{\frac{\alpha}{\pi}}. \quad (\text{B.12})$$

Here, similar to $m_{\text{dyn.}}^{(1)}$ the superscript (1) denotes that $G_0^{(1)}$ receives contribution from two-loop diagrams of order α that are shown in Fig. 3. These diagrams contribute to the composite effective action as it can be checked from (A.2). It would be interesting to perform a bottom-up calculation of $G_0^{(1)}$ from its definition (B.5) in the one-loop level. Calculating the expression in the parentheses in (B.5) up to order α and replacing $m_{\text{dyn.}}(G_0; T=0)$ from (B.11) leads to a nontrivial equation for G_0 , whose solution leads to an expression for G_0 that can be compared with $G_0^{(1)}$ from (B.12) in the lowest order of α correction.⁴¹

⁴¹ This calculation will be performed elsewhere [48].

2. Gap equation from the ring improved effective potential at zero temperature

To determine explicitly the contribution of ring diagrams to the dynamical mass and critical temperature, we will use in Sect. IV.B an alternative gap equation. It arises from the ring improved effective potential $\tilde{V}(eB, m_{dyn.}; T \neq 0)$ at finite temperature. At zero temperature, the ring improved effective potential is given in (A.3). The corresponding ring improved gap equation reads then

$$\frac{\partial \tilde{V}(m_{dyn.}, eB; T=0)}{\partial \langle \bar{\psi} \psi \rangle} = \tilde{G}_0 m_{dyn.}, \quad (\text{B.13})$$

where

$$\tilde{G}_0 = -\frac{1}{m_{dyn.} \Omega} \frac{\partial}{\partial \langle \bar{\psi} \psi \rangle} \left(-i \text{Tr} (S_{\text{LLL}}^{-1} \bar{S}_{\text{LLL}}) + \tilde{\Gamma}_2^{(\infty)} [\bar{S}_{\text{LLL}}, D_{\mu\nu}^{(0)}] + \mathcal{F}[D_{\mu\nu}^{(0)}] \right). \quad (\text{B.14})$$

Comparing to G_0 from (B.5) we get

$$G_0 = \tilde{G}_0 - \frac{1}{m_{dyn.}} \frac{\partial V_{ring}(m_{dyn.}, eB; T=0)}{\partial \langle \bar{\psi} \psi \rangle}, \quad (\text{B.15})$$

where V_{ring} is given in (A.6).

APPENDIX C: GAP EQUATION OF QED AT FINITE TEMPERATURE

1. Composite effective action in the LLL approximation at finite temperature

Let us consider the ladder LLL composite effective action (A.2) at zero temperature. Its generalization to finite temperature is indicated as $\bar{\Gamma}_T \equiv \Gamma_{\text{LLL}}[\bar{S}_{\text{LLL}}, D_{\mu\nu}^{(0)}; T]$, which is defined as

$$\bar{\Gamma}_{\text{LLL}}^T \equiv \Omega^{-1} \tilde{V}(m_{dyn.}, eB; T) - i \text{Tr} (S_{\text{LLL}}^{-1} \bar{S}_{\text{LLL}})_T + \tilde{\Gamma}_2^{(\infty)} [\bar{S}_{\text{LLL}}, D_{\mu\nu}^{(0)}; T] + \mathcal{F}[D_{\mu\nu}^{(0)}; T]. \quad (\text{C.1})$$

Here, $m_{dyn.} \equiv m_{dyn.}(T)$ is the temperature dependent dynamical mass. The ring improved effective potential, $\tilde{V}(m_{dyn.}, eB; T)$, is defined as

$$\tilde{V}(m_{dyn.}, eB; T) = V^{(1)}(m_{dyn.}, eB; T) + V_{ring}(m_{dyn.}, eB; T). \quad (\text{C.2})$$

Here, the one-loop effective potential at finite temperature is defined as in (A.4) by

$$V^{(1)}(m_{dyn.}, eB; T) \equiv -i \Omega^{-1} \text{Tr} \ln \bar{S}_{\text{LLL}}^T, \quad (\text{C.3})$$

and the ring potential is given as in (A.6) by

$$V_{ring}(m_{dyn.}, eB; T) \equiv \sum_{n=-\infty}^{\infty} \alpha^N \mathcal{R}_N^{(n)} [\bar{S}_{\text{LLL}}, D_{\mu\nu}^{(0)}; T]. \quad (\text{C.4})$$

In (C.3) the bare fermion propagator in the LLL is the generalization of (II.6)-(II.8) to finite temperature. For a general nonzero mass, the free fermion propagator at finite temperature including the contribution of all Landau levels is given by (II.19). The ring potential in (C.4) is defined in (III.9), where the

contribution of all diagrams in Fig. 1 and the diagram in (I.7) at finite temperature⁴² is taken into account. As it can be seen in (III.9) to determine the ring potential, we have to add over all $n \in]-\infty, \infty[$ that label the Matsubara frequencies ω_n . The summation over n in (C.4) denotes the same summation over n of Matsubara frequencies and $\mathcal{R}_N^{(n)}$ is the corresponding contribution of the N -th ring diagram to the n -th Matsubara frequency.

2. Gap equation from one-loop effective potential at finite temperature

In Sect. IV.A, the gap equation arising from one-loop effective potential is used to determine the dynamical mass (IV.5) and the critical temperature (IV.8) at finite temperature. The gap equation from one-loop effective potential at finite T is given by

$$\frac{\partial V^{(1)}(m_{dyn.}, eB; T)}{\partial \langle \bar{\psi} \psi \rangle} \equiv G m_{dyn.}. \quad (C.5)$$

It is indeed a generalization of (B.4)-(B.5) to finite temperature. Using the ladder LLL composite effective action (C.1), the effective coupling of QED in the LLL dominant regime at finite temperature, G , can be defined as

$$G \equiv -\frac{1}{m_{dyn.}} \frac{\partial}{\partial \langle \bar{\psi} \psi \rangle} \left(-i \text{Tr} (S_{\text{LLL}}^{-1} \bar{S}_{\text{LLL}})_T + \alpha \mathcal{R}_1[\bar{S}_{\text{LLL}}, D_{\mu\nu}^{(0)}; T] + \tilde{\Gamma}_2^{(1)}[\bar{S}_{\text{LLL}}, D_{\mu\nu}^{(0)}; T] + \mathcal{F}[D_{\mu\nu}^{(0)}; T] \right). \quad (C.6)$$

In Sect. IV.A, we will use this gap equation to determine the dynamical mass $m_{dyn.}^{(1)}(G; T)$ and the critical temperature $T_c^{(1)}(G)$ in the lowest order of α correction in ladder (rainbow) LLL approximation [see (IV.5) for the dynamical mass and (IV.10) for the critical temperature].

3. Gap equation from ring improved effective potential at finite temperature

The gap equation arising from the ring improved effective potential at finite temperature can be given most easily as a generalization of (B.13)-(B.14) to finite temperature. It is given by

$$\frac{\partial \tilde{V}(m_{dyn.}, eB; T)}{\partial \langle \bar{\psi} \psi \rangle} = \tilde{G} m_{dyn.}, \quad (C.7)$$

where \tilde{G} is defined by

$$\tilde{G} = -\frac{1}{m_{dyn.} \Omega} \frac{\partial}{\partial \langle \bar{\psi} \psi \rangle} \left(-i \text{Tr} (S_{\text{LLL}}^{-1} \bar{S}_{\text{LLL}})_T + \tilde{\Gamma}_2^{(\infty)}[\bar{S}_{\text{LLL}}, D_{\mu\nu}^{(0)}; T] + \mathcal{F}[D_{\mu\nu}^{(0)}; T] \right). \quad (C.8)$$

Comparing to G from (C.6) we get

$$G = \tilde{G} - \frac{1}{m_{dyn.}} \frac{\partial V_{ring}(m_{dyn.}, eB; T)}{\partial \langle \bar{\psi} \psi \rangle}. \quad (C.9)$$

⁴² This is the $N = 1$ term in (III.9).

4. Gap equations used in sections IV.B- IV.D

The general form of the gap equations (C.7)-(C.8) are not exactly the gap equations that are used in Sect. IV.B - IV.D to determine the full dynamical mass and critical temperature of QED in the ladder LLL approximation. There, we have used the ring potential in three different approaches $\aleph = \{\text{IR, static, strong}\}$. To give the general definition of the gap equation corresponding to all these three approaches, we will indicate the ring potential in the \aleph -approach by $V_{ring}^{\aleph}(m_{dyn.}, eB; T)$ and use the separation

$$V_{ring}(m_{dyn.}, eB; T) \equiv V_{ring}^{\aleph}(m_{dyn.}, eB; T) + \bar{V}_{ring}^{\aleph}(m_{dyn.}, eB; T). \quad (\text{C.10})$$

In Sect. IV.B, IV.C and IV.D, the superscript $\aleph = \text{IR}$, $\aleph = \text{static}$ and $\aleph = \text{strong}$, respectively. We define further the ring improved effective potential corresponding to \aleph -approach by one-loop effective potential (C.2) and the ring potential in \aleph -approach

$$\tilde{V}^{\aleph}(m_{dyn.}, eB; T) = V^{(1)}(m_{dyn.}, eB; T) + V_{ring}^{\aleph}(m_{dyn.}, eB; T). \quad (\text{C.11})$$

The gap equation in the corresponding \aleph -approach is therefore given by

$$\frac{\partial \tilde{V}^{\aleph}(m_{dyn.}, eB; T)}{\partial \langle \bar{\psi} \psi \rangle} = \tilde{G}^{\aleph} m_{dyn.}, \quad (\text{C.12})$$

where $m_{dyn.} = m_{dyn.}^{\aleph}$ and the corresponding coupling, \tilde{G}^{\aleph} is given by

$$\begin{aligned} \tilde{G}^{\aleph} = & -\frac{1}{m_{dyn.} \Omega} \frac{\partial}{\partial \langle \bar{\psi} \psi \rangle} \left\{ -i \text{Tr} (S_{\text{LLL}}^{-1} \bar{S}_{\text{LLL}})_T \right. \\ & \left. + \Omega^{-1} \bar{V}_{ring}^{\aleph}(m_{dyn.}, eB; T) + \tilde{\Gamma}_2^{(\infty)}[\bar{S}_{\text{LLL}}, D_{\mu\nu}^{(0)}; T] + \mathcal{F}[D_{\mu\nu}^{(0)}; T] \right\}. \end{aligned} \quad (\text{C.13})$$

We have therefore

$$\tilde{G} = \tilde{G}^{\aleph} - \frac{1}{m_{dyn.}} \frac{\partial V_{ring}^{\aleph}(m_{dyn.}, eB; T)}{\partial \langle \bar{\psi} \psi \rangle}. \quad (\text{C.14})$$

Let us finally give an example to clarify the above notation. In Sect. IV.B for instance, we have used the ring potential in the IR limit. In particular, this is determined by $n = 0$ in (C.4). Using the definitions

$$\begin{aligned} V_{ring}^{\text{IR}}(m_{dyn.}, eB; T) & \equiv \Omega^{-1} \sum_{N=1}^{\infty} \alpha^N \mathcal{R}_N^{(n=0)}[\bar{S}_{\text{LLL}}, D_{\mu\nu}^{(0)}; T], \\ \bar{V}_{ring}^{\text{IR}}(m_{dyn.}, eB; T) & \equiv \Omega^{-1} \sum_{\substack{n=-\infty \\ n \neq 0}}^{\infty} \sum_{N=1}^{\infty} \alpha^N \mathcal{R}_N^{(n)}[\bar{S}_{\text{LLL}}, D_{\mu\nu}^{(0)}; T], \end{aligned} \quad (\text{C.15})$$

to separate zero and nonzero Matsubara frequencies, the gap equation in the IR approach is given by

$$\frac{\partial \tilde{V}^{\text{IR}}(m_{dyn.}, eB; T)}{\partial \langle \bar{\psi} \psi \rangle} = \tilde{G}^{\text{IR}} m_{dyn.}, \quad (\text{C.16})$$

where the corresponding coupling is given by

$$\begin{aligned} \tilde{G}^{\text{IR}} = & -\frac{1}{m_{dyn.} \Omega} \frac{\partial}{\partial \langle \bar{\psi} \psi \rangle} \left\{ -i \text{Tr} (S_{\text{LLL}}^{-1} \bar{S}_{\text{LLL}})_T \right. \\ & \left. + \Omega^{-1} \bar{V}_{ring}^{\text{IR}}(m_{dyn.}, eB; T) + \tilde{\Gamma}_2^{(\infty)}[\bar{S}_{\text{LLL}}, D_{\mu\nu}^{(0)}; T] + \mathcal{F}[D_{\mu\nu}^{(0)}; T] \right\}. \end{aligned} \quad (\text{C.17})$$

-
- [1] D. A. Kirzhnits, *Weinberg model in the hot universe*, JETP Lett. **15**, 529 (1972) [Pisma Zh. Eksp. Teor. Fiz. **15**, 745 (1972)].
 - [2] S. Weinberg, *Gauge and global symmetries at high temperature*, Phys. Rev. D **9**, 3357 (1974).
 - [3] L. Dolan and R. Jackiw, *Symmetry behavior at finite temperature*, Phys. Rev. D **9**, 3320 (1974).
 - [4] D. A. Kirzhnits and A. D. Linde, *Symmetry Behavior In Gauge Theories*, Annals Phys. **101**, 195 (1976).
 - [5] A. D. Sakharov, *Violation of CP invariance, C asymmetry, and baryon asymmetry of the universe*, Pisma Zh. Eksp. Teor. Fiz. **5**, 32 (1967) [JETP Lett. **5**, 24 (1967 SOPUA,34,392-393.1991 UFNAA,161,61-64.1991)].
 - [6] K. Takahashi, *Perturbative calculations at finite temperatures*, Z. Phys. C **26**, 601 (1985).
 - [7] M. E. Carrington, *The effective potential at finite temperature in the Standard Model*, Phys. Rev. D **45**, 2933 (1992).
 - [8] M. B. Gavela, P. Hernandez, J. Orloff and O. Pene, *Standard Model CP violation and baryon asymmetry*, Mod. Phys. Lett. A **9**, 795 (1994).
K. Kajantie, M. Laine, K. Rummukainen and M. E. Shaposhnikov, *The Electroweak phase transition: A non-perturbative analysis*, Nucl. Phys. B **466**, 189 (1996).
 - [9] M. Giovannini and M. E. Shaposhnikov, *Primordial magnetic fields, anomalous isocurvature fluctuations and big bang nucleosynthesis*, Phys. Rev. Lett. **80**, 22 (1998).
P. Elmfors, K. Enqvist and K. Kainulainen, *Strongly first order electroweak phase transition induced by primordial hypermagnetic fields*, Phys. Lett. B **440**, 269 (1998).
 - [10] V. Skalozub and M. Bordag, *Ring diagrams and electroweak phase transition in a magnetic field*, Int. J. Mod. Phys. A **15**, 349 (2000).
 - [11] V. Skalozub and V. Demchik, *Electroweak phase transition in strong magnetic fields in the standard model of elementary particles*, [arXiv:hep-th/9912071].
 - [12] A. Sanchez, A. Ayala and G. Piccinelli, *Effective potential at finite temperature in a constant hypermagnetic field: Ring diagrams in the standard model*, Phys. Rev. D **75**, 043004 (2007).
 - [13] M. E. Tejeda-Yeomans, J. Navarro, A. Sanchez, G. Piccinelli and A. Ayala, *MSM self-energies at finite temperature in the presence of weak magnetic fields: Towards a full symmetry restoration study*, arXiv:0804.3433 [hep-ph].
 - [14] J. I. Kapusta and C. Gale, *Finite Temperature Field Theory: Principles and Applications*, Second Edition, Cambridge University Press (2006).
 - [15] H. Perez Rojas and A. E. Shabad, *Polarization of relativistic electrons and positron gas in a strong magnetic field; Propagation of electromagnetic waves*, Ann. Phys. **121**, 432 (1979).
 - [16] J. Alexandre, *Vacuum polarization in thermal QED with an external magnetic field*, Phys. Rev. D **63**, 073010 (2001).
 - [17] E. Braaten and R. D. Pisarski, *Deducing hard thermal loops from Ward identities*, Nucl. Phys. B **339**, 310 (1990).
J. O. Andersen, E. Braaten and M. Strickland, *Hard-thermal-loop resummation of the free energy of a hot gluon plasma*, Phys. Rev. Lett. **83**, 2139 (1999).
 - [18] C. x. Zhai and B. M. Kastening, *The Free energy of hot gauge theories with fermions through g^{**5}* , Phys. Rev. D **52**, 7232 (1995).
E. Braaten and A. Nieto, *Free energy of QCD at high temperature*, Phys. Rev. D **53**, 3421 (1996).
 - [19] T. Toimela, *The next term in the thermodynamic potential of QCD*, Phys. Lett. B **124**, 407 (1983).
 - [20] V. P. Gusynin, V. A. Miransky and I. A. Shovkovy, *Dimensional reduction and catalysis of dynamical symmetry breaking by a magnetic field*, Nucl. Phys. B **462**, 249 (1996).

- [21] V. P. Gusynin, V. A. Miransky and I. A. Shovkovy, *Theory of the magnetic catalysis of chiral symmetry breaking in QED*, Nucl. Phys. B **563**, 361 (1999).
- [22] V. P. Gusynin, V. A. Miransky and I. A. Shovkovy, *Large N dynamics in QED in a magnetic field*, Phys. Rev. D **67**, 107703 (2003).
V. P. Gusynin, V. A. Miransky and I. A. Shovkovy, *Dynamical chiral symmetry breaking in QED in a magnetic field: Toward exact results*, Phys. Rev. Lett. **83**, 1291 (1999).
V. P. Gusynin, V. A. Miransky and I. A. Shovkovy, *Dynamical chiral symmetry breaking by a magnetic field in QED*, Phys. Rev. D **52**, 4747 (1995).
V. P. Gusynin, V. A. Miransky and I. A. Shovkovy, *Dimensional reduction and dynamical chiral symmetry breaking by a magnetic field in (3+1)-dimensions*, Phys. Lett. B **349**, 477 (1995).
C. N. Leung and S. Y. Wang, *Gauge independent approach to chiral symmetry breaking in a strong magnetic field*, Nucl. Phys. B **747** (2006) 266 ; *ibid.*, *Gauge independence and chiral symmetry breaking in a strong magnetic field*, [arXiv:hep-ph/0503298].
S. Y. Wang, *Dynamical electron mass in a strong magnetic field*, Phys. Rev. D **77**, 025031 (2008).
A. A. Osipov, B. Hiller, A. H. Blin and J. da Providencia, *Dynamical chiral symmetry breaking by a magnetic field and multi-quark interactions*, Phys. Lett. B **650**, 262 (2007).
K. G. Klimenko and V. C. Zhukovsky, *Does there arise a significant enhancement of the dynamical quark mass in a strong magnetic field?*, arXiv:0803.2191 [hep-ph].
E. Rojas, A. Ayala, A. Bashir and A. Raya, *Dynamical mass generation in QED with magnetic fields: arbitrary field strength and coupling constant*, Phys. Rev. D **77**, 093004 (2008).
- [23] K. Farakos, G. Koutsoumbas and N. E. Mavromatos, *Dynamical flavour symmetry breaking by a magnetic field in lattice QED(3)*, Phys. Lett. B **431**, 147 (1998).
K. Farakos and N. E. Mavromatos, *Hidden non-Abelian gauge symmetries in doped planar antiferromagnets*, Phys. Rev. B **57**, 3017 (1998).
G. W. Semenoff, I. A. Shovkovy and L. C. R. Wijewardhana, *Phase transition induced by a magnetic field*, Mod. Phys. Lett. A **13**, 1143 (1998).
E. J. Ferrer, V. P. Gusynin and V. de la Incera, *Magnetic field induced gap and kink behavior of thermal conductivity in cuprates*, Mod. Phys. Lett. B **16**, 107 (2002).
E. J. Ferrer, V. P. Gusynin and V. de la Incera, *Thermal conductivity in 3D NJL model under external magnetic field*, Eur. Phys. J. B **33**, 397 (2003).
- [24] E. Elizalde, E. J. Ferrer and V. de la Incera, *Neutrino propagation in a strongly magnetized medium*, Phys. Rev. D **70**, 043012 (2004).
E. J. Ferrer and V. de la Incera, *Neutrino propagation and oscillations in a strong magnetic field*, Int. J. Mod. Phys. A **19**, 5385 (2004).
- [25] N. O. Agasian and S. M. Fedorov, *Quark-hadron phase transition in a magnetic field*, arXiv:0803.3156 [hep-ph].
E. S. Fraga and A. J. Mizher, *Chiral transition in a strong magnetic background*, arXiv:0804.1452 [hep-ph].
- [26] A. E. Shabad and V. V. Usov, *Modified Coulomb Law in a Strongly Magnetized Vacuum*, Phys. Rev. Lett. **98**, 180403 (2007).
- [27] D. E. Kharzeev, L. D. McLerran and H. J. Warringa, *The effects of topological charge change in heavy ion collisions: 'Event by event P and CP violation'*, arXiv:0711.0950 [hep-ph].
- [28] J. S. Schwinger, *On gauge invariance and vacuum polarization*, Phys. Rev. **82**, 664 (1951).
- [29] G. Calucci and R. Ragazzon, *Nonlogarithmic terms in the strong field dependence of the photon propagator*, J. Phys. A **27**, 2161 (1994).
- [30] A. V. Kuznetsov and N. V. Mikheev, *Electron mass operator in a strong magnetic field and dynamical chiral symmetry breaking*, Phys. Rev. Lett. **89**, 011601 (2002).
- [31] V. P. Gusynin and I. A. Shovkovy, *Chiral symmetry breaking in QED in a magnetic field at finite temperature*, Phys. Rev. D **56**, 5251 (1997).

- [32] J. M. Cornwall, R. Jackiw and E. Tomboulis, *Effective Action For Composite Operators*, Phys. Rev. D **10**, 2428 (1974).
- [33] H. T. Sato, *Thermodynamic fermion loop in a constant magnetic field*, J. Math. Phys. **39**, 4540 (1998).
S. Kanemura, H. T. Sato and H. Tochimura, *Thermodynamic Gross-Neveu model under constant electromagnetic field*, Nucl. Phys. B **517**, 567 (1998).
- [34] C. Schubert, *Perturbative quantum field theory in the string-inspired formalism*, Phys. Rept. **355**, 73 (2001).
- [35] E. V. Gorbar and V. A. Miransky, *Relativistic field theories in a magnetic background as noncommutative field theories*, Phys. Rev. D **70**, 105007 (2004).
- [36] A. J. Salim and N. Sadooghi, *Dynamics of $O(N)$ model in a strong magnetic background field as a modified noncommutative field theory*, Phys. Rev. D **73**, 065023 (2006).
- [37] V. P. Gusynin, V. A. Miransky and I. A. Shovkovy, *Dynamical flavor symmetry breaking by a magnetic field in $(2+1)$ -dimensions*, Phys. Rev. D **52**, 4718 (1995).
- [38] T. K. Chyi, C. W. Hwang, W. F. Kao, G. L. Lin, K. W. Ng and J. J. Tseng, *The weak-field expansion for processes in a homogeneous background magnetic field*, Phys. Rev. D **62**, 105014 (2000).
- [39] P. N. Meisinger and M. C. Ogilvie, *Complete high temperature expansions for one-loop finite temperature effects*, Phys. Rev. D **65**, 056013 (2002).
- [40] I. Gradshteyn and I. Ryzhik, *Table of Integrals, Series and Products*, 5th ed., (Academic Press, San Diego, 1994).
- [41] D. Ebert and V. C. Zhukovsky, *Chiral phase transitions in strong chromomagnetic fields at finite temperature and dimensional reduction*, Mod. Phys. Lett. A **12**, 2567 (1997).
- [42] K. Sohrabi, S. Fayyazbakhsh and N. Sadooghi, work in progress.
- [43] E. Elizalde, E. J. Ferrer and V. de la Incera, *Beyond-constant-mass-approximation magnetic catalysis in the gauge Higgs-Yukawa model*, Phys. Rev. D **68**, 096004 (2003).
J. Alexandre, K. Farakos and G. Koutsoumbas, *QED in a strong external magnetic field: Beyond the constant mass approximation*, Phys. Rev. D **62**, 105017 (2000).
- [44] E. J. Ferrer and V. de la Incera, *Ward-Takahashi identity with external field in ladder QED*, Phys. Rev. D **58**, 065008 (1998).
- [45] R. M. Corless, G. H. Gonnet, D. E. G. Hare, D. J. Jeffrey and D. E. Knuth, *On the Lambert W function*, Adv. in Comp. Math. **5**, 329 (1996).
- [46] V. A. Miransky, *Dynamical symmetry breaking in quantum field theories*, World Scientific, 1993.
- [47] I. A. Akhiezer and S. V. Peletminski, ZhETF (USSR) **38**, 1829 (1960) [JETP (Sov. Phys.) **11**, 1316 (1960)].
J. I. Kapusta, *Quantum Chromodynamics At High Temperature*, Nucl. Phys. B **148**, 461 (1979).
- [48] N. Sadooghi and K. Sohrabi, work in progress.